UNIVERSITY OF PISA

Doctoral School of

Neuroscience and Sciences of Endocrine System and Metabolism

Molecular, Metabolic and Functional Exploring of Nervous System and Sense Organs

Ph.D. Thesis

SSD: M-PSI/02

Wake-like activities and electrical silences in the human sleeping brain: functional roles and spatio-temporal dynamics in the thalamo-cortical network

Dr. Eng. Marco Laurino

Supervisor:
Dr. Angelo Gemignani, M.D.

Ph.D. Director:
Prof. Riccardo Zucchi, M.D.

May 21, 2014

To my family

Abstract

As pointed out by several papers, the less than one hertz oscillations or *Sleep Slow Oscillations* (SSOs) are the electrophysiological stigmata of the mammalian sleep. This cellular behavior, mainly involving thalamus and cortex, consisted of hyperpolarized phases (lasting 500 msec, down states) followed by depolarized ones (lasting 500 msec, up states). The electrical silence during down states, on the one hand, prevents any synaptic and network activity and on the other hand, creates the ionic conditions for a rebound of neural discharge (huge synaptic and network activity during up state). The presence of down states clearly marks the phenomenon of cortical bistability, which in turn reflects a deep hyperpolarization sustained by the opening of different K^+-channels. According to the *Integrated Information Theory* of Giulio Tononi, down states prevent the emergence of large-scale neural integrations and thus induce the break down of functional connectivity. This allows a functional segregation of independent cortical modules, which represents the *condicio sine qua non* for sleep unconsciousness. Other functional roles endowed in the SSO are memory consolidation and synaptic downscaling. The aim of this thesis is to investigate, via EEG, in human spontaneous and evoked SSOs: (i) the relationships between wake-like activities and electrical silence; (ii) the role of the thalamus; (iii) the quenching of sensory processing and thus of consciousness. Regarding point (i) we have found a positive bump preceding the down state characterized by an increase of high frequency activities. The presence of this high frequency activity before down state suggests a cortical ignition mechanism for the spontaneous SSO. As far as point (ii) is concerned, we have investigated how the thalamus influences the cortical expression of the SSOs. To this aim, we have studied SSO features in a case of *Fatal Familial Insomnia* (FFI) with a selective thalamic neurodegeneration of nuclei mainly involved in spindle generation. In the FFI patient, we have found a reduction of SSO event rate, some morphological alterations of SSO structure, and a significant reduction in grouping high frequency activity during up state. As for point (iii), we studied *K-Complexes* (KCs), namely SSOs evoked by sensory stimulations. The main results of this study are: a positive wave (P200) precedes the down state (N550); the topology of P200 latency depends on the sensory modality of stimulation (acoustic, tactile and visual) with earliest waves in the related primary sensory areas; the P200 travels as a cortical excitation inducing N550 and P900 (up state) in associative fronto-central

areas; when KCs are not evoked the P200-like excitations have lower amplitude compared to evoked KC P200; the down state latency topology is affected by the proneness to bistability, i.e. the amount of K^+-channel that favor a synchronized falling into down state. As a whole the results of the thesis indicate that *Slow Wave Sleep* (SWS) is not a mere quiescent state but rather an active state in which changes of neural dynamics allow a well orchestrated interplay of unconscious behavior and memory consolidation. The final consequence is the maintenance of homeostasis. The SSO is the cellular phenomenon capable to coalesce wake-like activities and electrical silences, synthesizing at microscopic level the macroscopic complexity of SWS. This thesis allowed exploring thalamo-cortical dynamics by studying spontaneous and evoked SSOs. In synthesis the human-environment interaction (including visceral stimuli) during sleep overlaps that of wakefulness, since thalamus and cortical areas devoted to the first step of sensory processing are identical. The difference between wake and sleep is only sustained by the down state. In conclusion the study of SSO clarifies many issues linked to sleep and in particular to the real efficacy of a good sleep. This opens the door to the application of SSO study in different preclinical or clinical conditions.

Contents

List of Tables

List of Figures

Introduction

The sleeping brain is far from being in a quiescent state. If this is intuitively true for REM sleep, during which oneiric activity takes place, it is also true for *Slow Wave Sleep* (SWS), during which consciousness is abolished.

This thesis is aimed to identify in humans the complexity of SWS by describing the coexistence of wake-like activities with sleep ones, highlighting their functions in the light of the homeostatic role of sleep.

At neural level, a wide variety of activity patterns are detectable during SWS. Some of these patterns overlap those of wakefulness; on the contrary others are paradigmatic of sleep. The cellular phenomenon that coalesces fragments of wake and sleep is the less than one hertz oscillation, or *Slow Oscillation*. This cellular pattern has been discovered by Mircea Steriade [1] in 1993 in anesthetized animals and then confirmed in natural sleeping animals [2]. Neurons that undergo Slow Oscillation show brief periods of electrical silence (about 500 ms of no synaptic and network activity) followed by equal lasting periods of huge neural discharge (high synaptic and network activity). This pattern mainly involves pyramidal neurons endowed in the V and III cortical layer as well as other cortical interneurons with excitatory and inhibitory properties [1, 3]. In other words, all cortical neurons are driven by sleep mechanisms to oscillate from activity to no-activity. Nevertheless, sleep is not a homogeneous phenomenon [2]. Indeed, the Slow Oscillation shows temporal varying patterns in function of cortical topology. In animal models, the Slow Oscillation origins preferentially in whisker barrels cortical area and spreads towards anterior and posterior regions [4]. This seems to be related to higher plasticity mechanisms in this specific region with respect to other cortical areas. Indeed, the cat uses whisker barrels for exploring the out world and to learn new behavioral modalities for improving its survival chances or for satisfying its appetitive needs. The strict relationship between sleep and

learning is strengthened by a role of Slow Oscillation in memory consolidation during sleep [5, 6, 7, 8, 9].

Acherman and Borbely published a paper [10] in 1997, describing the presence of less than one hertz in humans, but only in 2004 Marcello Massimini in one paper [11] and Jan Born in another one [12] have described the criteria for detecting less than one hertz oscillations from human EEG. Starting from these studies less than one hertz oscillations in humans have been referred to as *Sleep Slow Oscillations* (SSO). In 2009 and 2010, Danilo Menicucci and Andrea Piarulli, respectively, have enlarged the criteria using the *likeness rule method* [13, 14].

All these papers confirmed that SSOs show a distinct origin location (frontal areas), a cortical spreading at a mean speed of 5 meters per second with an antero-posterior gradient, and a higher detection rate in fronto-centro-parietal areas.

Hence, it is plausible that SSO also in humans origins are linked to brain plasticity mechanisms since frontal regions are the cortical areas where the probability of formation of hebbian circuits is higher with respect to other cortical regions.

Studies in computo [15, 16, 17], in vitro [18] and in animal models [19, 20] show that the electrophysiological basis of the stigma of SWS, i.e. the down state, is mainly sustained by a deep hyperpolarization induced by the opening of different types of K^+-channels, from voltage-gated to activity-dependent until membrane leakage. In humans this mechanism is expected, since patients with auto-antibodies for voltage-gated K^+-channels (Morvan's Chorea) show a state of *agrypnia excitata*, i.e. the abolishment of Slow Wave Sleep [21, 22].

As aforementioned, the down state is followed by the up state. This is true also in humans. Indeed some papers based on fMRI signal [23, 24] revealed regional BOLD increases synchronized with SSO. From a biophysical point of view, BOLD signal is mainly sustained by a local increase of cerebral blood flow, which in turn is boosted by an increase of synaptic activity. In this line, what fMRI sees is only a local increase of metabolic demand that during SSO can occur only during the up state. EEGraphic characterization of the up state, not only in term of spectral activity but also in term of temporal relationship with the down state, is still an open issue. The latter aspect is not a scientific sophism since several works in animals showed up states preceding down states. Up to now it is not clear what happens before and after the down state.

Chapter 1 of this thesis tries to highlight this issue in humans by applying a spectral analysis of EEG signals in epochs preceding and following the down state [25]. The main results of chapter 1 are: (i) down states of spontaneous SSOs are preceded by a positive bump of wake-like-activity whose role is to ignite the

opening of K^+-channels; (ii) up states following down states are mainly composed by sigma activity, which represent a thalamic rhythm. As a consequence, down states are framed by fast EEG activities.

The identification of these wake-like-activities and their relationships with the down state will allow better describing the concept of coalescence of rhythms coined by Mircea Steriade in one of his milestone papers [26]. Another issue that is still open in literature concerns the thalamic role in the physiology of SSO. The thalamus and its nuclei have always been considered pivotal for slowing cortical activity and for providing large-scale synchronizations [27]. The thalamic role has been questioned when Mircea Steriade's group published some papers addressing the cortical presence of Slow Oscillations in thalamectomized cats [28]. These works highlighted that the ablation of thalamus did not prevent the cortical expression of Slow Oscillations. In other words according to these results, the thalamus has been deemphasized as a key region for the physiology of less than one hertz oscillations.

However, other more recent works from the Mircea Steriade's group [26] and from Crunelli's group [29] identified the role of the thalamus in crowning spindles upon the up state of the Slow Oscillations. This thalamic activity seems to play a role in plastic mechanisms occurring during SWS, such as memory consolidation [8, 9]. Despite some data supporting a thalamic role, the thalamo-cortical interplay for priming cerebral cortex to boost slow oscillations is still under debate.

Chapter 2 of this thesis is dedicated to solving this issue in humans by using a pathological model of selective thalamic neurodegeneration that affects the medio-dorsal nucleus, the Fatal Familial Insomnia (FFI) [30]. The main results of this study are: (i) a dramatic reduction of SSO detection rate in the FFI patient; (ii) a significant reduction of spindle activity crowned upon the SSO up state, that it is more severe in cortical areas receiving medio-dorsal thalamic pathways. In summary this study, for the first time in humans, demonstrates a key role of the thalamus in the physiology of SSO.

Finally, is there a link between SSO and consciousness? Does the SSO represent the neural activity that preserves sleep when sensory systems are activated by environmental noise? From a computational point of view [31], the presence of the electrical silence (down state) represents the emphcondicio sine qua non for quenching consciousness. Indeed these micro-epochs, during which network activity is abolished, prevent large-scale functional integrated patterns that underlie the optimal mutual information milieu necessary for the emergence of consciousness at a specific critical point [32]. The arising question is: what is the functional role

of unconsciousness? From a heuristic standpoint, unconsciousness allows activity in segregated networks and hence the optimization of synaptic load associated to what we have learn during wake [33, 34]. In other words, unconsciousness is the price that the brain has to pay in order to afford plastic mechanisms of wakefulness. This theory is getting consolidated for animal. Does the same mechanism take place also in humans for inducing unconsciousness and hence, on the one hand, maintaining sleep and on the other hand optimizing neural network activities?

Chapter 3 addresses the cortical response to sensory stimuli during SWS [35]. This cortical response, called K-Complex, has been firstly documented in 1938 by Loomis et al [36]. Mircea Steriade's group highlighted that K-Complexes and SSOs share the same electrophysiological mechanism. i.e. the alternation of down-and-up states [37, 38, 39]. Furthermore, up to now, the K-Complex has been considered as an *aspecific cortical response*, without any link to the sensory modalities that evoked it. In other words, the topology of K-Complexes typically encompasses fronto-central areas without involving primary sensory cortices. Are primary sensory areas really insensitive to the external world or some complex process happens? Subjectively, we have all experienced perception while sleeping, e.g. sudden awakenings due to nocturnal earthquakes. It is worth nothing that we can awake without any sensory awareness. This last chapter clarifies how the sleeping brain interacts with external environment. We administered to healthy subjects simple acoustic, tactile and visual stimuli while sleep was getting deeper. High-density EEG showed that, for 200 milliseconds, sleeping brain starts processing stimuli in specific sensory cortical areas, but this very activity can induce a diffuse half-a-second's electrical silence in higher-level cortical areas, which erases consciousness and protects sleep.

This study, at our best knowledge, for the first time shows a sensory-dependent cortical response and following cortical dynamics for preventing awakening.

Chapter 1

Sleep Fast Rhythms modulate NREM bistability

During NREM sleep neurons undergo synchronized bistability (electrical-silence and wake-like-firing alternation), generating the EEG *sleep-slow-oscillation* (SSO), consisting of sharp negative peak (down state) followed by shallow positive shoulder (up state). Up states sweep the cortex after their down states. As down states are idiosyncratic with any activity, are there activities anticipating the down states within the same SSO? This issue is related to which phenomena facilitate neural bistability. We studied SSO coalescence with leading and chasing fast rhythms (FR) via FR time-frequency characterization, and correlating FR to SSO occurrence and size. Results show: (i) SSO groups FR up to 150Hz; (ii) FR increments anticipate SSO onsets (pre-down state peaks); (iii) topological associations between leading FR in σ (12-18Hz) and β/low γ (18-42Hz) bands and SSO rate/size; (iv) temporal associations between SSO amplitude/slopes and coalescing σ and β/low γ magnitudes. Consequently, cortical excitability, measured by leading FR, influences NREM bistability. Furthermore, pre-down state peaks are putative candidates for triggering/propagating SSOs.

1.1 Introduction

During NREM sleep, membrane potential of almost all cortical neurons undergo transitions to a temporary hyperpolarized state with a nearly absolute synaptic stillness (down state), followed by a depolarized state of intense firing (up state). This biphasic oscillation has a time scale larger than 1 second, hence the name slow oscillation. Several lines of evidence indicate that this oscillation is a

default-mode activity of brain circuits specifically during sleep [40, 26, 41], due to the joint properties of intra-cortical networks and cortico-thalamo-cortical modules [29]. The slow oscillation is locally tuned as consequence of plastic changes induced by learning [42, 43, 44] and its grouping of spindle and β activities has been considered relevant for establishing reiterative processing of memories during NREM sleep [45, 46, 47]. Nevertheless, little is known about the spatial and temporal organization of the fast rhythms coalescent with slow oscillations. As far as the EEG correlates in human sleep are concerned, the atom of this bistable behavior has been identified in the graphoelement termed sleep slow oscillation (SSO) [11]. SSOs start with a sharp negative peak related to the down state phase followed by a shallow positive half wave. Typically, SSOs emerge from the background activity in random points on the cortex and propagate across it [11]. Consequently the whole process behaves as a single event (SSO event).

Standing on the concept of SSO event, herein we study the modulation of rhythms such as spindles or faster activities during the different phases of SSO. To this aim we performed EEG recordings in ten non-sleep-deprived individuals during their first sleep cycle as described in a recent paper from our group [13] and, starting from hundreds of isolated SSO events (detection algorithm described elsewhere [14] we found that patterns of fast rhythms anticipate and modulate SSO occurrence and shape.

1.2 Materials and methods

1.2.1 Subjects, Recordings and Sleep Slow Oscillation detection

Ten non-sleep-deprived male volunteers (age 18-30, right-handed according to the Edinburgh Handedness Inventory, EHI) participate to the study. Inclusion criteria were any medications for at least 1 year; no personal or family history of sleep disorders and no medical, neurological or psychiatric disorders, as assessed by semi-structured interviews. They gave written informed consent and the experiment was in line with the University of Pisa Ethical Committee guidelines.

We selected participants who had the same daily activity, i.e. students at the University of Pisa (Italy), spending at least 6 hours in class and reading scientific books. After an adaptation night, all volunteers were allowed to sleep at their usual bedtime and EEG recordings were carried out during the first sleep episode of the night.

A 40-channel (32-ch for EEG, 8-ch for auxiliary signals) monopolar amplifier

(Nuamps, Neuroscan, Compumedics, El Paso, TX) was used to acquire signals with a sampling rate of 1 KHz and electrode impedance belows 5 KOhm. Scalp EEG signals were referenced to the FCz potential and then offline re-referenced to the average mastoid potential.

EEG epochs with artifacts were detected on the basis of automated threshold-crossing detection algorithms [14]. After confirmatory visual inspection, most of them were discarded. At the end of the preprocessing steps, recordings showed more than 90% of artifact-free epochs. These epochs were scored according to the AASM standards [48].

Slow waves in these epochs were detected automatically by using the algorithm proposed by Piarulli et al.[14] that generalized the detection algorithm of Massimini and colleagues [11]. This detection algorithm starts scanning the band pass (0.5-4 Hz) filtered EEG signals in order to find patterns satisfying three criteria: (1) a negative zero crossing and a subsequent positive zero crossing, separated by 0.3-1 s; (2) a negative peak between the two zero crossings with voltage $< -80\mu$V; and (3) a negative-to-positive peak-to-peak amplitude $> 140\mu$V. Then, for each detected sleep slow oscillation concurrent sub-threshold SSOs are detected on the basis of the correlation between their angular phase time courses. This likeness rule completes the mapping of each SSO event and improves its characterization over the scalp.

Definition of the morphological parameters of the SSO

Three basic morphological parameters of the SSO have been considered (Panel a of Figure 1). The SSO amplitude was defined as the negative peak to positive peak amplitude, whereas the slopes corresponded to the steepness of the signal between the first zero crossing (Z1) and the negative peak – slope 1 – and between the negative peak and the second zero-crossing (Z2) – slope 2. All parameters have been measured on the signal pre-filtered in the delta band (low-frequency stop = 0.1 Hz, low-frequency pass = 0.5 Hz, high-frequency pass = 4.0 Hz, high-frequency stop = 4.4 Hz).

1.2.2 Time-frequency analysis of SSO events

We investigated fast rhythms accompanying SSOs by computing the time-frequency power spectrum (spectrogram) of all waves belonging to isolated events. We analyzed only temporally isolated events to avoid potential biasing related

to the activity of other contiguous SSO events. To this aim, events were selected more distant than 4 s from the previous and 4 s from the following, with time distances measured between the negative peaks of the waves.

We studied the spectrogram in a 5 s interval including the wave, from 2 s before the SSO negative peak to 3 s after. This time interval was chosen in order to include in the analysis a baseline epoch before the SSO onset and a recovery epoch after the SSO offset, both lasting at least 1 s.

The spectrogram had a resolution of 66ms and 6 Hz and was calculated by the Fast Fourier Transform applied on Hamming weighted sliding-windows on each 5 s EEG interval. Each window was of 166 ms with a 60% overlap between contiguous windows.

Throughout the study, the analyses were performed on the power integrated in three frequency bands: σ (12-18 Hz), β/low γ (18-42 Hz) and high γ (60-144 Hz). For each frequency band, we split the time course in 5 consecutive non-overlapping phases, each related to a definite SSO interval (Figure 1, panel b): a baseline phase (BP), a pre-down state phase (PDP), a down state phase (DP), an up state phase (UP) and a recovery phase (RP). BP is defined from 2s before to 1s before the negative peak of the SSO, whereas the RP is in the last second, from 2s after to 3s after the negative peak of the SSO. The other 3 phases correspond to time windows encompassing the extremal points of the power according to the following: PDP is related to the first maximum of σ and β power that occurs distinctly before the down state onset, DP accounts for the drop of fast rhythms concurrent with the negative peak, and UP accounts for the maximum of fast rhythms, taking place during the positive phase of the SSO.

The power of oscillations within each band and during each wave phase was characterized by measures in salient intervals within each phase. We termed these estimates power reference values (PRVs). As shown in the panel b) of Figure 1.1, for the characterization of BP and RP, we considered the mean value of the power time course within the phase, whereas PRVs for PDP, DP, and UP were estimated by averaging the power within an interval centered in the power maximum/minimum of the phase: the usage of neighborhood averaging allows making these PRVs robust against the presence of outliers in the power spectrum. The PVR of the UP was the mean value in a 400 ms neighborhood of the power maximum within 1.5 s starting from the negative peak (this interval always included the positive peak of the wave, as a posteriori verified). The PVR for the DP was the power mean value in a 400 ms neighborhood of the power minimum searched over the interval between the first zero crossing and the positive peak. The PRV for the PDP was

the mean value in a 400 ms neighborhood of the power maximum searched over the interval from the end of BP interval to the left boundary of DP neighborhood.

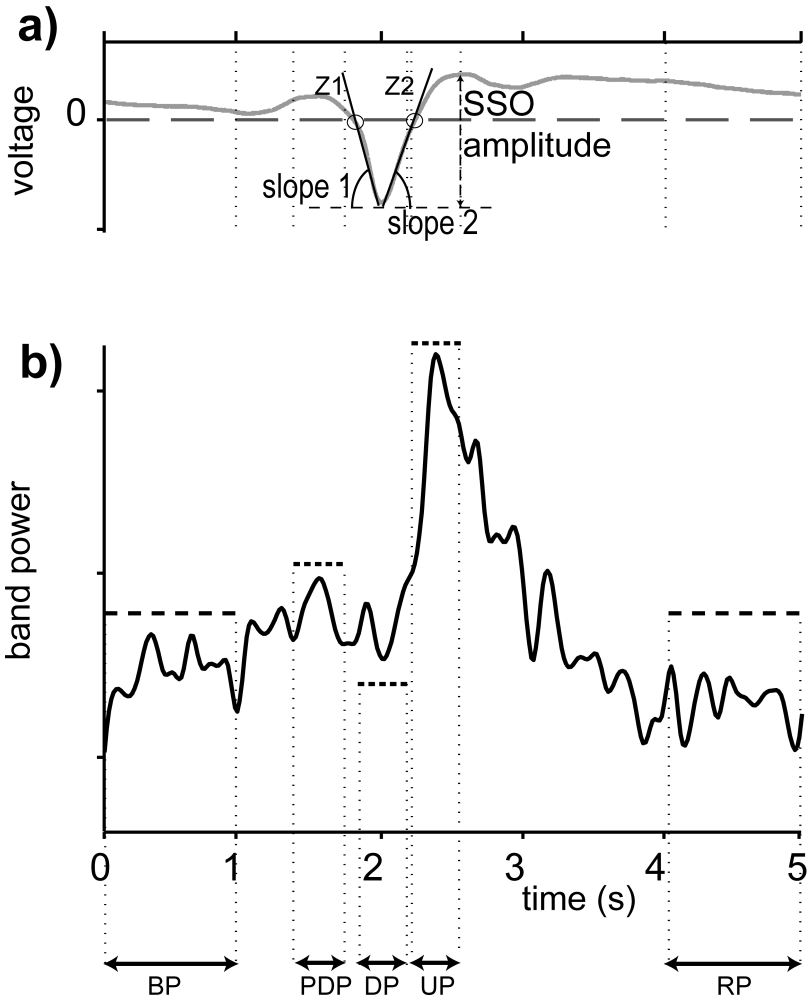

Figure 1.1. a) Graphical definition of SSO shape parameters. SSO amplitude was defined as the negative to positive peak amplitude. Slopes to and from the negative peak were defined as the steepness from the first zero-crossing (Z1) before the negative peak to the peak itself, and the steepness from the negative peak to the following zero-crossing (Z2). **b) Graphical definition of phase reference values (PRVs).** For each band, PRVs for baseline phase (BP) and recovery phase (RP) were the mean value of the power time course within the phase. The PVR of the up state phase (UP) was the mean value in a 400 ms neighborhood of the power maximum evaluated over a 1.5 s interval starting from the negative peak. The PVR for the down state phase (DP) was the power mean value in a 400 ms neighborhood of the power minimum evaluated over the interval between the negative zero crossing and the positive peak. The PRV for the pre-down state phase (PDP) was the mean value in a 400 ms neighborhood of the power maximum evaluated over the interval from the end of BP interval to the left bound of DP neighborhood.

1.2.3 Statistical Analysis

In order to study the course of FR with the slow wave phases and the effects related to sleep stages, we used repeated-measures ANOVAs. We analyzed PRVs trends by means of repeated-measures ANOVA with the sleep stage as a between-subjects factor (two levels corresponding to stage N2 and stage N3) and wave phase, (5 levels, i.e. BP, PDP, DP, UP, RP) as a within-subject factor. We applied the same statistical model to PRV data split for frequency band. For this analysis, regardless of the varying subset of electrodes involved in each SSO event, we choose to characterize each event focusing on two special waves: the origin wave and the wave with the higher amplitude (max wave). This choice enables us to investigate fast rhythms both at the cortical emergence of the event and at the location of its greatest neuronal assembly involvement. In addition, we investigated associations of FR expression to the shape and the rate of SSOs by means of correlation analyses (Pearson correlation, threshold of significance $p < 0.01$). Before performing the statistical tests, PRVs were transformed from μV^2 to dB in order to have values with a distribution not significantly different from a normal one, according to the Lilliefors test. We performed a first set of correlations to highlight associations between the scalp distributions of morphological parameters, rate of SSO occurrence and FR expression. Thus, correlations were performed between the average maps of PRVs on one side, and the average maps of SSO amplitude, SSO slopes and SSO rate of occurrence on the other.

A second set of correlation analyses was focused on investigating potential temporal association between wave shape and coalescent FRs, namely we verified whether increases in SSO size are coupled with enhancements of FRs expression. To this aim, given the electrode, we estimated the correlations between morphological parameters and PRVs series.

1.3 Results

1.3.1 A fast rhythms increase anticipates the SSO emergence

We investigated fast rhythms accompanying SSOs of all waves belonging to isolated events. Within the recordings, 20% of the events were isolated, namely a total of 630 events: according to the AASM standard [48] among them 40% belonged to sleep stage N2 and 60% to N3. On average (Figure 1.2, panel a), isolated SSO waves have a transient positive deflection followed by a deep negative peak

and by a large positive sweep.

Superimposing the group-averaged SSO template to the group-averaged spectrogram (Figure 1.2, panel b), a full band power increase during the wave in comparison to the first second, taken as baseline, is apparent. In addition, the spectrogram shows that an increase of power takes place definitely before the SSO onset: a behavior even more evident from the time course of power content integrated in the frequency bands (Figure 1.2, panel c).

The statistical analysis indicated that the modulation of fast rhythms with the phase of the SSO is overt for all bands with wave phase effect $p < 0.01$ both for origin and max waves (Figure 1.3). The highest PRVs were measured during UP for all bands ($p < 0.001$ compared to BP) and notably a second significant peak corresponded to PDP ($p < 0.001$ compared to BP for all bands). This latter peak, on average, occurs from 200 ms (β/low γ and high γ) to 120 ms (σ) before the SSO first zero crossing (Z1 point in Figure 1.1) and is weaker than the UP peak (p¡0.05). Finally, σ power within the DP is slightly higher ($p < 0.05$) than the BP level, which was expected since the interval across the negative peak includes the initial part of the transition to the SSO depolarizing phase [11] and unfortunately its PRV cannot provide a pure estimate of the fast rhythms during the neural stillness.

1.3.2 Sleep stage affects fast rhythms along with the wave phase

The progressive weakening of rapid activities as NREM sleep deepens is a widely described feature of sleep. In line with this general behavior, we find that the expression of fast rhythms in the σ, β/low γ bands during the SSO is greater during N2 than during N3 (sleep stage effect has $p < 0.001$ both for origin and max waves). At variance, no significant effect holds for high γ. Notably, for the σ rhythm differences between sleep stages are dependent on the wave phase (the interaction wave phase*sleep stage is significant – $p < 0.01$): the power levels during PDP, DP and UP are significantly different between sleep stages (related post-hocs have $p < 0.01$) whereas both baseline and recovery levels are similar (Figure 1.4). These findings are stable during the propagation since both origin and max wave analyses yield the same results.

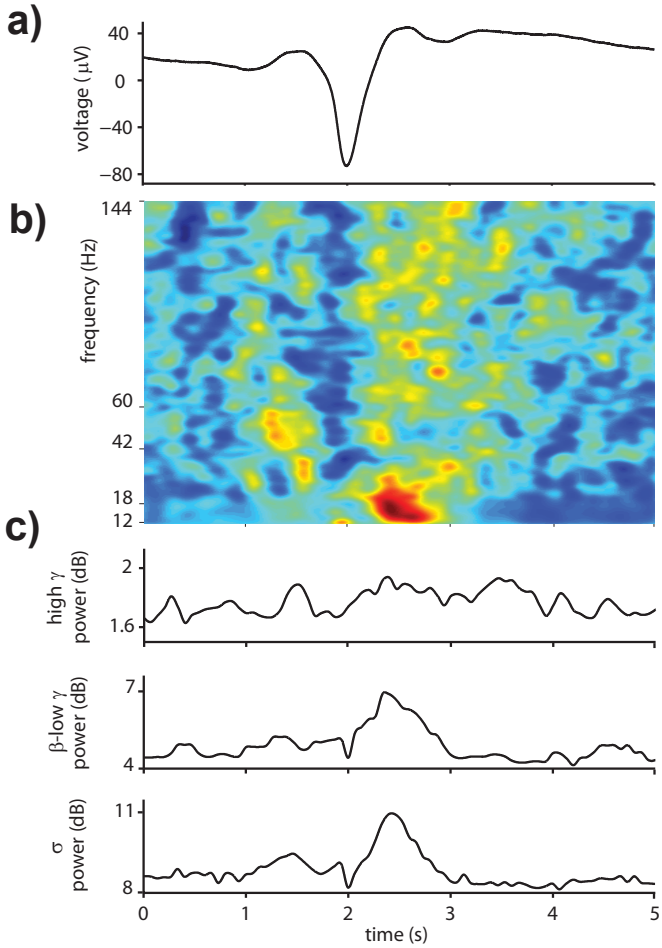

Figure 1.2. Time-frequency analysis of SSO events. a) Group average of the isolated SSO waves plotted as template of the SSOs belonging to the isolated events. **b)** Group-averaged spectrogram triggered on the SSO negative peak: the averaging has been performed between all single-wave spectrograms, irrespectively from electrode location, sleep stage or subject. In order to allow the graphical representation of the spectrogram we normalize the value of each time point to the range of the time point values related to its frequency bin $(P(t) - min(P(t))/(max(P(t)) - min(P(t))))$. This normalization highlights the course of power as function of wave phases despite the great decrease of power as function of frequency. The group-averaged spectrogram indicates that SSOs modulate fast rhythms up to high-γ frequencies. **c)** Group average time courses of power content integrated from the spectrogram in the σ, β/low γ, and high γ bands. Band power time courses highlights that, in addition to the up state-related fast activity peak, an increase of power happens definitely before the SSO emergence.

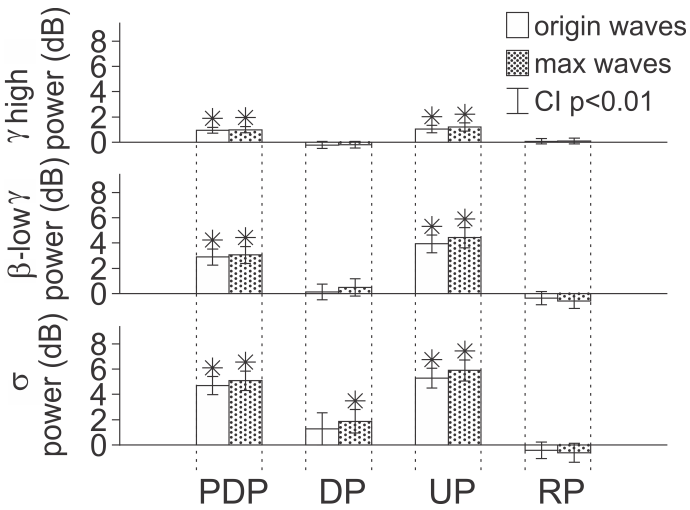

Figure 1.3. Changes of fast rhythms compared to the preceding baseline phase. Fast rhythms expression from σ to high γ have significant increases ($p < 0.01$) both during PDP ad UP; this holds both for origin waves (empty bars) and for max waves (dotted bars). Error-bars indicate confidence intervals of PRV increases and asterisks mark significant changes compared to the matched baseline PRV.

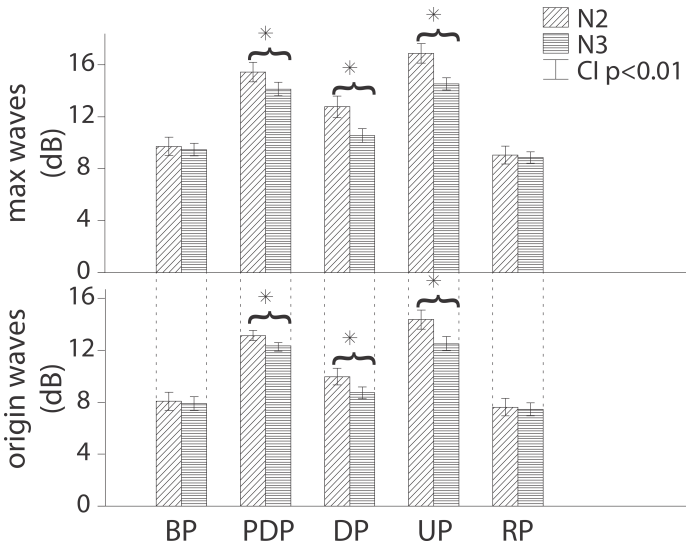

Figure 1.4. Interaction between wave phase and sleep stage in the σ band. The expression of σ rhythms, both during origin waves and max waves, changes from sleep stage N2 to N3 distinctly during PDP, DP and UP. Error-bars indicate confidence intervals of PRV split for sleep stage and asterisks mark significant differences between stages.

1.3.3 Scalp distribution of baseline fast rhythms maps cortical proneness to SSO

Evidences in literature indicate that the cortical proneness to SSO depends on cortical areas: the rate of SSO occurrence peaks on the fronto-central region [11], and the maps of indices related to neuronal involvement and synchronization (such as the SSOs amplitude and slopes considered in the following) have nearly the same spatial distribution [13].

Thus, we mapped the mean power of fast rhythms coalescing with the SSO in order to verify whether their expression have the same distribution over the scalp. This analysis considered all waves belonging to the SSO events. By splitting per electrode, Figure 1.5 shows group-average head plots forσ, β/low γ and high γ power bands during the five phases.

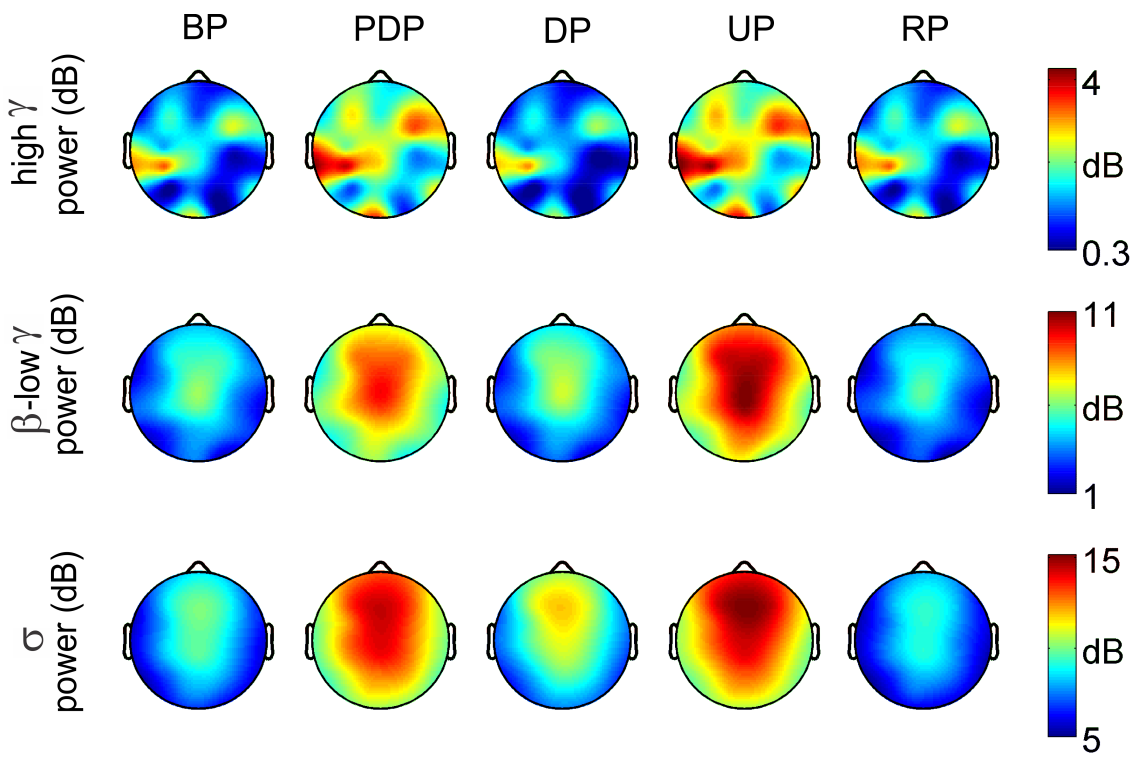

Figure 1.5. Group-average head plots for σ, β/low γ and high γ power bands during the five SSO phases. The power scalp distribution of both σ and β/low γ activities has a fronto-central prevalence overlapping SSO rate and morphology maps (Figure 1.6). At variance, high γ activity has a maximal expression over areas surrounding the somatosensory regions.

As far as σ and β/low γ bands are concerned, areas with the greater power

during both PDP and UP are those with greater probability of showing SSOs and vice versa. Also, these power scalp-distributions parallel the maps of SSO amplitude and slopes (Figure 1.6).

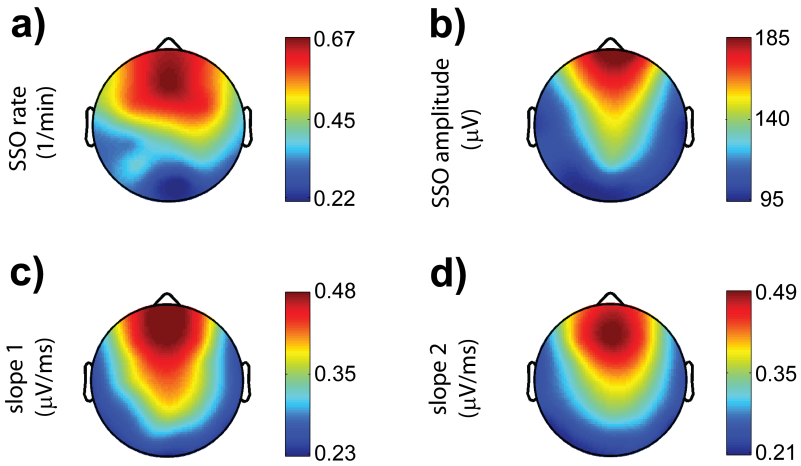

Figure 1.6. Topographic plots of isolated SSO events. Scalp distribution of rate (a), amplitude (b), slope 1 (c) and slope 2 (d) of isolated SSO. The maps nearby overlap with the distribution of power in the σ and β/low γ bands.

It is of notable relevance that the same associations are already present for BP PRV distributions that correlate with the same morphological parameters as well as with the detection probability. Figure 1.7 illustrates these significant linear relationships indicating that a signature of cortical proneness is present in the cortex electrical activity more than 1s before the SSO onset.

1.3.4 The shape of SSOs is influenced by coalescent fast rhythms

In addition to the area-dependent effects described in the previous section, we investigated the coordinated changes of fast rhythms and wave shape during the sleep time. Thus, given the area, namely electrode per electrode, we estimated the correlations between wave shape and coalescent fast rhythms expression. We found significant associations ($r > 0.3$ have a significance $p < 0.01$) between morphological parameters and PRVs of σ and β/low γ bands, whereas no association was identified with the high γ rhythms.

Figure 1.8 refers to the σ rhythms and shows the correlation maps as function of the wave phase. The maps related to the wave amplitude are similar to those referring to wave slopes: significant associations hold for a bulk of fronto-central

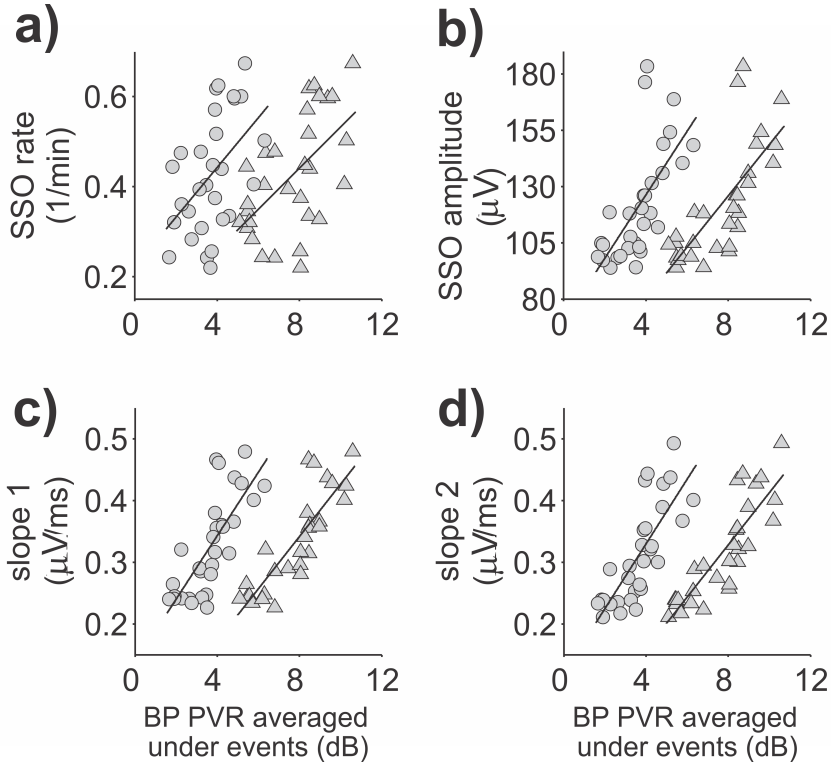

Figure 1.7. Baseline phase power scalp distribution parallels SSO shape and detection probabilility maps. a) Areas with the greater power in σ (a triangle indicates each electrode mean PRV) and β/low γ (a circle indicates each electrode mean PRV) bands during BP have a greater probability of showing a SSO: correlation was $r = 0.57$ ($p < 0.001$) for σ and was $r = 0.51$ ($p < 0.004$) for β/low γ. Moreover, the average BP power level per electrode parallels maps of SSO amplitude (b) slope 1 (c) and slope 2 (d) (refer to Figure 1.8 in the Materials and Method section for SSO morphological parameter definitions). For the association with the SSO amplitude correlations were $r = 0.75$ ($p < 0.001$) for σ and was $r = 0.67$ ($p < 0.001$) for β/low γ. For the association with the slope 1 correlations were $r = 0.87$ ($p < 0.001$) for σ and was $r = 0.77$ ($p < 0.001$) for β/low γ. For the association with the slope 2 correlations were $r = 0.86$ ($p < 0.001$) for σ and was $r = 0.78$ ($p < 0.001$) for β/low γ.

electrodes and have the greatest correlation coefficients during PDP and UP. The β/low γ rhythms have very similar maps (data not shown).

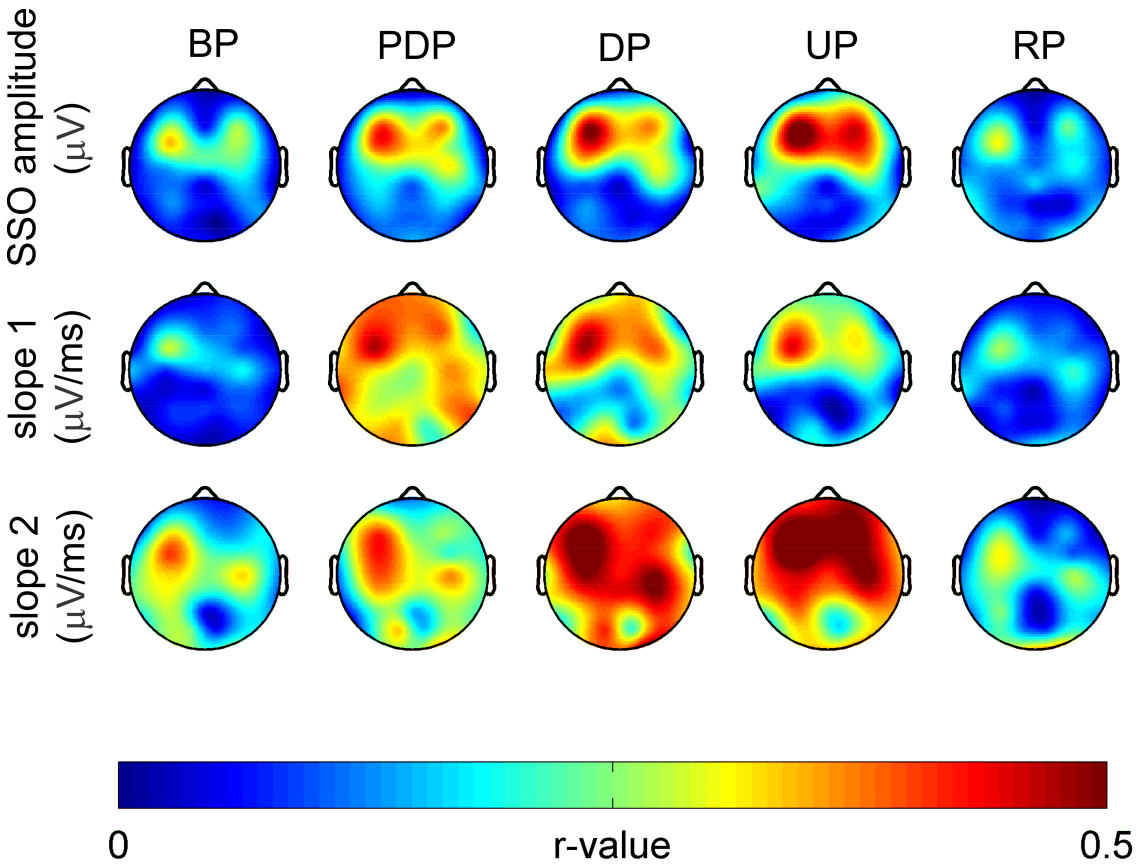

Figure 1.8. Local changes of fast rhythms expression is associated with shape modifications of the current SSO. PRVs in the σ band correlates with both SSO amplitude and slopes in a bulk of fronto-central electrodes. Correlation coefficients $r > 0.3$ were significant with $p < 0.01$.

1.4 Discussion and conclusions

Our study demonstrates how the alternation of stillness and activity occurring during NREM sleep groups rapid EEG oscillations in a broad frequency band. Extending Molle and colleagues observations of σ and β activities in humans [12] we show that the expression of rhythms up to high γ depends on the SSO phase as previously shown in animal models [27]. These high-frequency activations are spread over a broad band, without the distinct spectral peaks recently demonstrated by microelectrodes implanted in epileptic patients [49]. We also report

evidence of another broadband activation preceding the down state (in the PDP): at variance with the absence of an up state before the down state of K-complexes in N2 (namely, before the down state of SSOs during N2 [38]) reported in a different set of epileptic patients [50], on healthy humans this activation takes place both during N2 and N3. At our best knowledge, no other study on humans have highlighted this activation; on the contrary, in animal models, a pre-down state activation was explicitly reported by Crunelli et al. [51], who discussed thalamocortical volleys subtending and preceding the onset of a SSO. This activation is a posteriori recognizable in figures of previously published papers, either studying animals [52] or humans [12].

It is plausible that such a triphasic (high/low/high power) fast rhythms pattern becomes evident only when considering isolated and complete SSOs. Actually, in animal models most of the reported recordings [53, 54, 1] focus on stationary slow oscillations while the only study on humans dealing with spindle-activity-grouping during slow oscillations [12] analyzed separately positive-half and negative-half slow waves. In both cases it is impossible to recover the dynamics of fast rhythms expression during a whole SSO. Actually, the definition of the SSO event as well as the focus on isolated ones allow both searching for causal links between SSO phases and fast rhythms expression and defining baseline and recovery phases enclosing each SSO event.

We find that the triphasic pattern of fast rhythms is always present and already full-fledged at the SSO origin: therefore, this structured coalescence results to be a constitutive part of the SSO event from its genesis in the interplay between cortical, reticular thalamic and thalamocortical neurons [29]. We also identified a specific behavior for the σ component of fast rhythms as far as its dependence from sleep stage is concerned. The fact that σ power decreases with sleep deepening specifically during PDP, DP and UP without affecting baseline and recovery could be related to the behavior of thalamocortical neurons specifically active during the SSO. Indeed, thalamocortical neurons switch from a spindle to a clock-like delta activity with the transition from N2 to N3 [55, 56]. By mapping on the scalp the expression of fast rhythms during SSOs, we identify a clear link with maps of SSO occurrence and shape. This direct association could be related to the set up of the synaptic-based cortical oscillator subtending the SSO [29]. Many players contribute to the network properties [57, 58, 53, 59, 60, 1, 61]: as far as the neuronal component is concerned, both excitatory and inhibitory cortical neurons are involved since the cellular up state component of the SSO is facilitated either by spontaneously occurring coincidence of excitatory neurotransmitter

release at a few synaptic sites ([20] or by the reduction of inhibitory activities [62]. Different balances of excitation and inhibition between cortical areas could explain the spatial differences of fast rhythms activities, and could link their power distributions to the varying cortical SSO proneness. Moreover, also a thalamic influence could modulate the power distribution on the scalp [63].

In addition to these area-dependent effects, we investigated the predictability of SSO shape from the concurrent pattern of fast rhythms and we found that in the central areas fast rhythms, including the anticipatory ones, strongly influence the shaping of the SSO. The correlation maps measuring this association show the highest coefficients during PDP and UP linking down state duration [52] and neural synchronization correlates [64], such as SSO amplitude and slopes, to the amount of preceding and following fast rhythms. Which factors modulate the expression of fast rhythms during time and, in turn, alter the local network proneness to fall into the SSO is a question whose answer is still far from our reach. However, it is worth noting that correlations not vanishing with the SSO end (agreement of BP and RP maps) suggest the existence of mechanisms producing ongoing fast rhythms with a dynamics slower than the SSO duration. On the other hand, the sampling of fast rhythms expression during every isolated SSO event highlights an event-by-event variability: thus the dynamics of ongoing fast rhythms is faster than the typical waiting time between isolated SSOs. Fronto-central areas with the greater SSO shape predictability are nearly overlapping those having the highest rate of SSO detection: both phenomena could be related to the proximity of the two main SSO sources, that is the left insula and the frontal gyrus [65].

Conclusions

The data reported here complete the description of the spontaneous slow oscillations sweeping the cerebral cortex during NREM sleep. Moreover, we show that the probability of observing a SSO and its shape are linked to the expression of ongoing fast rhythms. A greater cortical excitability measured by the BP fast rhythms expression seems to promote the NREM bistability by triggering a depolarization avalanche that we detect as the fast rhythms peak in the pre-down state phase. The shape of the coalescing pattern of activities is invariant with the propagation and the wave front sweeping through the cortex during each SSO event could be the avalanche of depolarization occurring before the negative sweep of the SSO instead of the negative peak itself [50]. Regarding

the functional implications of the links between SSO and fast rhythms, many works highlighted the homeostatic equilibrium between cortical activity during wakefulness and sleep need as demonstrated by the local increased slow wave activity in areas previously involved in tasks [42, 43, 66, 46]: as a matter of fact a playback of learning-related neural patterns has been identified during NREM sleep and involves both hippocampal and cortical networks [67, 68, 69]. Here we find relationships between SSOs and concurrent fast rhythms that putatively could be EEG markers of the speculated cycling process for iteratively recalling and storing information acquired during wakefulness [70, 47].

Chapter 2

Thalamic contribution to Sleep Slow Oscillation features: Fatal Familial Insomnia case study

The objective of this study was the studying the thalamic role in the cortical expression of the Sleep Slow Oscillation (SSO) in humans by comparing SSO features in a case of Fatal Familial Insomnia (FFI) and a group of controls. We characterize SSOs in a 51-year-old male with FFI carrying the D178N mutation and the methionine/methionine homozygosity at the polymorphic 129 codon of the PRNP gene and in eight gender and age-matched healthy controls. Polysomnographic (21 EEG electrodes, two consecutive nights) and volumetric- (Diffusion tensor imaging Magnetic Resonance Imaging DTI MRI) evaluations were carried out for the patient in the middle course of the disease (five months after the onset of insomnia; disease duration: 10 months). We measured a set of features describing each SSO event: the wave shape, the event-origin location, the number and the location of all waves belonging to the event, and the grouping of spindle activity as a function of the SSO phase. We found that the FFI individual showed a marked reduction of SSO event rate and wave morphological alterations as well as a significant reduction in grouping spindle activity, especially in frontal areas. These alterations paralleled DTI changes in the thalamus and the cingulate cortex. This work gives a quantitative picture of spontaneous SSO activity during the NREM sleep of a FFI individual. The results suggest that a thalamic neurodegeneration specifically alters the cortical expression of the SSO. This characterization also provides indications about cortico-thalamic interplays in SSO activity in humans.

2.1 Introduction

Slow (< 1 Hz) rhythms in the sleeping brain and their electrophysiological expressions, namely the Sleep Slow Oscillations (SSOs), are increasingly attracting the attention of neurophysiologists and clinicians. Specifically, the SSO graphoelement is the EEG expression of the slow wave sleep (SWS) phenomena [44, 34].

Electrophysiological studies in animal models have revealed that cortical neurons show a coordinated switching behavior of the membrane potential during the SSO: they synchronously oscillate between a state of hyperpolarization (down state) and a state of wake-like depolarization (up state), both lasting several hundreds of ms [8]. This behavior represents the fundamental cellular phenomenon underlying different slow and fast neural activities in SWS, such as K-complexes, delta waves and spindles [26]. The SSO in the human EEG corresponds to a sharp negative peak (related to the down-state) followed by a shallow positive half wave (related to the up-state). The positive phase of each SSO has also the property of grouping spindles and faster activities [11, 12]. Indeed, it has been observed in animal models and in humans that periods of cortical hyperpolarization (down-state) are followed by strong rebounds of spindle activity which represent the grouping influence of the SSO on thalamo-cortical cells[12, 71]. This property has been considered relevant for establishing reiterative processing of memories during NREM sleep [45].

Furthermore, the SSO originates mainly in frontal regions [11] and propagates across variable cortical territories at a typical speed of a few m/s, preferentially in a fronto-posterior direction [13]. From the point of view of scalp signal analysis, each SSO is concurrently detected on a variable set of EEG electrodes, with delays related to the propagation. Consequently, each set of quasi-simultaneous SSO constitutes a propagating SSO event [11, 13].

From an anatomical standpoint, the SSO in cortex survives to extensive thalamic lesions or destruction of thalamocortical neurons [72], although it is detectable in thalamocortical neurons (TCN) of various thalamic nuclei and in neurons belonging to the nucleus reticularis thalami (NRT) [29]. In addition, animal models indicate that intact thalamo-cortical circuits have substantial influence on the generation and synchronization of the cortical SSO [63].

From these considerations a question arises which is still under debate: is the human SSO generated in the neocortex and then imposed on thalamic territories or is it generated by a mutual interplay between thalamus and cerebral cortex?

Experimental models of selective thalamic lesions in humans can help in answering the above mentioned question. Two models appear to be particularly suited for selectively studying the thalamic role in the physiology of SSO: i) the bilateral or unilateral thalamic strokes, with limitations related to the inter-subjects variability, and ii) an autosomal dominant hereditary disease, clinically characterized by loss of sleep, dysautonomia and motor signs, and pathologically characterized by selective thalamic degeneration [73, 22], named Fatal Familial Insomnia (FFI). This work copes with the study of the thalamic role in the physiology of SSO, by using the latter clinical condition.

FFI is linked to a missense mutation at codon 178 of the prion protein gene PRNP [74] and to the presence of the methionine (M) codon at position 129 in the mutated allele of the PRNP [75]. In addition, among FFI patients, MM homozygous at codon 129, have shorter disease duration (9-10 months) compared with the MV heterozygous patients ($>$ 24 months) [76]. Longitudinal, serial 24-h polygraphic recordings demonstrate the progressive reduction of spindles and delta sleep (synchronized sleep), which disappear later in the course of the disease [77, 78]. In FFI, CT and MRI scans are unremarkable, but longitudinal PET (18 FDG-PET) scans disclosed an hypometabolism confined to the thalamus in the earlier stages of the disease; studies [79] using the same longitudinal PET (18 FDG-PET) techniques showed that in carriers of FFI mutation the thalamic hypometabolism may precede the disease onset by several months [80].These studies confirm that the hallmark of FFI, particularly in early stage of the disease, is a thalamic dysfunction that may be associated with a less pronounced dysfunction of the frontomesial cortex (limbic and paralimbic cortical regions).

We evaluated the polysomnographic recording obtained in a FFI subject (D178N–129M) at a middle stage of the disease, when the pathological process is mainly bounded in the thalamus and NREM sleep is still detectable and compared the FFI patient with a set of age/sex matched healthy controls. The purpose of this study is determining the influence of a thalamic dysfunction on the SSO physiology.

After a general evaluation of the changes in the sleep macro-structure as well as of the power spectra, we focused the analysis on SSO activity. We found that in the FFI individual the SSO rate is dramatically reduced, the SSO segment related to the transition from down-state to up-state has a greater duration, and the SSO ability to group spindle activity is greatly impaired. These findings parallel a selective thalamic neurodegeneration identified through MRI evaluations.

These results indicate that thalamo-cortical interplays are crucial for the SSO synchronization in humans and, as a byproduct, suggest that the study of SSO in

presimptomatic FFI carriers is a useful tool for identifying of preclinical thalamic dysfunctions.

2.2 Material and Methods

2.2.1 Case report

A Caucasian 51-year-old male patient, born in North East Italy, was admitted because of a 5 months history of sub-acute onset of *inability to sleep*. His wife reported additional peculiar oneiric episodes during the night, characterized by gestures mimicking daily-life activities, such as pointing to something, eating or drinking. Since the beginning of these symptoms, he also developed hypertension, erectile dysfunction, fluctuating episodic diplopia and a weight loss of about 7 kilograms. The neurological examination showed short-term memory deficit; impaired horizontal and vertical saccadic eyes movements, spontaneous and evoked myoclonus. He was member of an FFI family already published: he is the V-59 subject of the genealogical tree described in literature [74]. Analyses of DNA extracted from peripheral leukocytes, revealed both the D178N mutation and the methionine/methionine homozigosity at the polymorphic 129 codon of the PRNP gene. He died 10 months after the onset of sleep problems for a sudden, generalized autonomic failure, complicated with infections.

MRI study

The FFI patient was studied in a 1.5 Tesla GE system. A T1-weighted axial volumetric image was acquired using the FSPGR sequence (TI=600 ms; TE=5.1 ms; TR=12.5 ms; 25.6 cm square FOV, 1 mm slice thickness; in-plane resolution=256x256), while axial DTI images were obtained (5 mm slice thickness without inter-slice gap) using a single-shot SE-EPI sequence with TE=89.2 ms, TR=10 s, 32 cm^2 FOV, in-plane resolution=256x256. Five T2-weighted scans without diffusion gradients, 25 with direction-encoding gradients at strengths, corresponding to b-value 900 s/mm^2, were acquired. Ten healthy individuals of similar ages, who had previously undergone the same MR exams, were selected from our database of studies, for comparison purposes.

2.2.2 Data analysis of the FFI individual and healthy controls

DTI processing was performed using the FMRIB software library (`http://www.fmrib.ox.ac.uk/fsl`). We acquired DTI-EPI images to compensate for the effect of eddy current distortions using the image registration software FLIRT. Parameter maps for mean diffusivity (MD) were determined voxel-wise using the program DTIFIT. The volumetric image was segmented into multiple cortical, subcortical and white matter regions using the software tool FreeSurfer (`http://surfer.nmr.mgh.harvard.edu/`). Segmentation labels were transferred to the DTI image volumes by aligning the unweighted EPI images to the T1-weighted volume, first by an affine registration, then by a non-linear one (FLIRT and FNIRT from the FMRIB software library). Regions of interests were selected from a sulcal-and gyral-based cortical parcellation atlas provided by Freesurfer [81], corresponding to regions reportedly involved in slow wave sleep activity [65]. The regions of interest comprised the thalamus, the superior, middle, and (opercular, orbital and triangular parts of the) inferior gyri of the frontal cortex, the cingulate gyri (divided into the main part and isthmus), the frontal middle and inferior, pericallosal and cingulate sulci, and the precuneus. For these areas, the median bilateral MD was calculated, while the structure volume was estimated using FreeSurfer. A t-statistic was calculated for the control group assuming a normal distribution and a probability that the patient observation derived from the same group was estimated, using the formula of Geissen, taking $p < 0.05$ as significant.

Sleep study of the FFI individual and the healthy controls

The FFI patient was hospitalized for two consecutive days. He was allowed to sleep ad libitum, living in a temperature (24±1 °C) and humidity (40-50%) controlled room, lying in bed except when eating, in a light-dark schedule (dark period: 11 pm-7 am). The patient was placed on a 1.800 kcal/day diet divided into three meals (8 a.m., 12 a.m., 6 p.m.) and three snacks (10 a.m., 4 p.m., 11 p.m.). The EEG activity of the FFI patient was recorded during the dark period for two consecutive days, the first night being an adaptation night, so that only the second night recording was considered for the analysis.

The case of this study has been compared with a group of 8 middle-aged, healthy males. Control subjects were selected according to these criteria: age between 45 and 55 years, no personal or family history for sleep disorders and for other medical, psychiatric or neurological disorders, drug free for at least six months. Volunteers were not sleep deprived and after an adaptation night

they were allowed to sleep at the usual bedtime. All experimental procedures were performed according to the ethical guidelines of the Ethical Committees of University of Bologna, Italy.

Sleep EEG recording and preprocessing

EEG recordings were collected by Nihon Kohden Neurofax EEG-1200 64-channels Electroencephalograph (NIHON KOHDEN CORPORATION 1-31-4 Nishiochiai, Shinjuku-ku, Tokyo 161-8560, Japan). The EEG was acquired from 21 electrodes positioned according to the 10-20 International Electrodes Placement System; each electrode was referred to a reference electrode in midline position between Fz and Cz. All signals were sampled at a frequency of 500 Hz, 16 bit resolution and 0.016–120 Hz band pass filtered.

Polysomnographic recording included two electrooculographic (EOG) channels, submental EMG, tibialis anterior bilateral EMG, abdominal effort and EKG. Signal treatment (from pre-processing to SSO wave analyses) was implemented using Matlab (MathWorks, Natick, MA, USA). All maps were obtained using EEGLAB Toolbox [82]. EEG raw data were offline re-referenced to mastoid electrodes average potential in order to obtain monopolar-like potentials [83].

2.2.3 EEG data analysis

Sleep stages (wake, N1, N2, N3 and REM sleep) were scored offline according to AASM scoring criteria [48] by visual and spectral inspection of 30 s EEG epochs. For the comparison of sleep EEGs between the FFI case and the controls, we also matched the sleep time duration of the FFI case with a portion of the control's sleep recordings: to this aim, we used only the first sleep cycle data of control subjects.

Epochs belonging to N2 and N3 stages and free from artifacts (i.e. epochs without movements or arousals) were selected for two independent analyses:

(I) Estimation of power spectral distribution of the sleep EEG signals;

(II) Detection and analysis of SSOs.

In order to identify the differences between the FFI case and the control group, for each parameter we compared the patient value to the control sample distribution, calculating its t-score.

Power spectral distribution of the sleep EEG signals

EEG power spectra related to the N2 and N3 sleep stages of each subject were calculated via periodogram (Hamming windowed Fast Fourier Transform with window length of 30 s), estimated on the corresponding EEG epochs. Spectral power of the EEG signal was calculated for all EEG electrodes in frequency bands, defined as delta (δ: 0.3-4 Hz), theta (θ: 4-8 Hz), alpha (α: 8-12 Hz) and sigma (σ: 12-15 Hz, spindle activity).

Detection and characterization of the SSOs

SSO analysis was performed on the waves detected from each EEG channel. SSOs were detected using the Likeness Method proposed by our group in previous works [13, 14]. In summary, our method detects only full-fledged SSO events, i.e. events with at least one wave that during its propagation reaches the archetypal amplitude criteria, but also allows the selection of channels containing sub-threshold SSOs that effectively completes the mapping of each propagating event. As a consequence of the typical waxing and waning behavior of SSO events, these sets of small waves often include the first and last ones occurring in the event. Specifications for the detection the of full-fledged SSO were: a) two zero crossings separated by 0.3–1.0 s, the first one having a negative slope; b) a negative peak between the two zero crossings with a voltage less than -55 μV; c) a negative-to-positive peak amplitude of at least 100 μV. Typically, these detection criteria are satisfied both by K-complexes during N2 and by slow waves during N3. Herein with the term SSOs we refer both to all waves satisfying the aforementioned criteria, and to those supplemented with our likelihood method.

The SSO behavior of each subject was characterized through the study of:

(I) the mean rate of SSOs occurrence;

(II) the scalp distributions of the origin sites, and of waves detection;

(III) a set of morphological features that specify the waves shape;

(IV) the SSO positive phase ability to group the spindle activity by the SSO positive phase.

Within each SSO event, we used the delays between the wave negative peaks to identify the origin site: the electrode with the earliest negative peak indicated the origin site of the event. As far as the wave shape is concerned, we had previously

defined seven morphological features that fully characterize the morphology of each SSO [13] (see Figure 2.1 and 2.2]: three amplitude features [N (negative peak) amplitude; P (positive peak) amplitude; NP (negative-to-positive peak) amplitude], two time features (the interval between the negative peak and positive peak - NP time; the first zero crossing to negative peak time - ZN time), and two steepness features (the slope of the signal between the first zero crossing and the negative peak - slope 1; the slope between the negative peak and the second zero crossing - slope 2).

Here, we considered an additional feature in the frequency domain that we named spindle grouping, namely an estimate of the change of the σ activity (12-15 Hz) passing from the downstate to the upstate of each SSO. To this aim, power estimates were calculated by using a Hamming windowed FFT with a window length of 500 ms: downstate power estimate was derived centering the FFT on the negative peak, while the upstate window was centered on the positive peak of each SSO (T1 and T2 time windows in Figure 2.8 and 2.9, respectively. We defined the spindle grouping as the difference between the positive peak σ power and the negative peak σ power.

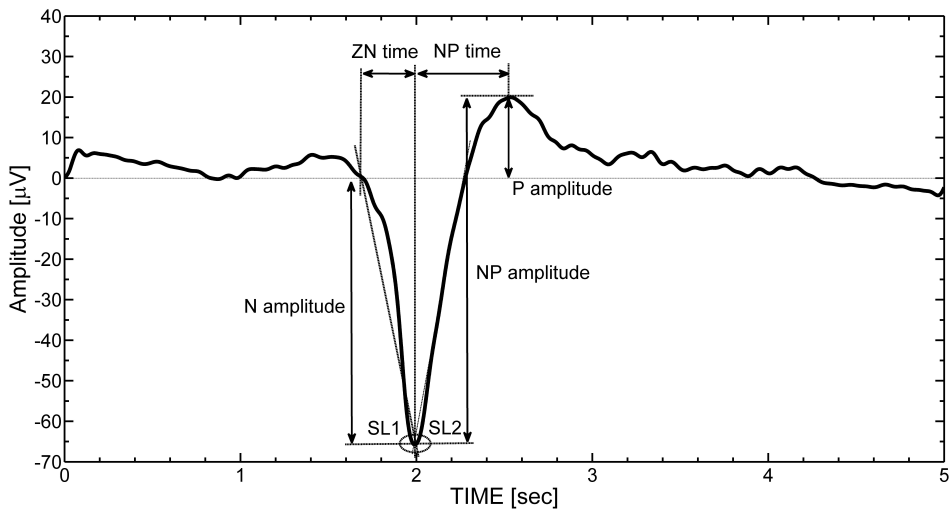

Figure 2.1. SSO template of control subjects. SSO template illustrating the seven morphological features of control subjects.

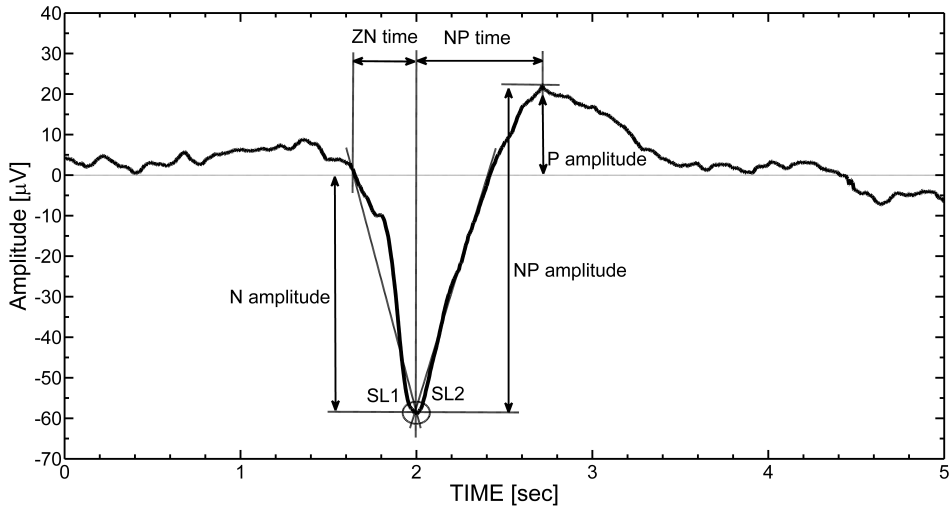

Figure 2.2. SSO template of FFI patient. SSO template illustrating the seven morphological features of FFi patient.

2.3 Results

2.3.1 Neuroimaging study

In two out of 14 selected regions of interest the patient demonstrated a mean diffusivity (MD) value significantly outside the distribution of the controls: in the thalamus (0.819×10-3 mm^2/s against controls mean±SD 0.779±0.015 ×10-3 mm^2/s; p=0.03) and in the cingulate (0.825×10-3 mm^2/s against controls 0.794±0.009 ×10-3 mm^2/s; p=0.013) MD was elevated in the patient. The volume of these and all others structures selected was normal compared to the healthy controls ($p > 0.05$; data not shown).

2.3.2 Changes of macrostructure and power spectrum in NREM sleep of the FFI patient

In the FFI patient, the polysomnographic analysis shows a marked reduction of total sleep time and a severe alteration of the cyclic sleep organization. Typical NREM sleep graphoelements (K-complexes, delta waves and sleep spindles) were markedly reduced with a predominance of stage 1 sleep intermixed with REM sleep with and without atonia. Thus, no physiological sleep cycles were identifiable in the FFI patient and 40.8 min of N2 sleep stage and 39 min of N3 sleep stage

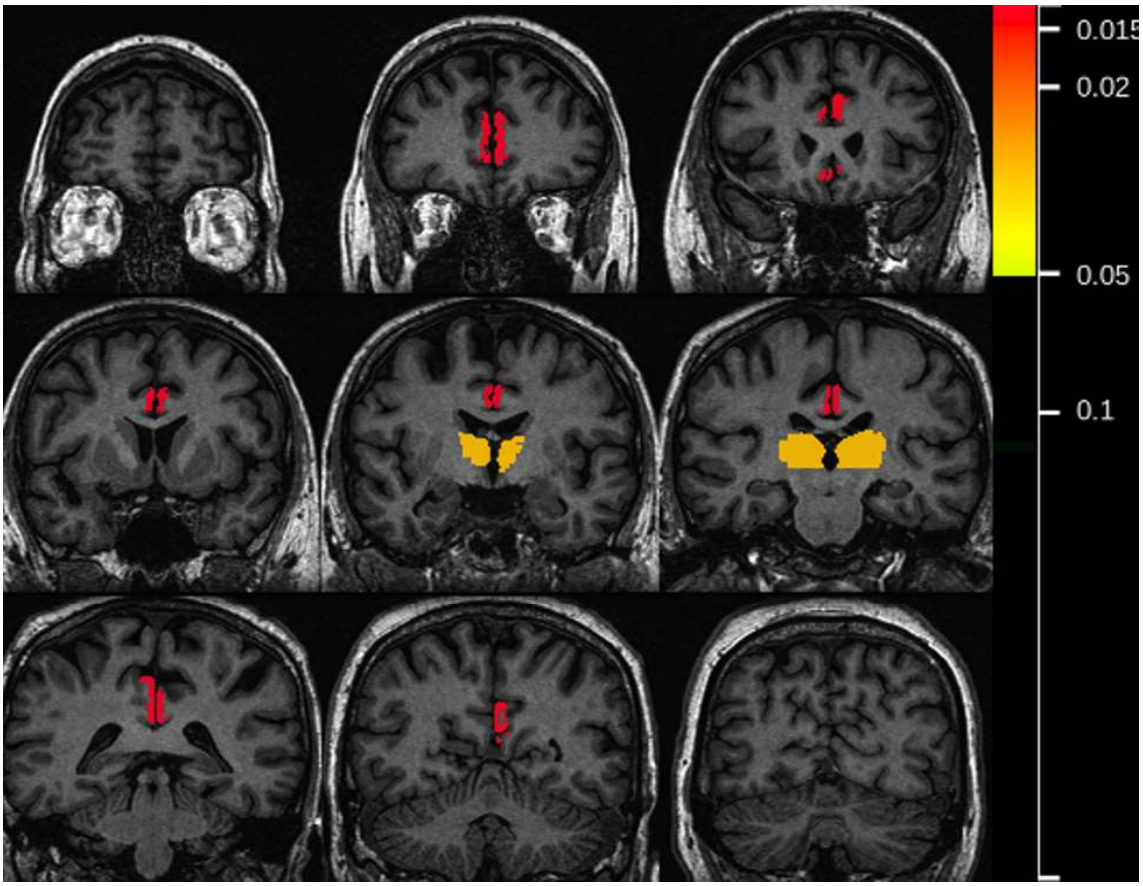

Figure 2.3. MRI study of FFI patient. The regions of interest for which patient's MD was significantly altered with respect to controls are shown, displayed as p-values (see color scale at right), back projected onto ROIs selected by FreeSurfer, superimposed on T1 coronal images of patient. The figure highlights a bilateral involvement of thalamus and cingulate cortex.

were derived from the whole night recording. Figure 2.4, bottom panel, shows the FFI patient sleep structure during the night compared to that of a representative healthy control (upper panel).

All controls showed a physiological sleep EEG pattern, reaching the deepest stages of NREM sleep (stage N3, or SWS), with K-complexes, spindles and delta waves. The sleep staging allows the recognition of the first cycle for each individual (Figure 2.4). In healthy controls NREM stage durations of the first sleep cycle were on average: 32 (SD 16) min for N2 stage and 32 (SD 11) min for N3 stage.

As far as the power spectral distribution of the sleep EEG signals is concerned, delta and sigma activity during both N2 and N3 stage were significantly lower in the FFI patient with respect to controls (Figure 2.5); this considerable reduction was

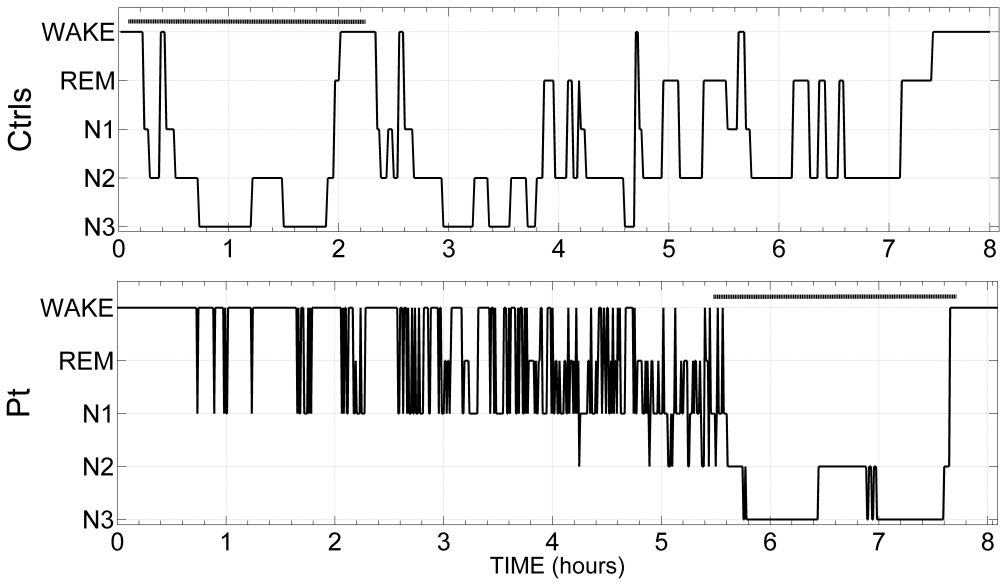

Figure 2.4. Hypnogram comparison. Hypnograms of the FFI patient (bottom panel) and of a representative healthy control (upper panel). The dotted lines cover the NREM sleep epochs used for the analysis of both power spectrum and SSO features. N1, N2, N3 (Slow Wave Sleep) indicate sleep stages according to AASM scoring criteria.

detected in all cortical areas ($p < 0.05$ for all electrodes). It is worth nothing that the physiological increase of delta activity from shallow to deep sleep observed in controls is also present in the FFI individual; at variance, sigma activity does not show any change, shifting from N2 to N3. No significant changes have been observed for theta and alpha activities, which seem to be spared by thalamic neurodegeneration (Figure 2.5).

2.3.3 Sleep Slow Oscillation changes in the FFI patient

The rate of SSO events during both N2 and N3 stage were significantly lower in the FFI individual with respect to controls (Figure 2.6). The SSO detection rate showed, like for delta activity, a relative increase from N2 to N3 stage both for the FFI individual and the controls.

The reduction of SSO detection rate observed in the FFI individual uniformly encompassed all cortical areas. As a result the scalp distribution of SSO origins and detections in the FFI individual remained unaltered with respect to healthy controls: the origins were mainly detectable in frontal areas while detections were

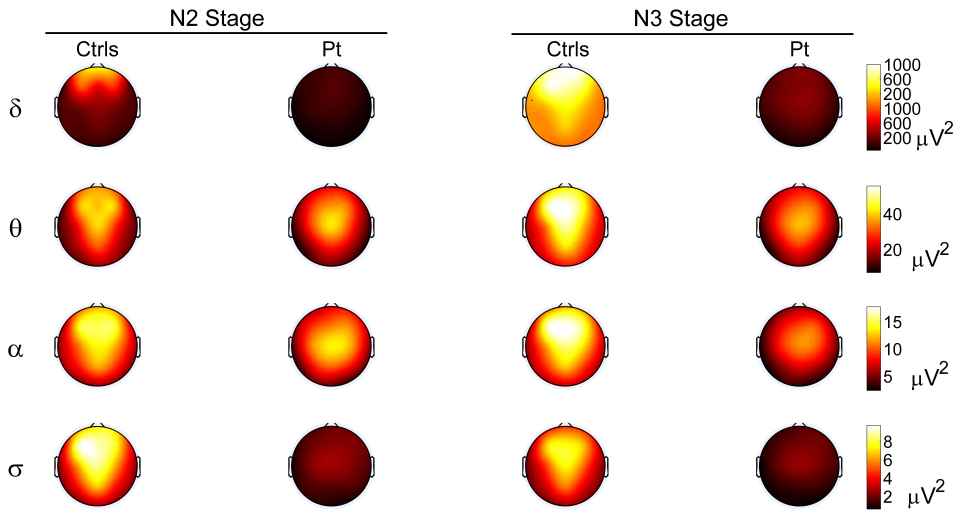

Figure 2.5. Power spectra topology. Topological characterization of sleep EEG power spectra for controls (Ctrls) and FFI patient (Pt) in N2 and N3 stages. Each row corresponds to a power band: delta (δ: 0.3-4 Hz), theta (θ: 4-8 Hz), alpha (α: 8-12 Hz) and sigma (σ: 12-15 Hz). Powers are expressed in μV^2.

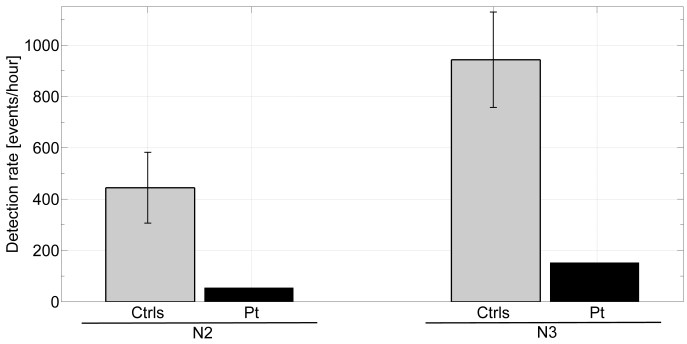

Figure 2.6. SSO event detection rates. SSO event detection rates for the controls (Ctrls) and the FFI patient (Pt) in N2 and N3 stages. For the controls, the bar indicates the group average with the corresponding confidence interval (p=0.95).

maximal over medio-frontal and parietal areas (Figure 2.7).

The analysis of wave shape highlighted two distinct morphological changes: the FFI individual had a mean NP time increase ($p < 0.001$) and a mean slope 2 reduction ($p < 0.01$), as can be seen from the Table 2.1.

Figure 2.8 and 2.9 illustrates the pathognomonic feature occurring in the SSO, with respect to the grouping effect of the positive peak on spindles (sigma activity). In healthy controls the superimposition of raw data (Fz electrode) to the same EEG epoch filtered in delta and sigma bands highlights a specific temporal link between the SSO positive peak and the crowning spindle (Figure 2.8). In the FFI

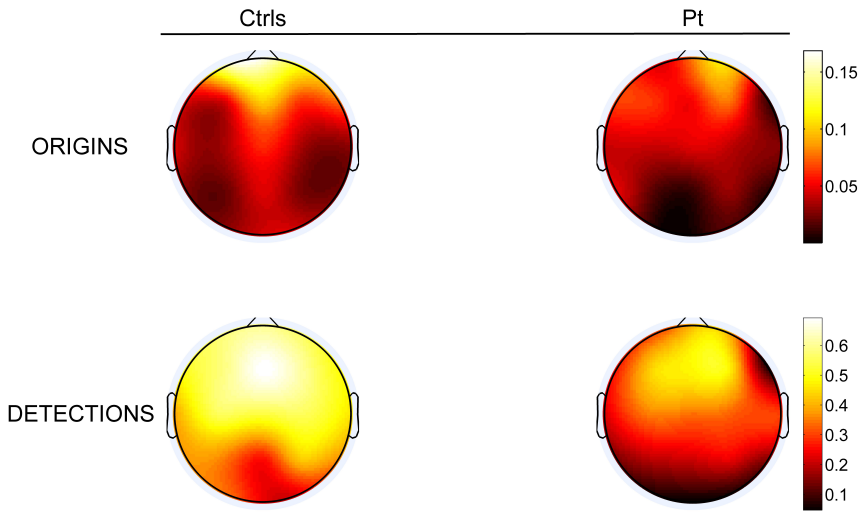

Figure 2.7. SSO origin and detection maps. SSO origin and detection maps for the controls (Ctrls) and the FFI patient (Pt). For Ctrls, the figure shows the grand-mean of the maps over individuals. Each map represents the frequency (reported as percentage) of SSO event origins or SSO detections for each electrode.

Features	Ctrls mean (SE)	Pt mean	p-values
NP amplitude (mV)	96.3 (5.5)	84.2	NS
N amplitude (mV)	-65.5 (4.7)	-56.6	NS
P amplitude (mV)	34.9 (3.1)	29.1	NS
NP time (ms)	490.2 (18.5)	612.6	< 0.001
ZN time (ms)	268.6 (8.2)	280.6	NS
Slope 1 (mV/ms)	-0.241 (0.01)	-0.224	NS
Slope 2 (mV/ms)	0.218(0.014)	0.147	< 0.01

Table 2.1. Morphological comparison of SSOs. Mean values of each morphological feature of SSO for the control group (Ctrls) and the FFI patient (Pt). SE stands for standard error.

individual this association was undetectable (Figure 2.9).

The lack of grouping effect on spindle activity sustained by the SSO positive peak in the FFI individual shows a specific scalp distribution. As depicted in Figure 2.10, in the FFI individual the reduction of sigma activity encompassed all electrodes with a greater impairment in frontal leads.

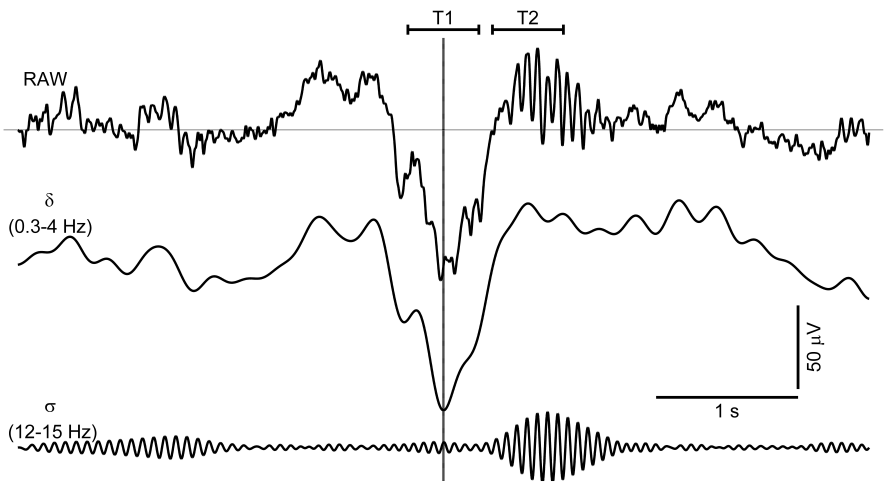

Figure 2.8. Frequency decomposition of a raw EEG epoch from Fz lead containing a SSO of a control subject. Upper trace is the raw signal, the intermediate one is the signal in the delta band (δ, 0.3-4 Hz) and the lower the signal in the sigma band (σ, 12-15 Hz). Bandpass filtered signals have been derived using a Chebyshev II filter with no attenuation at pass-band and -60 dB at the low and high stop-bands. T1 and T2 are 500 ms widows encompassing the SSO negative and positive peak, respectively, used for the spectral analysis of sigma activity for each electrode (see Figure 2.10).

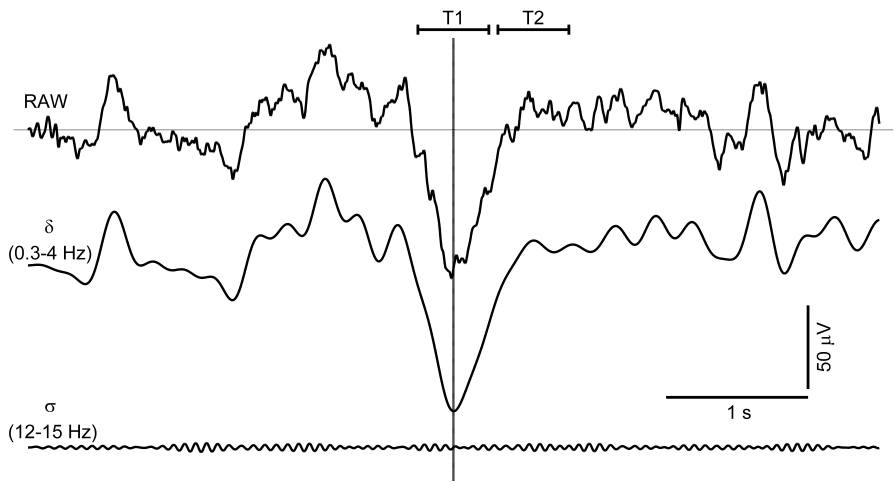

Figure 2.9. Frequency decomposition of a raw EEG epoch from Fz lead containing a SSO of FFI subject. Upper trace is the raw signal, the intermediate one is the signal in the delta band (δ, 0.3-4 Hz) and the lower the signal in the sigma band (σ, 12-15 Hz). Bandpass filtered signals have been derived using a Chebyshev II filter with no attenuation at pass-band and -60 dB at the low and high stop-bands. T1 and T2 are 500 ms widows encompassing the SSO negative and positive peak, respectively, used for the spectral analysis of sigma activity for each electrode (see Figure 2.10). The lack of crowning spindle in the FFI patient is clearly depicted.

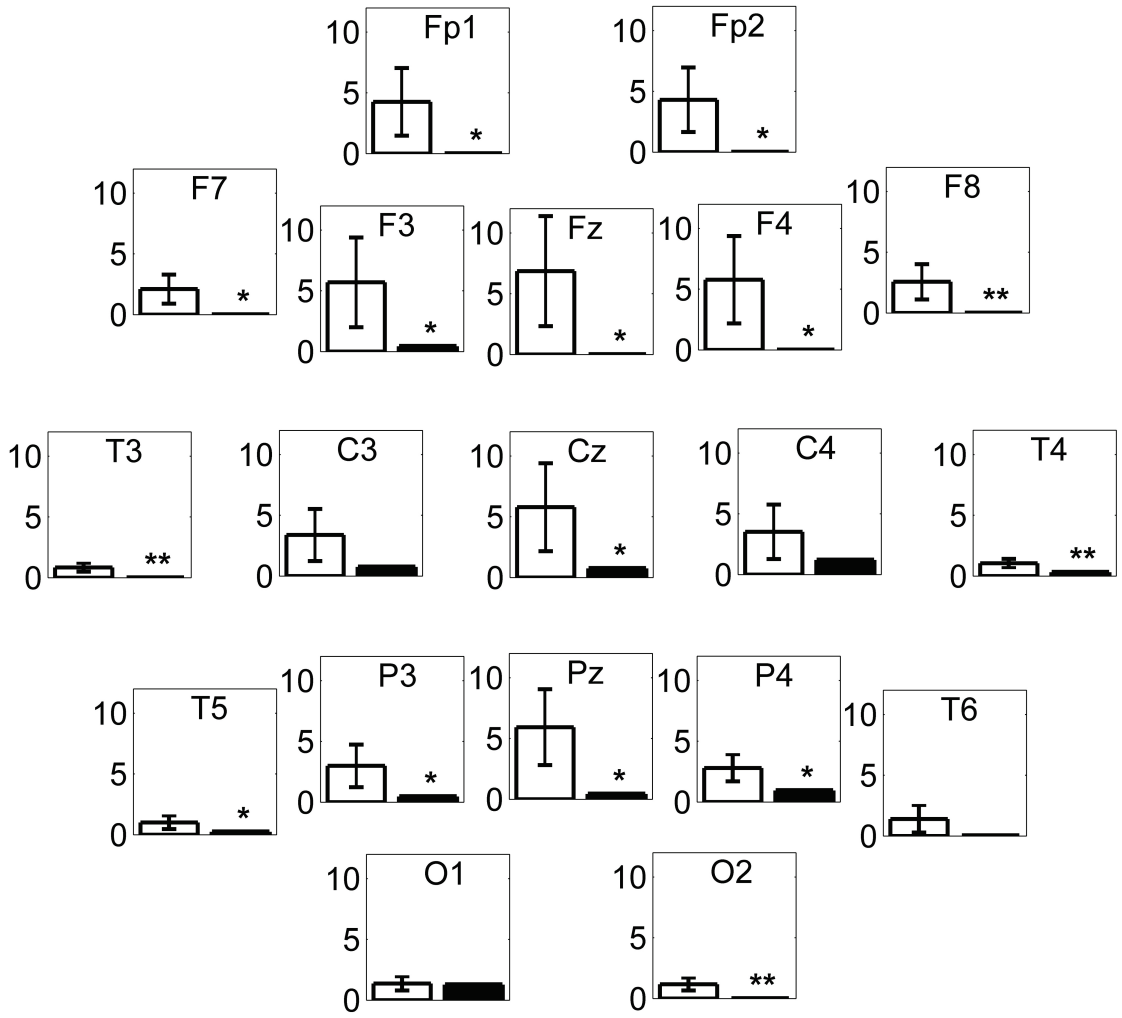

Figure 2.10. Spindle grouping maps. Spindle grouping, as the difference, expressed in μV^2, of sigma powers between up and down states of each SSO, for each lead in controls (white bars) and FFI patient (black bars). For controls, the bars indicate the group average with 95% confidence interval. Asterisks indicate significances of sigma grouping between controls and FFI patient ($* : p < 0.05$, $** : p < 0.01$).

2.4 Discussion and conclusion

The present study shows that in one D178N–129M FFI individual, at middle stage of the disease, the SSO behavior was impaired. The SSO changes seen in the patient were a severe reduction in rate, distinct shape alterations as well as an impairment of the grouping effect on spindle activity.

Our patient had the typical rapid course of the D178N–129M type of FFI characterized by loss of sleep and disturbances of autonomic functioning followed by mild somatomotor abnormalities. This clinical picture corresponds to the neuropathologic hallmark of FFI [73, 84, 85] that is a severe atrophy of the anterior ventral and mediodorsal thalamic nuclei with loss of 80% to 90% of the neurons and two-to-three fold increase in astroglial cells, whereas spongiosis is conspicuously absent. The other thalamic nuclei are less and inconsistently affected whereas atrophy of the inferior olives is also commonly found. The involvement of other brain regions, particularly the cerebral cortex, is a function of the disease duration, which, in turn, is largely related to the genotype at codon 129 PRNP. For instance, the neocortex is affected by spongiosis, gliosis, and, to a lesser extent, by neuronal loss, only in cases of more than 18 months' disease duration [85].

Thus, we can consider our short duration case of FFI, evaluated 5 months after the onset of the disease, as a good model of a selective thalamic dysfunction. This was confirmed by DTI study that showing microstructural degenerative alterations without volume changes only in the thalamus and cingulate, it repeated the results obtained with PET (18 FDG-PET) in a group of FFI patients and healthy carrier of D178N–129M genotype [79, 80].

This study was based on comparisons between the case and a group of age-matched healthy controls. Concerning the significant SSO changes, despite the fact that in general multiple testing could imply the increase of false positive errors, in this case no correction had to be done, since we kept under control the false positive probability of each single test (i.e. the probability of mis-indicating as significantly changed a certain variable). In other words, we did not have to control the probability of having mis-classified one or more features among the set of the tested ones.

We confirmed deficits in delta and spindle activity of the FFI patient. These results are in line with the well-known assumption that the thalamus has a critical role in the generation of typical graphoelements of SWS, such as spindles (sigma activity), K-complexes and delta waves (delta activity). Remarkably, the data on the role of the thalamus in the physiology of SSO has so far been less consistent.

The hypothesis of SSO as being a purely cortical phenomenon is supported by the following:

(I) transections of the cortico-thalamic afferents abolish SSO in thalamo-cortical cells and NRT neurons [86, 87];

(II) athalamic animals keep on expressing SSO [20];

(III) the discovery of intrinsically oscillating neurons in layer V and IV [88].

In order to identify, in humans, a thalamic role in SSO behavior, we herein statistically characterized the spontaneous SSO activity in one D178N–129M FFI individual, compared with 8 age/gender-matched non-deprived volunteers. The descriptive statistics shown in Table 2.1 constitute, up to our knowledge, the first result for FFI, with the limitations deriving from being a single-case study. The FFI individual showed a dramatic lower rate of SSO events during NREM stages N2 and N3. The study of both origin and detection scalp distributions indicates that also in the FFI individual the frontal area network is more prone to produce SSOs than networks in the posterior and temporal areas. The finding of a similar mean event size in the FFI individual compared to controls also indicates that the SSO spreading capability is spared by the thalamic neurodegeneration. This is in line with data showing that the cortical travel is mainly sustained by cortico-cortical mechanisms [89].

In the FFI case the wave shape has shown specific morphologic alterations such as NP time increase and slope 2 reduction, which could be related to a reduced thalamic synchronization on the cortical neuronal pool coming out from the downstate of the SSO [90, 51].

Finally, our results in the FFI individual show a consistent lack of spindle activity concurrent with the depolarizing phase of SSO, which is in turn consistent with thalamo-cortical cells impairments in oscillating in spindle frequency, and hence reverberating it on the cortex through thalamo-cortical volleys. Actually, both animal and human data indicate that SSOs have the capability of grouping spindles [26, 12]. These studies demonstrate that the depolarization of neocortical pyramidal cells during the up-state drives the generation of spindle oscillations in thalamo-cortical feedback loops. Our data are thus consistent with the observations that (i) in athalamic animals SSO is still present at a cortical level while spindles are suppressed [86]; (ii) in animal models ibotenic acid selective lesions of the dorsomedian thalamic nuclei induce a loss of sleep spindles [91].

As depicted in Figure 2.10 we have also identified a topological alteration of sigma activity grouped by the SSO up-state. The more dramatic reduction has been observed in frontal electrodes, which detect neural activity modulated by thalamic volleys starting from anterior and dorsomedian thalamic nuclei. As aforementioned, these nuclei are selectively degenerated in FFI [92, 93]. Based on studies using in vivo and in vitro techniques, the dorsal thalamus is known to play a key role in the generation of spindles [94]. In particular, sleep spindles seem to be affected by stereotactic lesions in medial thalamic structures in humans; moreover, spindle activity in the cat was modified by lesioning the dorsomedian thalamic nucleus [91]. We cannot exclude that loss of sleep spindles in FFI could be associated also to the neurodegeneration of the nucleus reticularis [93]. It is difficult to precisely ascertain to what an extent this nucleus is affected in FFI. Anatomical connections between the reticularis and the dorsomedian thalamic nucleus have been traced: in particular, this nucleus receives afferents from the oral pole of the reticular nucleus [95]. Therefore, degeneration of the dorsomedian thalamic nucleus could be in itself responsible for the loss of spindling activity in FFI, either isolated or crowned on the depolarizing phase of SSO.

In our patient, these SSO changes seem to be related to specific structural and selective thalamic alterations or to its functional effect on the cingulate [79, 80], as indicated by DTI and Spectroscopy MRI.

Conclusions

Given the limited research available in humans, we can only speculate about the mechanisms mediating thalamic reticular nucleus and thalamo-cortical nuclei deficits in FFI underlying alterations of cortical SSO behavior. Recently, a review [29], mainly focused on electrophysiological recordings in animals, stated that *"slow oscillation originates from the dynamic interplay of three cardinal oscillators: the synaptically based cortical oscillator and two thalamic oscillators, the thalamocortical and NRT neurons"*. Our data support this hypothesis of a bidirectional cortico-thalamic interplay in generating and modulating the SSO features.

Future studies will be needed to establish whether SSO deficits are present in other neurologic disorders, including unilateral and bilateral thalamic strokes. These conditions, together with the FFI studied herein, represent the only available human models for studying a thalamic-lesion effect on sleep, and in particular on SSOs. Such studies, while contributing to unravel the SSO mechanisms in humans, will help in establishing new diagnostic and therapeutic approaches

that may ameliorate both symptoms and SSO activity in FFI patients. Possible approaches consist in techniques that have been shown to increase SSOs rate production, such as (i) transcranial magnetic stimulation in combination with high-density EEG and fMRI will be needed to evaluate the functioning of cortico-thalamic reticular nucleus-thalamic-cortical loops in FFI; (ii) transcranial direct current stimulation for evoking SSOs [44]. Finally, the results obtained in this single case study, with relative speculations, also suggest that the study of SSO in presimptomatic FFI carriers can represent a useful tool for the early identification of preclinical thalamic dysfunctions.

Chapter 3

Mapping the sleeping brain while quenching sensory processing

During non-REM sleep the largest EEG response evoked by sensory stimulation is the K-complex (eKC), composed of an initial positive bump (P200) followed by a bistable cortical response: a giant negative deflection (N550) and a large positive one (P900), respectively reflecting down states and up states of <1Hz oscillations. Sensory-modality-independent topology of N550 and P900, with maximal detection rate on fronto-central areas, has been consistently reported, suggesting that sensory inputs arise to the cortex avoiding specific primary sensory areas. However, these studies neglected latencies of all KC components as a function of electrode sites. Our aim is to identify, component by component, which topological/dynamical properties of eKCs depend on stimulus modality and which are mainly related to local cortical properties. We measured temporal and morphological features of acoustic, tactile and visual eKCs to disentangle specific sensory excitatory activities from aspecific responses due to local bistability proneness, measured by means of N550 descending steepness (synchronization in falling into down state). While confirming the sensory-modality independence of N550 and P900 topology with maximal detection rate in fronto-central areas, four main original results emerge from this study: (i) the topology of P200 latency depends on the sensory modality with earliest waves in the stimulation-related primary sensory areas; (ii) P200 rapidly travels as a cortical excitation; (iii) P200-like excitations when KCs are not evoked are detected over the scalp with significantly smaller amplitudes in fronto-central areas, compared to eKC P200s; (iv) N550 latency mirrors its mean local steepness which is function of topological proneness to bistability. From these results we can describe the emergence N550/P900 complex

as the interplay between a waxing P200 cortical travel and higher fronto-central proneness to bistability. In conclusion, eKCs exhibit a physiological dichotomy: P200 acts as a traveling cortical excitation whose function is to induce the bistable cortical response (N550/P900), which in turn is crucial for maintaining sleep and unconsciousness.

3.1 Introduction

It is widely known that the sleeping brain reacts to simple sensory stimuli with stereotypical EEG responses [36, 96]. After state-independent early phases of processing related to synaptic excitation from afferent thalamic inputs, sensory stimuli during non-rapid eye movement (NREM) sleep trigger a pattern composed of 3 distinctive waves:

- a positive component (**P200**) at the conventional latency of 200 ms;
- a giant negative component (**N550**) at the conventional latency of 550 ms;
- a positive component (**P900**) at the conventional latency of 900 ms.

P200 amplitude increases from wakefulness, light sleep, to deep sleep [97, 98, 99], while the biphasic component of N550 and P900 waves is strictly related to NREM sleep [100]. The whole complex has been named K-complex (KC) in the electroencephalogram (EEG) jargon, and can be triphasic [101], namely when P200 is detected and considered, or biphasic when P200 is undetectable or overlooked [50, 102].

Not only are KCs elicited by sensory stimuli, but they normally also spontaneously arise in the cortical mantle [103]. Spontaneous and evoked KCs and the Sleep Slow Oscillation (SSO, i.e. less than 1Hz oscillations) spontaneously occurring in Slow Wave Sleep stem from the same cellular dynamics [83, 39]: membrane potentials of large cortical neural assemblies intermittently switch between K+-dependent hyperpolarization (down state) with neuronal stillness and depolarization with strong synaptic activity (up state) [53, 17, 104]. The giant N550 deflection is generated by the down state, while the following positive P900 bump reflects the up state [37].

Many studies have established that evoked KCs (eKCs) from different sensory modalities (i.e. acoustic, respiratory occlusion, tactile, visual) result in superimposable topologies of cortical detection of N550 and P900, with amplitudes

symmetrically distributed over the scalp, invariably with a maximum on fronto-central areas [105, 106, 101]. However, these studies did not take into account the possible different latencies of KC components as a function of electrode sites. Here we investigate whether latencies are more specific than amplitudes as markers of wave source localization over the cortex in order to map a sensory-modality-dependent cortical response.

Methodologically, focusing on latencies requires the study of the topology of cortical activity in many different time points. As a result, our sensory mapping is naturally dynamic, allowing a study of KCs as *traveling waves*, a property well established for SSOs [11, 13]. As early stated, KCs and SSOs share the same cellular mechanisms, so it is expected that also eKCs could propagate over the cortex from distinctive sites of origin. An indication of this property has been reported in cats: sensory stimuli administered during sleep induced a localized response in cortical areas receiving sensory-specific thalamic projections that subsequently propagated on cortical mantle [38] That study was based on recordings obtained via implanted electrodes.

Thus, the aim of the study is to identify, component by component, which topological and dynamical properties depend on the stimulus modality and which others are mainly related to local cortical properties. In particular, focus will be on the spatiotemporal properties of eKC components in order to verify propagation mechanisms and to see which component propagation is real or apparent. We will look for causal relations in the propagation patterns to see, component-by-component, and modality-by-modality (acoustic, tactile and visual stimuli), whether detected propagation is caused by a real wave of excitation or it is mainly apparent, i.e. caused by independent interactions with gradients of the local cortical proneness to bistability. We will also discuss our results in terms of relationships between eKCs components and sensory processing, and in particular how the human sleeping brain quenches consciousness of sensory stimuli.

3.2 Methods

3.2.1 Participants and experimental protocol

Fourteen healthy volunteers (right-handed males, age 20–26 years) participated in this study and gave their informed consent. No one reported history of medical diseases and of psychiatric and neurological disorders, nor audiological or visual deficits. Subjects were instructed to avoid alcohol and caffeine starting from 24

hours before the experiment. Each of them spent two consecutive nights in the sleep laboratory, the first as adaptation night. High-density sleep EEG recordings were collected in the second night during which subjects underwent sensory stimulations during NREM sleep stages.The Ethical Committee of Pisa University approved this study.

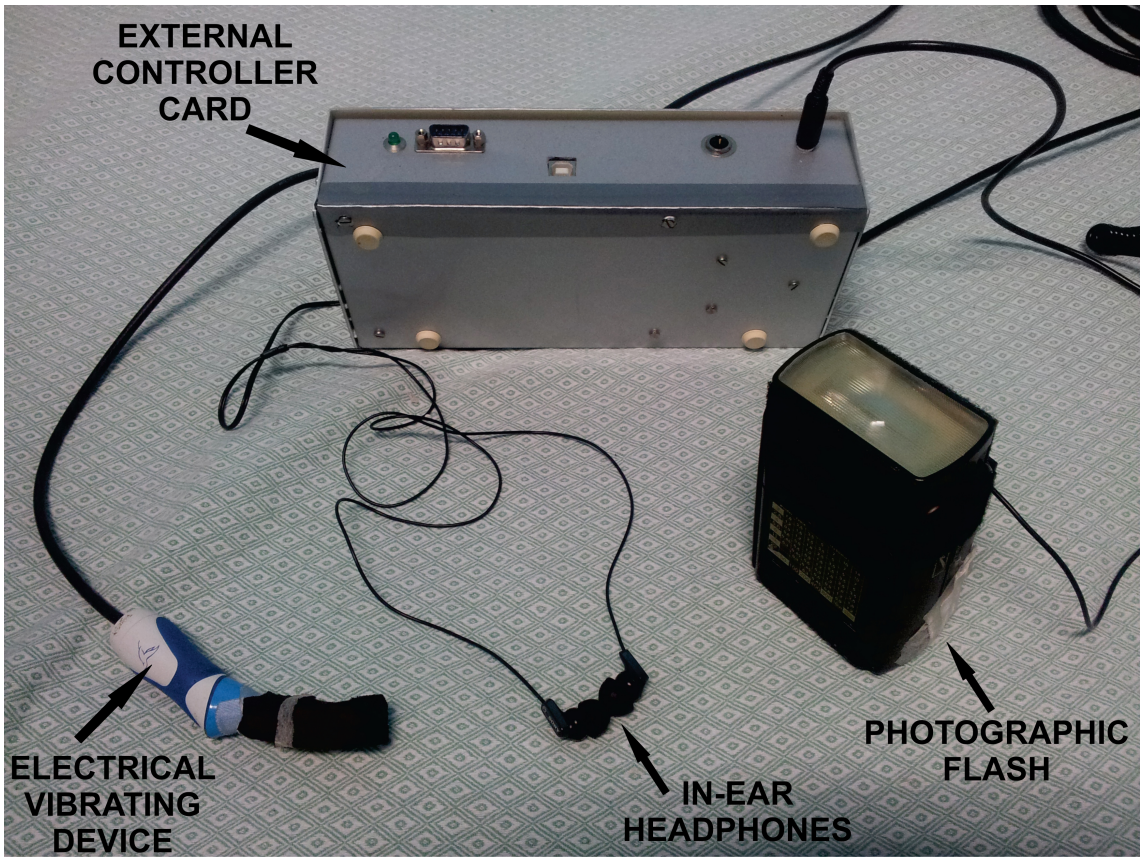

Figure 3.1. Dedicated hardware system for stimuli administration. The system is composed by: a external controlling card connected with Personal Computer, a photographic full-field flash, some in-ear headphones and a vibrating motor. The three stimulus actuators are controlled by the external card.

The experimenter performed real-time EEG visual scoring in order to establish current sleep stage. Stimulation was carried out during N2 and N3 stages, except interruptions during awakenings and arousals, and consisted in sequences of random-ordered auditory, tactile and visual stimuli having inter-stimulus interval between 15 s and 20 s, sampled from a uniform distribution.

Acoustic stimuli were pure tones of 1000 Hz lasting for 50ms (5ms rise and fall times), and they were delivered through in-ear headphones (XBA, Sony)

at an intensity of 60 dB sound pressure level. Tactile stimuli were mechanical vibrations (pallesthesia) of 300 Hz (50 ms duration; 20 ms rise and fall times) delivered through electrical vibrating device placed on the middle finger of the right hand. Visual stimuli consisted in a light flash (<1 ms duration) delivered with a photographic flash (32 Z − 2, Metz), oriented to the room ceiling. The administration of stimuli is controlled by a dedicated PC, it is also developed an ad-hoc software that controls a external electronic card, and the stimulus actuators is controlled by this card (see Figure 3.1).

3.2.2 High-density EEG recording

High-density EEG recordings were carried out using the Net Amps 300 (GES300; Electrical Geodesic Inc., Eugene, OR, USA) with 128-electrodes HydroCel Geodesic Sensor Nets. The Electrical Geodesic system adopts the vertex electrode (Cz) as the on-line recording reference. Electrode impendence values were maintained below 50 KOhm. Data were collected using the Net Station software, Version 4.4.2, (Electrical Geodesic Inc., Eugene, OR, USA) in the 0.01–500 Hz band, with 500 Hz sampling rate.

3.2.3 Data analysis

Selection and features of evoked K-complexes

EEG data were off-line re-referenced to the average potential of the mastoid electrodes in order to obtain monopolar-like potentials [11]. Off-line sleep staging was performed according to AASM scoring criteria [48] by visual screening in the time and frequency domain of 30 s EEG epochs. Epochs contaminated by artifacts (e.g. movements, muscle contraction) were discarded from following analysis. Then, in each artifact-free EEG epoch, we rejected from the analysis individual channels with low quality signal [14] and we selected trials of eKCs satisfying two criteria: 1) full-fledged, i.e. fulfilling the detection criteria of spontaneous SSOs [14] and; 2) temporally-isolated, i.e. without any spontaneous SSO event occurring from 3s before to 4s after the eKC negative peak (N550).

Each full-fledged and isolated eKC was characterized by means of three morphological features [25]: the peak-to-peak amplitude (NP amplitude), the slope of the signal between the first zero crossing and the negative peak (Slope 1) and the slope between the negative peak and the second zero crossing (Slope 2). Each eKC

response was also segmented in order to study the dynamics of its main components [107, 108]; for each eKC we extracted the P200 (maximum local positive peak between 220-350 ms), the N350 (minimum local negative peak between 300-450 ms), the N550 (minimum local negative peak between 450-750 ms) and the P900 (maximum local positive peak between 700-1400 ms).

In order to complete the description of the sleeping-brain behavior when the cortex interacts with an excitatory stimulus, we also studied EEG traces following stimuli not evoking KC (for brevity we use herein the acronym of non-evoked K-complex, **N-eKC**). In order to have a clear distinction between eKCs and N-eKCs, we made a further selection to avoid sub-threshold eKCs. To this aim we only considered the events with no trace of KC that effectively corresponded to negative deflections smaller, in absolute value, than 10 μV in the interval 0-750 ms after the stimulus. By construction, N-eKCs did not have the N550/P900 component complex; thus the segmentation procedure was applied only for the P200 component. All analyses have been performed by using Matlab (MathWorks, Natick, MA, USA), while scalp maps were obtained using EEGLAB Toolbox [82].

Propagation of evoked K-complexes

In principle, both geometrical (the distance from the stimulus-specific sensory areas) and local (the proneness to bistability) properties could generate delays in eKC waves detected under different electrodes. In order to highlight the effect of geometrical vs. local factors we adopted two sorting criteria for electrodes: (i) the distance from primary sensory areas; or (ii) the local proneness to cortical bistability indicated by Slope 1. Thus, we considered: (1) the latency distance scatter plot; (2) the latency-Slope 1 scatter plot. Finally (3), we performed the comparison of latencies between primary sensory areas and other cortical regions as a function of sleep stage.

1) The latency-distance scatter plot was defined using the averaged latency of each electrode in the x-axis and the electrode distance from primary sensory areas in the y-axis. The distance was defined as the Euclidean distance (by using the 3-D coordinates of electrodes) between each electrode site and the geometric centroid of the set of electrodes over each primary sensory area. For acoustic stimuli we had two centroids corresponding to the bilateral cortical projection of primary acoustic areas. In this case we selected the minimal distance. We based the electrode localization on a three-shell spherical head model registered to the Talairach stereo-tactic space available as a digitized MRI (MNI305) from

the Montreal Neurological Institute [109]. Electrodes related to acoustic stimuli were over the 41 and 42 Broadman areas (BA), electrodes related to tactile stimuli were over the 3, 1, and 2 BA and electrodes related to visual stimuli were over the 17 and 18 BA. For each latency component, the latency-distance scatter plot was used to evaluate the consistency of a cortico-cortical propagation model from the primary sensory areas to adjacent ones over large cortical territories, and, in case of consistency, to estimate the component propagation speed. The consistency of the surface propagation model was indicated by the goodness (r^2, with the corresponding p-value) of the linear regression with latencies as independent variable and distances as dependent one (robust fit performed with a bisquare weighting function), while the speed of propagation corresponded to the slope of the fit. Only positive slope correspond to causal excitation transport. The significance alpha level of regression was set to 0.05.

2) The latency-Slope 1 scatter plot was defined using the averaged latency of each electrode in the x-axis and the averaged values of Slope 1 for each electrode in the y-axis.Further analysis is the same as for latency-distance scatter plot with the difference that proneness-driven apparent travel corresponds to negative slope of the linear regression of the plot: longer (shorter) delays are expected in sites with lower (higher) proneness to bistability, i.e. with lower (higher) values of Slope 1.

3) The comparison of latencies between primary sensory areas vs. other cortical regions was performed with a analyses of variance (univariate analysis of variance, with significance level set to $p = 0.05$) to model the latencies of each eKC component as a function of three between-subject factors (volunteer, 14 levels; sleep stage: N2 or N3; sensory modality of stimulation: acoustic, tactile or visual) and a within-subject factor (electrode site: over primary sensory areas or over other cortical regions with respect to each type of stimulations). All the data were previously tested (Lilliefors test) for normality of distribution. The usage of analysis of variance allowed further confirmation of components deriving from primary sensory areas and of those mainly depending on local cortical properties, which could also depend on sleep deepening.

3.3 Results

Whole-night EEG recordings were performed on fourteen subjects reaching the deepest stages of NREM sleep, with spontaneous KCs, spindles and delta waves. During N2 and N3 sleep stages we delivered to each subject 160±90

acoustic stimuli, 180±80 tactile ones and 200±100 visual ones (mean ± SD). Only a portion of delivered stimuli successfully evoked KCs: on average (mean ± SD), for each subject, acoustic stimuli evoked 92±50 KCs, tactile stimuli evoked 42±30 KCs and visual stimuli evoked 35±25 KCs. Among eKCs, we selected the temporally-isolated ones (see Methods for definition of isolated eKCs) for the following analysis resulting in the following numbers of isolated eKCs: 47±30 for acoustic stimuli, 25±18 for tactile ones and 16±9 for visual ones. Here the mean is intended over subjects (± SD).

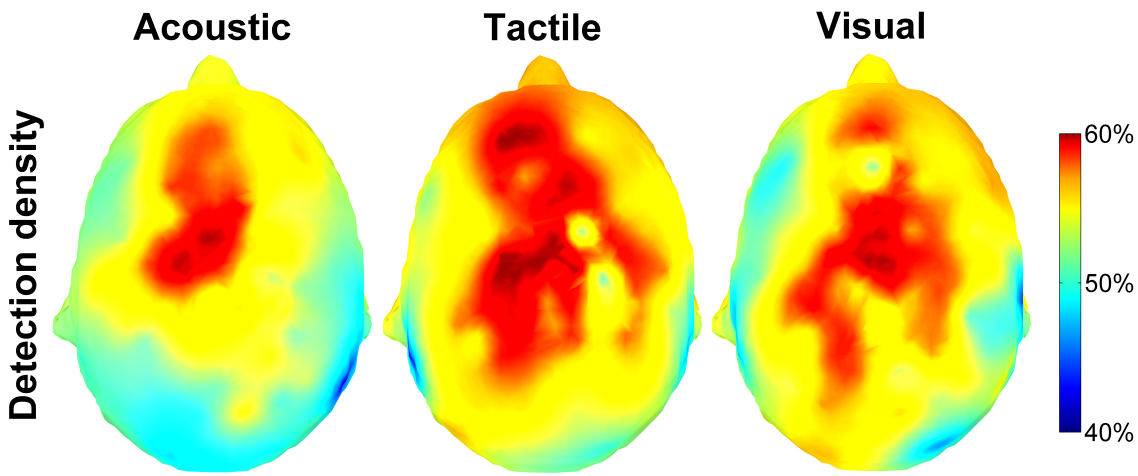

Figure 3.2. Detection density map of evoked K-complexes. The detection density map illustrates the probability of detecting the eKC shape under each electrode, for each sensory stimulation modality (% of eKC events affecting each electrode). Irrespectively from the stimulation modality, almost 60% of eKCs were detected over the fronto-central regions.

Among the traces not showing a full-fledged KC (N-eKC), only a subset did not show any trace of bistability, i.e. with a very small negative deflection of N550 ($> -10\mu$V): on average (mean ± SD), for each subject we obtained 22±13, 42±24 and 32±25 N-eKCs for acoustic, tactile and visual stimuli, respectively.

Maps of eKC detections did not show any topological specificity with respect to stimulus modality: maximum values were invariably found in fronto-central areas (Figure 3.2). Each isolated eKC was also characterized by means of three morphological features:

- negative-to-positive peak (NP) amplitude reflecting how many neurons are involved in generating eKC;

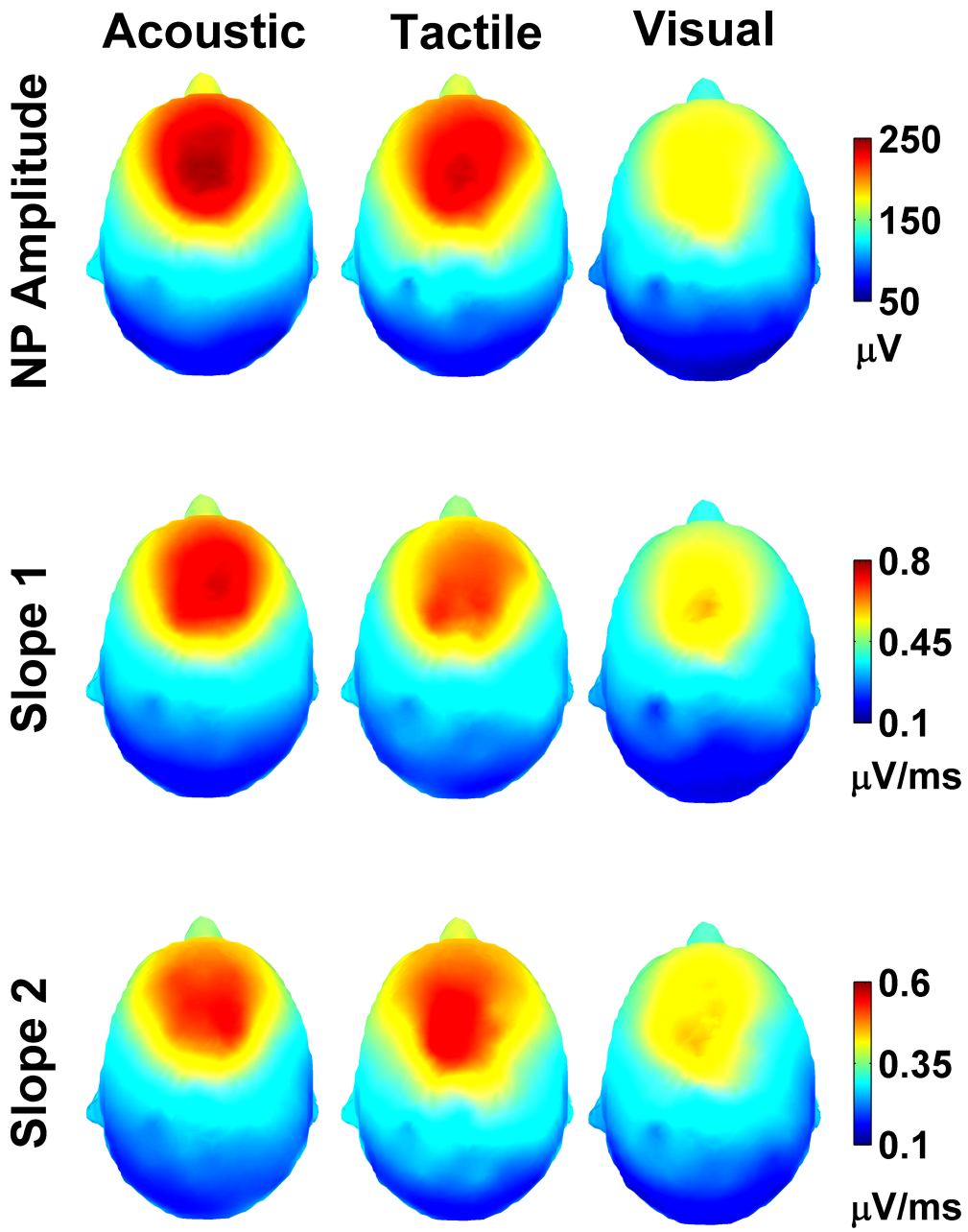

Figure 3.3. Maps of evoked K-complexes morphological features. The grand average maps of NP amplitude, Slope 1 ad Slope 2 for the three stimulation modalities are shown. These measures are tight related to the N550 component of eKC and represent different correlates of neuronal bistability proneness.

- Slope 1, by consensus [110, 13, 111] reflecting how many and how synchronously membrane K^+-channels open for hyperpolarizing cortical neurons;
- Slope 2 reflecting local recover of synaptic activity including a modulation induced by thalamocortical volleys [110, 30].

Higher values of Slope 1 indicate a higher degree of cortical proneness to bistability (index of bistability) [112]. As depicted in Figure 3.3, also the maps of NP amplitude, Slope 1 and Slope 2 are independent from sensory modality of stimulation and mirror maps of eKCs: maximum values are localized in fronto-central regions.

Table 3.1 provides the comparisons of NP amplitude, Slope 1 and Slope 2 with respect to the sleep stage factor, i.e. N2 versus N3, and to the cortical area factor, i.e. primary sensory areas versus other cortical regions. The values of Slope 1, Slope 2 and NP amplitude were greater during N3 than during N2 ($p<0.001$); remarkably, Slope 1, Slope 2 and NP amplitude detected in primary sensory areas showed significant lower values with respect to those in other cortical regions ($p<0.001$).

3.3.1 The triphasic structure of evoked K-complexes

Figure 3.4 shows the grand mean templates of EEG responses for the three sensory modalities of stimulation. Each line corresponds to the average shape recorded for each electrode and for each type of stimulation (average was over subjects and trials). The response shape was triphasic, i.e. three major positive–negative–positive waves (P200, N550 and P900) were always clearly visible. The latencies of the 3 different components, in terms of grand-average over the scalp and subjects, resulted as follows (mean ± SD): P200 at 274±35 ms, N550 at 650±150 ms and P900 at 1130±40 ms.

3.3.2 The topology of evoked K-complexes: the peculiar mapping of P200 latencies

Figure 3.5 shows the variability of the latency of the 3 different components as a function of topology and sensory modality of stimulation. The first main result of the study concerns the topology of P200 latency that appeared to be specifically dependent on the sensory modality. Remarkably, earliest P200 were located over the primary sensory cortical areas of the related sensory modality (Figure 3.5,

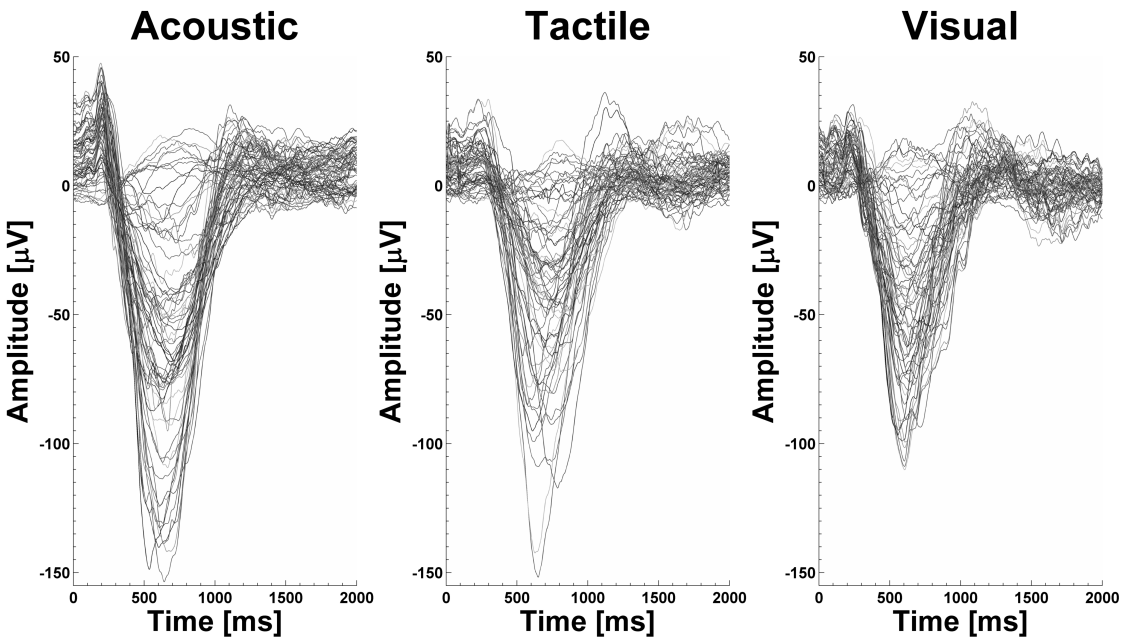

Figure 3.4. Triphasic structure of eKCs. Grand mean templates of the EEG responses following the sensory stimulations during NREM sleep have three evident major positive-negative-positive waves (P200, N550 and P900). Each line corresponds to the average shape recorded for each electrode and for each type of stimulation (averaged over subjects and trials and triggered setting t = 0 at stimulus onset).

first row). For the sake of clarity, the phrase *earliest P200* has the meaning of the electrode where P200 has the minimum latency within each eKC event. In particular, the map of earliest P200 related to (i) acoustic eKCs largely coincided with the primary auditory cortex, bilaterally (Broadman Area, BA 41 and 42); (ii) tactile eKCs coincided with the left primary somatosensory cortex (BA 3, 1 and 2); and (iii) visual eKCs coincided with the primary and secondary visual cortices (BA 17, 18 and 19).

We established the significance of the results depicted by the maps of Figure 3.5 by means of a quantitative analysis of variance (Table 3.1) on component latencies: for each sensory modality, the mean P200 latency was significantly lower for electrodes over primary sensory areas than for electrodes over other cortical regions ($p<0.001$ for all sensory modalities). Let us stress that the sleep deepening did not affect the aforementioned results on P200 latency, as shown in Table 3.1 .

Second and third rows of Figure 3.5 show the latency maps of the N550 and P900, which resulted independent from stimulation modality. The maps of latencies of N550 and P900 show a large similarity with the map of eKC detection:

earliest latencies were in the regions of maximal detections, i.e. in the fronto-central ones (Figure 3.2). In line with spontaneous KC literature [11], the probability detection of earliest N550 and P900 decreased along an antero-posterior gradient. The analysis of variance (Table 3.1) yields a clear stage effect, with shorter latencies in N3 for both N550 and P900, with respect to N2 ($p<0.001$). No significant effects were found comparing latencies on primary sensory areas and other cortical regions.

3.3.3 The dynamic properties of evoked K-complexes: real and apparent travels

The second important result of this study refers to dynamical properties of P200, i.e. how this cortical excitation really travels on the cortical mantle. As shown in Figure 3.5 (first row), the P200 of acoustic eKC first propagated bilaterally to the vertex and from it, along the central midline, to occipital and to frontal-lobes electrodes, which, surprisingly, were the last to be reached. For tactile eKCs the P200 propagated from the primary sensory area towards frontal and occipital regions. Finally, the P200 of visual eKCs travels along a posterior-frontal direction, ending its travel at the prefrontal regions.

The qualitative dynamical behavior of P200, depicted in Figure 3.5, has been validated by means of the latency-distance scatter plot, a quantitative approach allowing the evaluation of statistical significance of this behavior (see Methods). This analysis is shown in Figure 3.6 (first column). A clear direct proportionality between distances and latencies is clear and highly significant ($r^2>0.4$ for all modalities, p-value <0.001). The speeds of propagation stemming from the slope of each regression line were estimated in 9.7 m/s for acoustic eKCs, 8.0 m/s for tactile eKCs and 8.1 m/s for visual eKCs. At variance, the latency-distance scatter plot method applied to N550 and P900 is not consistent with a wave starting from the primary sensory areas since the fitting procedure yields negative slope (Figure 3.6, second and third columns).

The Figure 3.7 reports analogous results for latency-Slope 1 scatter plots (see Methods). We adopted Slope 1 as a measure of bistability proneness (see Discussion). Here the situation is opposite (Figure 3.7, second and third columns): while N550 and P900 display negative significant slope ($r^2>0.59$ for all modalities having p-value <0.001) suggesting they are driven by bistability proneness, P200 propagation is not explained by the proneness model (3.7, first column).

3.3.4 P200 amplitude-dependent trigger for eliciting N550 apparent travel

As depicted in Figure 3.8, first row, the amplitude of P200 of eKCs showed a clear antero-posterior gradient. At variance, looking for a positive peak in the same time window used for the search of eKC P200, resulted in detecting N-eKC putative P200s with an even distribution of amplitude over the scalp (Figure 3.8, second row). The comparison of the first and the second row of Figure 3.8 is summarized in the third row: eKCs P200 amplitudes were significantly larger over fronto-central areas.

We also estimated the latencies of N-eKC P200-like excitations obtaining highly variable, divergent maps as a function of the stimulation modality. We refer to the P200 associated to N-eKCs as *P200-like excitations* since we have detected the maximal positive deflection in interval 220-350 ms post-stimulus, in the same way we detected P200 for eKCs. In principle, it is not assured that the events detected by this procedure are related to the stimulus as small deflections may arise also for other mechanisms or by random fluctuations.

The third result of this study thus consists in unraveling the necessity of an ordered waxing P200 behavior for eliciting bistability. The N550 emerges in fronto-central areas only when P200 display in these regions larger amplitudes compared to the level of activity in the same time interval when the KC is not evoked.

The fast travel of P200 ignites the beginning of negative slope that marks the beginning of bistable behavior firstly in primary sensory areas and subsequently in other cortical regions, ending in the frontal areas. Sorting waves according to the distance from the primary sensory areas to the frontal ones, as shown in Figure 3.9, underlines the fast propagation of P200 (red line plotted over the butterfly plots) from primary sensory cortices to frontal ones, with similar dynamics for the three stimulation modalities. The apparent travel of N550 is also shown in Figure 3.9. Despite higher NP amplitude in fronto-central regions (see Figure 3.3, first row, and Table 3.1), the large difference in values of Slope 1 between primary sensory areas and frontal regions (Figure 3.3, second row, and Table 3.1) prevails in making N550 latencies smaller in fronto-central areas (Figure 3.9), In fact Figure 3.9 highlights a reverse path of N550 (negative slope of the dashed blue line plotted over the butterfly plots) latencies with respect to those of P200s (red line). The strong dependence of N550 latency from the values of Slope 1, index of local proneness to bistability, is the fourth result of this study. This result supports the apparent nature of N550 travel.

3.3.5 The Vertex Shape Wave

Besides, we occasionally detected the so called vertex shape wave (or N350), a local minimum amidst the negative slope to the N550 peak. This component had large latency variability, hence hidden by averaging procedures, and it was tightly localized over central areas. We performed for N350 the same analysis performed for the other components (P200, N550 and P900). In agreement with large body of literature (see for instance, [113, 114]) on N350 topology and dynamics, (i) detections took place exclusively in a tight central area surrounding the vertex, (ii) N350 did not show any propagation-like behavior and (iii) N350 displayed a latency of 380±40 ms (mean ± SE). Our butterfly plots (see Figure 3.9) display moderate evidences of N350, while they are inappreciable in Figure 3.9. The smoothed shape of N350 is caused by the fact that the signals are filtered in delta band (0.3-4.5 Hz) and this caused attenuation for this narrow component compared to the large N550 one.

Recalling that N350 was out of the main aim of our study, detection rate was not computed, but visual inspection suggests a low detection rate. This is in line with low detection rates for, respectively, rare auditory, frequent auditory and inspiratory-occlusion stimuli that have been reported to be not higher than 10%, 9%, and 5%, compared with K-complex elicitation of 38%, 17% and 22% (for a review see [107]). We recall that our butterfly plots make use of averaged templates and not of single event traces. It is therefore expected that even those vertex electrodes mostly affected by sporadic vertex-shape waves will display only some deviation, and not a large deflection.

We conjecture that other factors may yield a small number of N350 detections in our study. These include: (i) N350 is enhanced in the responses to deviant stimuli during oddball paradigms [115], different from the protocol we used; (ii) N350 is very dependent by the inter-stimulus interval, and an "unusually long refractory period" has been reported ([116].

3.3.6 P200 latency of non-evoked K-complexes

We refer to the P200 associated to non-evoked KCs (N-eKCs) as "P200-like excitations" since we have detected the maximal positive deflection in interval 220-350 ms after the stimulus, in the same way we detected P200 for eKCs. In principle, it is not assured that the events detected by this procedure are related to the stimulus as small deflections may arise also for other mechanisms or by random

fluctuations. Figure 3.10 shows the latency-distance scatter plots and latency maps of P200-like excitations as a function of stimulation modality. Similarly to what shown in Figure 3.6, distance is calculated from the centroid of primary sensory areas.

Both for acoustic and tactile stimuli the greatest differences that emerge from a comparison with the relative scatter plots in Figure 3.6 (first column, first and second row) are: (i) the regression lost statistical significance due to a scattered distribution; (ii) the latencies relative to the primary sensory areas do not have minimal latencies; (iii) dots relative to primary sensory areas are scattered as the others. These results are also well depicted by the latency maps (Figure 3.10, last column, first and second row) and indicate that detected excitations do not seem to follow the cortical pathways originating from primary sensory areas, at variance with eKCs P200s. We cannot therefore exclude that the detected P200-like excitations have a stimulus independent origin. In other words the non-emergence of neural bistability is linked to the absence of P200 travelling wave, and this is in line with a lack of a waxing/travelling behavior and hence to lower amplitudes in fronto-central areas (see Figure 3.8, first and second column).

For the visual stimulus a special discussion is in order. Figure 3.10 (third row) depicts that P200-like excitations seem to show a travelling behavior. The main difference with eKCs P200s are the following:

- there is a gap between 9 and 13 ms that divides electrodes pertaining to primary and accessory visual areas and remaining cortical areas;
- the dots are well ordered around the regression line, while in the case of eKCs there is a cluster of prefrontal electrodes with delayed response. This behavior is also displayed by the latency map (third column of Figure 3.10).

The evident postero-gradient of P200-like excitations could be ascribed to the well know anatomical connectivity which interconnect visual areas and connect them with other cortical regions. Let us recall the dorsal stream, the ventral streams, and the occipitofrontal fasciculus. While this may account for a default gradient for cortical excitation starting from primary visual area, a direct comparison between the visual latency maps of Figure 3.10 and of Figure 3.5 (first row, third column) shows that in the former the postero-antero gradient completely characterizes the map, in the latter a more complex structure of dynamics is present. This complex structure may be related to the cortical dynamics yielding bistability. One classical explanation of N-eKCs makes use of the concept of thalamic gating during sleep

that undergoes fluctuation in time [87] and explains amplitude changes of sensory evoked potentials during slow wave sleep [117].

As far as latencies of P200-like excitations are concerned, the structure-less maps and scatter plots of acoustic and tactile stimuli seem to be in accordance with a close or also semi-close thalamic gating while for visual stimuli this is masked by a default postero-anterior gradient driving excitation travels.

	Sleep Stage				Cortical area			
	N2	**N3**	**F-score**	**p-value**	**PSA**	**OCR**	**F-score**	**p-value**
P200 latency mean±SE (ms)	274.8±1.4	274.7±1.4	0.004	NS	270.4±1.5	279.1±1.3	33.074	<0.001
N550 latency mean±SE (ms)	698.2±5.2	607.2±5.2	250.419	<0.001	657.7±5.3	647.6±4.9	3.431	NS
P900 latency mean±SE (ms)	1192.8±8.9	1135.0±9.0	35.700	<0.001	1163.2±9.2	1164.5±8.4	0.021	NS
Slope 1 mean±SE (μV/ms)	0.37±0.01	0.41±0.01	10.315	<0.001	0.31±0.01	0.47±0.01	337.409	<0.001
Slope 2 mean±SE (μV/ms)	0.31±0.01	0.33±0.01	9.906	<0.001	0.26±0.01	0.37±0.01	316.448	<0.001
NP amplitude mean±SE (μV)	134.9±2.5	152.4±2.5	39.914	<0.001	120.1±2.6	167.3±2.4	320.915	<0.001

Table 3.1. Comparisons of the eKC latencies and morphological features as a function of sleep stage and cortical areas. Values are expressed in means and standard errors (SE); PSA: primary sensory area; OCR: other cortical regions. N2 and N3 sleep stages according to AASM criteria [48]. NS: not significant.

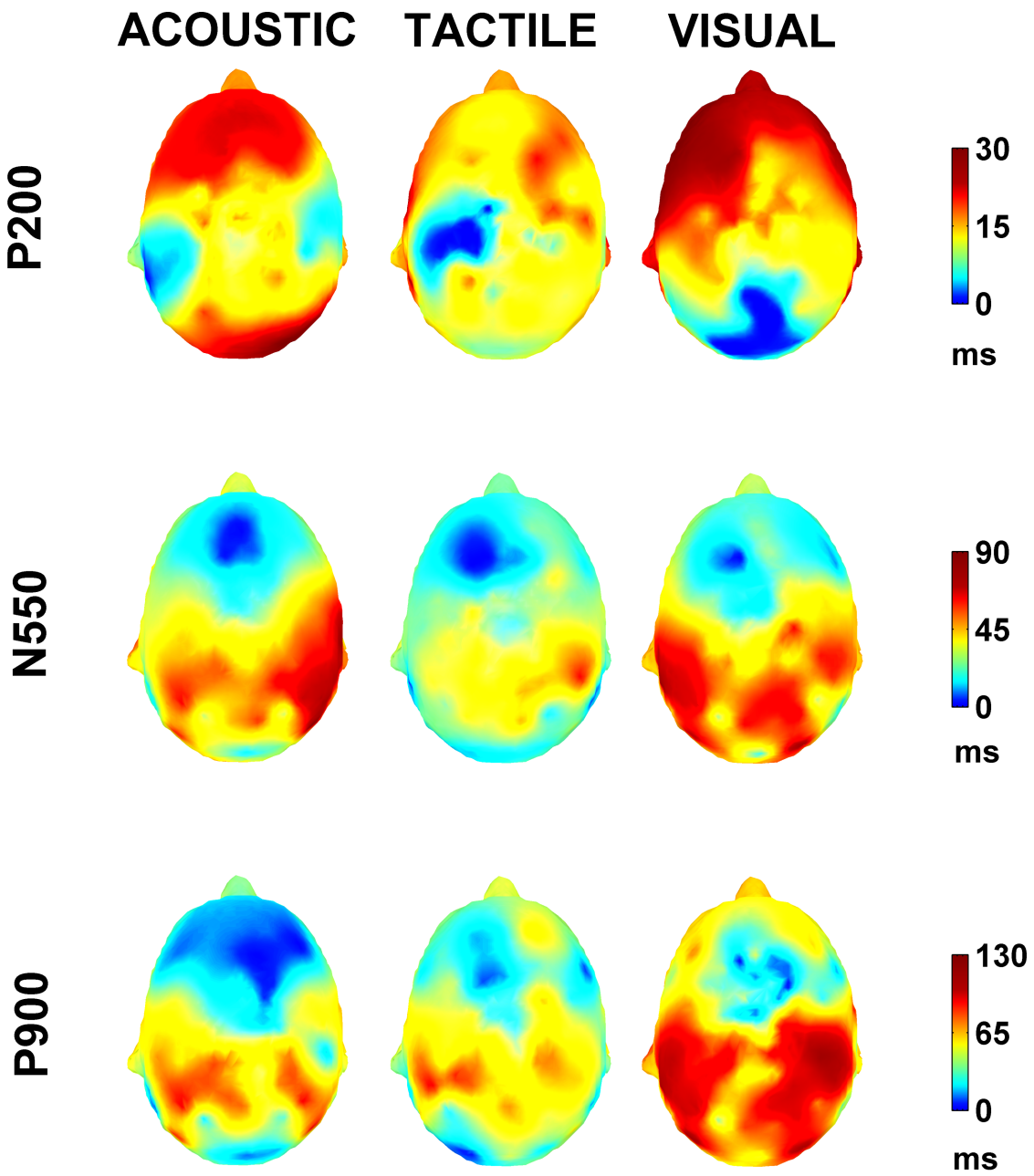

Figure 3.5. Spatial distribution of the latencies of eKC components. The grand average maps show components latency delays (for each component, delay equal to zero is set at the instant of the earliest latency) between electrodes, for the three stimulation modalities. Notice that P200 localization over the cortex based on latency maps indicated a sensory-modality-dependent cortical response peaked on primary sensory areas. At variance, N550 and P900 latencies maps account for the distribution of bistability proneness across the cortex.

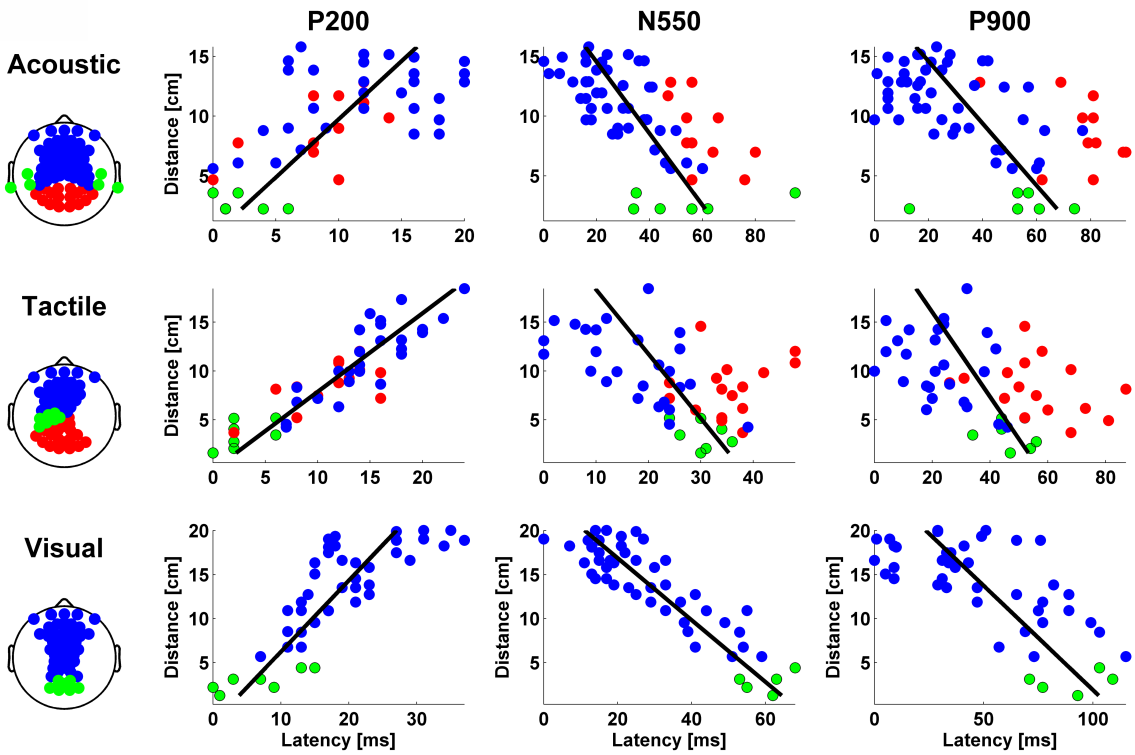

Figure 3.6. Models of component propagation: latency-distance scatter plots. Latency-distance scatter plots with the mean latency of each electrode in the x-axis and the electrode distance from primary sensory areas (PSA) in the y-axis. The electrodes over PSAs are indicated with green dots, the centro-frontal electrodes and the posterior electrodes with blue and red ones, respectively. For the visual stimulation the electrodes over PSA and posterior areas are overlapped (green dots). The distance is defined as the Euclidian distance (the 3-D coordinates) between each electrode site and the geometric centroid of electrodes over each PSA. In the case of acoustic stimulation we have two centroids corresponding to the bilateral acoustic PSAs, thus for each electrode the distance from PSA was defined as the minimal one between the two centroids. The black line of fitting over each scatter plot has been derived by robust linear regression. It is possible to note as P200 latencies are ordered according to the distance from the primary sensory areas (panel A) as activated by specific sensory stimulations.

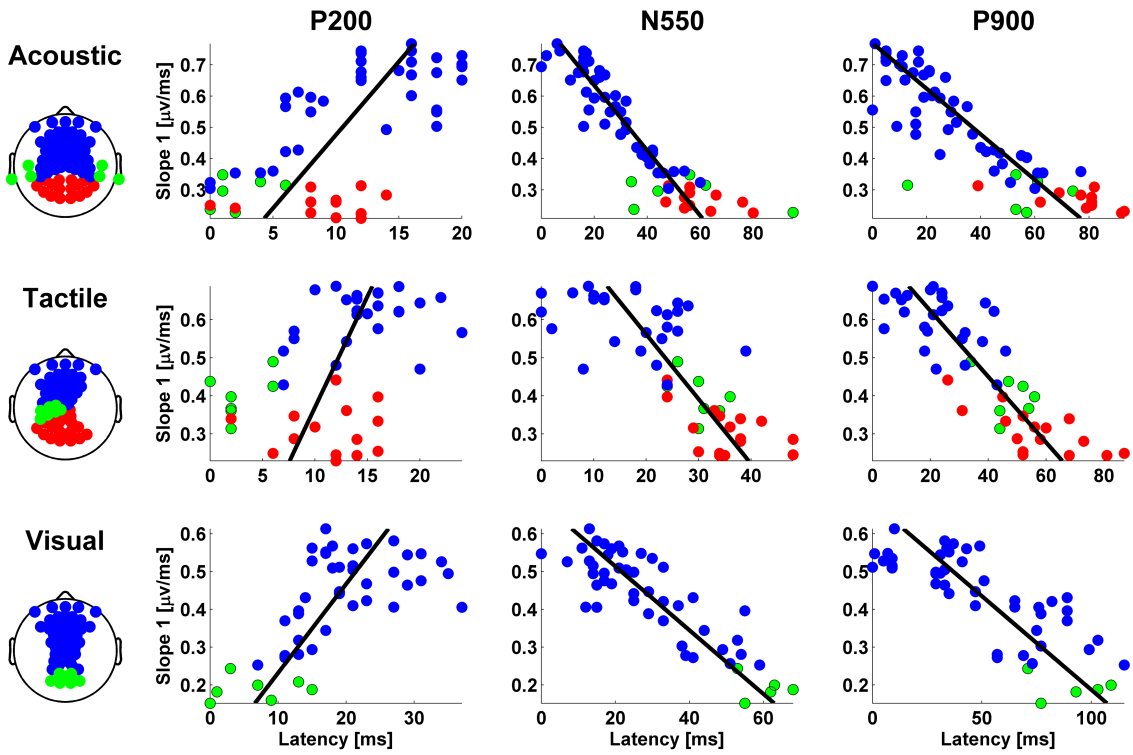

Figure 3.7. Models of component propagation: latency-Slope 1 scatter plots. The latency-Slope1 scatter plots with the mean latency of each electrode in the x-axis and the Slope1 of each electrode in the y-axis. Color dots and regression lines have been derived as in Figure 3.6. Notice as N550 and P900 showed the shortest latencies on fronto-central regions that were the last reached by P200 and their path followed the antero-posterior gradient of proneness to bistability (the greater is slope, the lower is the latency).

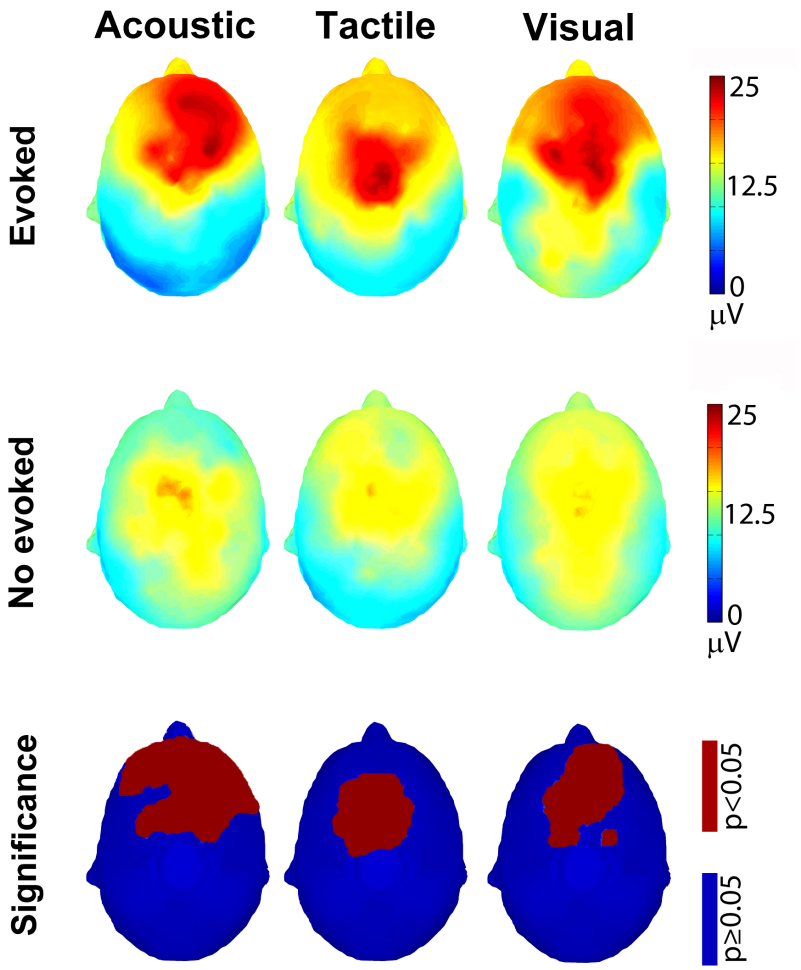

Figure 3.8. Amplitudes maps and comparison of eKC P200s and N-eKC P200-like excitations First and second lines show the grand average maps of P200 amplitude for the three stimulation modalities in the cases of eKC and N-eKC, respectively. Third line indicates the scalp regions of significant amplitude differences between eKC P200s compared to N-eKC P200-like excitations (red: $p<0.05$).

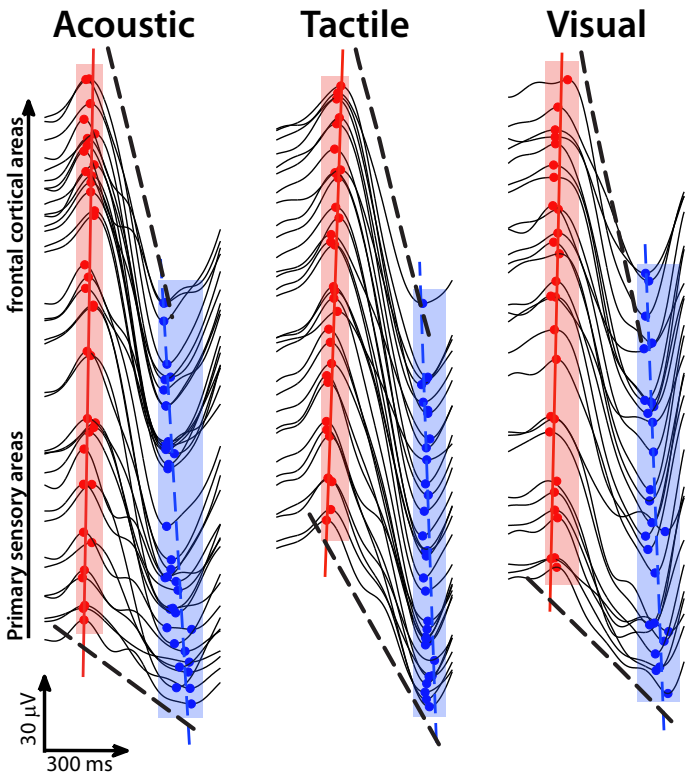

Figure 3.9. Real and apparent travels of P200 and N550 components. The figure contains averaged templates of P200 and N550 for each sensory modality of stimulation ordered according to the distance from primary sensory areas. Electrodes more posterior than those of primary sensory areas have been omitted. Red and blue dots explicitly draw local maxima (P200 peaks) and minima (N550 peaks), respectively. The red background highlights the time interval between P200 peaks and the red line indicates the speed of propagation of P200. Analogously, blue background and dashed line refer to the N550. Irrespective of the modality of stimulation, the traveling of P200 is real and faster than that of N550 and the high speed of propagation of the P200 excitation makes the "ignition" quasi simultaneous for N550, which is slower and apparent, insofar as the local minima are essentially driven by the negative descending Slope 1, whose high variability results in a relatively slow speed. Notice that the steepness of Slope 1 (black dashed lines) relative to primary sensory areas are much smaller than those relative to frontal ones; this is less evident for the tactile responses because the somatosensory hand area is close to areas with higher proneness.

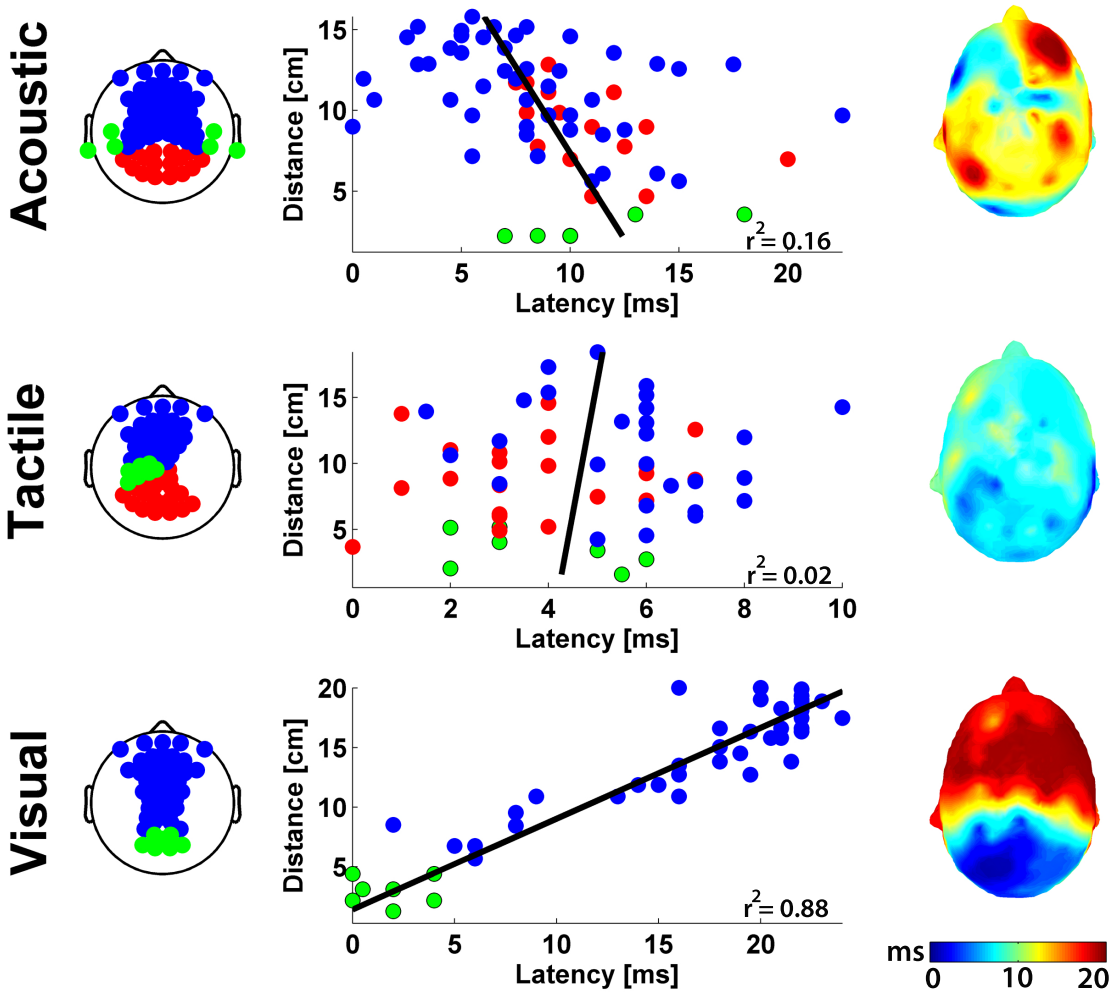

Figure 3.10. Latency maps and latency-distance scatter plots of N-eKC P200-like excitations.

3.4 Discussion and conclusions

In order to identify, in humans, the sensory processing during NREM sleep, we herein characterized the spatio-temporal features of evoked cortical responses, i.e. the K-complexes (eKCs) in 14 healthy volunteers by means of high-density EEG and 3 different sensory modalities. Owing to a stimulation administered during the whole night, we were able to collect a large number of eKCs for each sensory modality for all N2 and N3 stages. The rate of stimuli successfully evoking acoustic and tactile eKCs was in line with previous studies [118], while for visual stimuli we report a lower rate with respect to a previous study [115]. In our study, visual eKCs resulted sparse and with smaller amplitude compared to the other modalities. A possible explanation could be related to intensity and orientation of the light stimulator since we used a photographic flash oriented to the room ceiling while others studies [115] aligned the source directly toward the subject's head. On the other hand, our experimental set-up did not provoke any awakening (at variance with [115]).

Among the various results stemming from our extensive characterization of eKCs, four main original results emerge:

(I) The topology of P200 latency is dependent on the sensory modality with earliest waves in the stimulation-related primary sensory areas;

(II) P200 travels on the cortical mantle as a cortical excitation. On the basis of these results, a third finding is assessed:

(III) P200-like excitations of N-eKCs are detected over the scalp with amplitudes significantly smaller in fronto-central areas, compared to eKC P200s.

(IV) N550 latency mirrors its mean local steepness (Slope 1) which is function of topological proneness to bistability.

On the basis of these results, a global picture is assessed: N550 (down state) and P900 (up state) are driven by the interplay between amplitude-dependent P200 trigger and local proneness to bistability.

Let us now discuss the emerging picture in terms of an ideal bottom-up travel of a sensory input from periphery to cortical areas. This allows us to pinpoint each result in a unifying scenario and in an intuitive order.

3.4.1 P200 as a cortical excitation

As earlier described, P200 is the first detectable wave, with shortest latencies detected in the primary sensory areas of stimulation. This original result indicates that also during NREM sleep sensory stimuli follows wake-like sensory pathways, ascending to primary sensory areas from specific thalamic nuclei as suggested by previous works (for a review see [119]). Besides, we cannot exclude a contribution from aspecific thalamo-cortical cells [120]or even, as recently reported, by the brain stem [121], which theoretically generate a diffuse cortical response undetectable in terms of averaging. However, the specific wiring of sensory inputs provides the shortest possible processing time in term of perception in wakefulness[122], hence making this pathway the predominant one also during NREM sleep.

P200 as the earliest wave component of eKC is not an original result since Loomis has firstly reported that KCs can be triphasic [36]. A first hint of sensory-dependent P200 topology can be found as preliminary result in a recent review [115]. At variance with the results presented herein, however, they used sleep EEG recordings from 5 subjects and LORETA-based source analysis, thus showing a significant overlap of the reconstructed current densities only on somatosensory (by means of electrical median nerve stimulation) and visual primary areas.

Once elicited in the primary sensory area, P200 follows cortical pathways as a cortical excitation (point ii). We were able to validate ($p<0.001$) this behavior by means of the latency-distance scatter plot. In summary, the P200 evoked by the three sensory modalities spreads like a traveling wave packet with 10 m/s speed over the excitable cortical mantle.

The results of latency maps analysis (point i) and of latency-distance scatter plot (point ii) allow us to state that P200 origin is always located in the primary sensory areas (confirmed by analysis of variance in Table 1), activated by specific sensory stimulations [123], therefore by excitatory glutamatergic thalamo-cortical cells [4], and from there it propagates across the cortical mantle, triggering N550 and P900 components of eKCs, which show a topology independent from sensory modalities. From an electrophysiological standpoint, we recall that N550 and P900, respectively reflect a deep hyperpolarized phase with electrical silence (down state) and a following depolarized phase with huge synaptic activity (up state) [110, 13]. We purposely use the terms down and up state to underline that cellular mechanisms at the basis of N550 and P900 are the same of Sleep Slow Oscillations (SSO, <1Hz oscillations), i.e. the neuronal bistability whose presence paradigmatically defines NREM sleep.

3.4.2 P200 as a trigger for bistability

The role of P200 as a trigger of the following bistable complex resulted dependent on its amplitude as indicated by the comparison between P200 belonging to eKCs and P200-like excitations belonging to N-eKCs (point iii). As a matter of fact, we imagine a threshold effect, i.e., in order to induce bistability a waxing and efficient neuronal recruitment along P200 travel seems to be necessary. By efficient we mean that P200 needs to display larger amplitude in the fronto-central areas (see Fig. 6) because the integrative nature of these regions facilitates electrical reverberation exploiting recently formed up-scaled Hebbian circuits [34]. This effect is very much in congruence with the results obtained in vivo [124] and in vitro [62]. The work of [124] triggered sleep slow waves by means of transcranial magnetic stimulation demonstrating that the amplitude of the negative peak depended on stimulation intensity. The thorough study of [62] demonstrated that cortical down states are mainly related to the synchronicity of opening of activity-dependent K^+-channels, and are strongly modulated by electrical activity preceding the down state, both in term of its duration and in term of speed of silencing the network. In our case the electrical activity preceding the downstate is the P200 that during its cortical travel interacts with areas with different degree of proneness, in turn related to activity during wakefulness: higher is the proneness faster is the speed of network silencing. In this light, our group has previously [25] searched for wake-like activities surrounding the down state and the main result was that down states were preceded by a well-defined activity both in terms of shape (a bump) and spectral activity (from sigma to high gamma). We interpreted these results as an ignition for inducing bistability.

The spatiotemporally-varying neuronal recruitment shown by the P200 that conducts to evoking or not evoking the KC opens the new issue of which mechanisms drive this behavior. The thalamus could play a role in modulating the KC responses; in fact a classical explanation of N-eKCs makes use of the concept of thalamic gating during sleep that undergoes fluctuations in time as demonstrated by the study of [87] via intracellular recording. The work of [117] suggested that this mechanism explains amplitude changes of sensory evoked potentials during slow wave sleep, since recurrent thalamic hyperpolarization and cyclical shunting of the membrane of relay neurons play a role in preventing sensory inputs being transferred to the cortex. We conjecture that the thalamic gating may be one of the mechanisms strongly influencing the waxing behavior of P200 during its travel, favoring cortical neural recruitment instead of directly affecting the bistability

expression.

The thalamic role was already suggested in [25] for spontaneous SSOs showing how the activity preceding down states is characterized by the typical thalamic spectral rhythm (sigma band) as well as by other cortical activities, such as high gamma. Actually, the relationships between thalamic and cortical activities in triggering slow oscillations are more complex: experiments conducted on thalamo-cortical slices have shown that thalamocortical inputs facilitate while intra-cortical inputs suppress cortical up states[125]. In this view, our work highlights the role of thalamic input on sensory cortices in enhancing the probability to trigger up states, in particular P200 and all related mechanisms. Finally, based on our data we do not exclude the a priori possibility that thalamus could interplay with the cortical slow activity, by means of an intra-thalamic reversible transition between bursting mode and tonic firing mode [126, 127]. This effect is displayed by some fMRI studies showing a thalamic activation during evoked and spontaneous K-complexes [128, 113]. In principle, an intra-thalamic spread of such a transition would have the possibility of being projected as a cortical wave traveling on the cortical mantle. However there are evidences in animal models that allow considering this mechanism at least unlikely, since transection of cortico-cortical pathways though with intact thalamo-cortical connections abolished for both P200 and N550 any travel across the transected cortical territories [38]. Furthermore when thalamo-cortical cells fire in a wake-like mode during sleep, features and mapping of sleep slow oscillations and K-Complexes are profoundly altered. This is the case of selective thalamic neurodegeneration, such as Fatal Familial Insomnia (FFI). Indeed, a recent paper of our group and other colleagues [30] (that is extensively reported in chapter 2) showed that in a case of FFI, mainly involving the dorsal thalamus (and maybe the reticular thalamic nucleus, as described in literature), the rate of spontaneous sleep slow oscillation is dramatically collapsed as well as the possibility to identify specific features of up state, such as sigma activity crowning.

In conclusion, we stress again that the trigger is due to P200, which is a cortico-cortical traveling wave. However one may hypothesize an ancillary role of the thalamus in increasing and optimizing neural recruitment along the P200 travel.

3.4.3 Cortical proneness to bistability

We have stated that the bistable behavior is triggered by the P200 excitation. In this subsection we discuss how its outcome is favored and modulated by local

properties that we refer to as cortical proneness to bistability. Proneness is tied to how synchronously neurons open K^+-channels for falling in downstate [110], thus the Slope 1 feature is the most convenient EEG measure for mapping local cortical proneness.

Our results based on topology of NP amplitude, Slope 1 and Slope 2 (which correspond to how synchronously cortical neurons and thalamo-cortical cells discharge exiting from the down state, [110, 112] show that fronto-central regions display the largest values, depicting sharper eKCs with higher amplitude. Moreover, bistability-related morphological features of eKC (NP amplitude; Slopes 1 and 2) increase as sleep get deeper, in line with the increased bistability proneness indicated by the greater rate of spontaneous SSO in the deeper sleep stages [11, 13] and their maps substantially overlap that of detection rate (an a posteriori direct measure of proneness). As expected, N550 and P900 latencies diminish as sleep get deeper. Conversely P200 latencies are not affected by sleep deepening, hence by the degree of proneness to bistability.

We also confirm that the areas with highest proneness are the fronto-central ones with a clear antero-posterior gradient [106, 101]. Remarkably these maps overlap those of the latencies of N550 and P900 that, at variance with those of P200, are independent from sensory modalities of stimuli. This result confirms the well-known sensory-modality independence of the biphasic component (N550 and P900) of eKCs [103, 129] that corresponds to the bistable behavior.

3.4.4 The apparent travel of bistability

At this point we are forced to critically revise the concept of slow waves at $<$1 Hz as a traveling wave. We recall that spontaneous KCs and eKCs display similar depth profiles and current source density distributions, strongly indicating a common origin and a common generating mechanism [38, 39]. Furthermore, the analysis of the sleep slow oscillation as a traveling wave [11] showed that SSOs and spontaneous KCs have the same cortical dynamics, indicating that all slow waves at less than 1 Hz during sleep are a unitary phenomenon.

When looking at traveling waves, a classical distinction is made between group velocity and phase velocity; insofar as only the former really describes energy or information transmission [130]). This is true both for wave trains and for isolated wave packets, since local differences (such as the local proneness during NREM sleep) may simulate fast energy or information transmission apparently violating causal relations. In particular, it is odd that information may be transported by an

electrical silence (down state) that, mainly for its temporal precision and detection robustness, has been extensively used for monitoring the cortical travel of SSOs [11, 13]. Having this difference in mind, let us describe results on real and apparent traveling properties of the different eKCs components. We already discussed how P200 really transfers neural excitation over the cortex similarly to what happens in wakefulness owing to a waxing behavior. N550 and P900 reflect a completely different phenomenon. Our results show that N550 and P900 do not obey to a model corresponding to a travel along the path earlier traveled by P200 (see Figure 3.6; latency-distance scatter plots; see also Figure 3.9). In fact N550 and P900 showed the shortest latencies on fronto-central regions that were the last reached by P200 (Figure 3.9). On the contrary their path followed the antero-posterior gradient of proneness to bistability (point iv), as indicated by the latency-Slope 1 scatter plots (Figure 3.7; see also Figure 3.9), mirroring the reported cortical *travel* of SSOs [11, 13].

The emerging scenario is that of a bistability driven by the interplay between two necessary conditions: (i) the efficient cortical travel of P200 to integrative areas, and (ii) the higher proneness to bistability of these latter areas. The difference in proneness determines different latencies for the reference point of the negative peak of N550. Let us make a pictorial example to clarify the difference between group and phase velocity. Imagine a linear series of firecrackers in which one explosion ignites the fuse of the following one. This is what we mean by group velocity transport. This happens for P200 propagation. Alternatively, one may align the firecrackers with *parallel fuses* ordered with respect to the fuse length and ignite all of them simultaneously or quasi-simultaneously, as in the case of the fast cortical traveling trigger of P200. One sees a traveling wave but the order of explosions depends on the fuse length instead of the order of ignition. This is what we mean for phase velocity. In this metaphor, the shorter is the fuse, the higher the proneness to bistability, which explains topology and dynamics of N550 and P900. Metaphors aside, when we state that N550 shows an apparent travel we mean that the delays between negative peaks are not due to the propagation of the falling to down states succeeding P200 traveling along cortical territories, but that they are caused by different values of Slope 1 (see Table 3.1, second row of Figure 3.3 and Figure 3.9). The apparent travel of N550, well described in Figure 3.9, stems from the topological distribution of the values of Slope 1. As earlier anticipated in the Results section, the strong dependence of N550 latency from the values of Slope 1, index of local proneness to bistability, is the fourth result of this study (point iv). Indeed, the role of Figure 3.9 is that of pictorially showing how the apparent travel

follows the real travel of P200 excitation. By ordering waves from primary sensory areas to frontal ones, we see that the traveling of P200 is faster than that of N550. Therefore the relatively high speed of propagation of the P200 excitation makes the *ignition* quasi simultaneous for N550, whose high variability in Slope 1, with a greater steepness in frontal areas compared to the primary sensory areas, results in a relatively slow speed for the N550. This explains its apparent anterograde travel.

3.4.5 Conclusions

The results reported herein naturally lead to rethink the features and functions of less than 1 Hz oscillations, independently from whether evoked or spontaneous. We are now inclined to believe that, during sleep, information travel pertains to the P200 or to the positive bump of spontaneous SSOs occurring before the negative peak and that its travel cannot be inferred by the dynamics of N550 or SSO negative peak, that are trivially driven by the antero-posterior gradient of proneness to bistability. From a methodological and conceptual standpoint, following a traveling wave focusing on relative small positive bump is technically challenging; on the other hand, focusing on the negative peak is still convenient, but one has to consider that it is the expression of an earlier activity. The problem is that the negative component of the KC/SSO has time duration of several hundreds of milliseconds and the location of the negative peak, despite its precision, is only a particular point of the negative component and, in particular, it does not mark the local ignition of down states. In principle, the negative component, i.e. the onset of the falling into downstate, starts around the end of the P200 component both for primary sensory areas and for other cortical regions, including the fronto-central ones (see Figure 3.9). Thus, adopting the zero crossing point after the P200, also the negative component would presumably start right after the P200, therefore from primary sensory areas in the case of eKCs. Unfortunately precise location of the onset of bistability is challenging as, for instance, zero crossings are strongly dependent on drifts and filters adopted. This may represent a future direction for further researches.

How does sleep-related bistability quench consciousness in sensory processing? The higher proneness to bistability in fronto-central regions is crucial. Half a second of diffuse electrical silence of fronto-central neural circuits prevents the conscious processing of sensory inputs by means of a breakdown of large scale functional connectivity, in line with the results of [131] obtained by transcranial

magnetic stimulation and with recent results of our group on the non-emergence of the global workspace during NREM sleep [32].

However, the P200 early processing is also crucial. The relative low bistability proneness in the primary areas compared to the other cortical regions (established by analysis of variance in Table 1 and depicted in Figure 3.9) has the role of allowing the diffusion of a waxing P200 to higher-order associative cortical areas. At that level, the P200 propagation leads to two alternative outcomes: (1) the silencing of the integrated cortical response by the induced bistability; (2) the awakening due to increase of Reticular Ascending System (RAS) activity, which antagonize the opening of neural K^+-channels at cortical level [132, 133, 17]. This induces a large-scale cortical integrated activation, which is condicio sine qua non for the emergence of consciousness. As a result the awakened subject is fully aware of the stimulus that he/she received when asleep.

In conclusion, two words on the old dilemma about the nature of KCs: arousal as stated by many or sleep protection as advocated by as many others? We think that our study clarifies and settles this controversy (for a review see [134]) insofar as eKCs fully contain both properties with the traveling excitation P200 taking place almost exactly like in wakefulness (arousal) leaving the sleep-protection function to the classical bistable behavior (N550 and P900).

Conclusions

In this thesis, three studies aimed to identify the complexity of neural activity during *Slow Wave Sleep* (SWS) in humans have been described. In general, all studies reported in this thesis were focalized on the *Sleep Slow Oscillation* (SSO), a graphoelement that corresponds to a peculiar neural behavior: SSO consists of a sharp negative peak (down state or electrical silence) followed by a shallow positive shoulder (up state or huge neural discharge).

Three main questions were posed:

1. What are the functional relationships between wake-like activities and electrical silence within spontaneous SSOs?

2. Does the thalamus play a key role in the fine modulation of wake-like activities and electrical silence of spontaneous SSOs?

3. What are the roles of wake-like activities and electrical silence of evoked SSOs (K-Complexes) in quenching consciousness and maintaining sleep?

Functional relationships between wake-like activities and electrical silence within spontaneous SSOs

In this study, the cortical bistability (neurons undergo alternate electrical silence and wake-like firing) in SWS has been evaluated by means of electroencephalography (EEG). Three main results [25] emerge: (i) the identification an early positive bump composed by fast EEG rhythms which occurs immediately before the down state; (ii) the fact that early positive bump ignites the falling in the down state; (iii) fast EEG rhythms crowning the up state that operate in the iteratively recalling and storing information acquired during wakefulness.

In particular, the identification of an early positive bump composed by wake-like activities corroborates the hypothesis that an activity-dependent accumulation of calcium or adenosine diphosphate (ADP) triggers a potassium current and, thus, the down-state. This is in contrast with the author of [50] that suggests the need of additional mechanisms since he observed a lack of a local up state preceding the K-Complex.

The positive influence of fast EEG rhythms on bistability suggests a novel scenario about *a good sleep*. From a heuristic point of view, the study of an optimal level of *cortical noise* during NREM sleep (i.e. the amount of fast EEG rhythms) may favor the emergence of the early positive bump, thus the cortical bistability and its positive functions in maintaining sleep and consolidating memories. This aspect could be relevant when considering pathological conditions or pharmacological treatments: it would appear that the modulation of fast EEG rhythms during slow wave sleep could represent an appropriate target for the treatment of a variety of sleep disorders.

The thalamic role in the fine modulation of wake-like activities and electrical silence of spontaneous SSOs

In this study, original results found in humans through surface EEG about the role of thalamus in modulating dynamics of neuronal populations during SSO have been reported. To this aim a human pathological model of selective thalamic neurodegeneration, the Fatal Familial Insomnia, has been used. One FFI patient at the middle stage of the disease, compared with 8 matched healthy controls, has been studied.

The following question has been addressed: may thalamus play a crucial role in the expression of the different features of cortical SSOs?

The main results [30] of this study are: (i) the FFI individual shows a dramatic reduction of the SSO rate as well as alterations of the wave shape; (ii) the FFI individual shows a lack of spindle (sigma activity, 12-15 Hz) crowning the up state, and that this alteration shows a specific topology: the fronto-central areas are more affected than temporo-occipital ones. This topological result is in agreement with the thalamo-cortical efferents of dorsal thalamic nucleus, which sends its volleys mainly to anterior cortical territories.

Despite data are collected only from one patient affected by a rare pathology, they allowed for considering thalamus as a pivotal region for triggering SSO and for grouping fast cortical rhythms also in humans. These original findings could

be important for sleep neurophysiology and sleep medicine. Since the discovery of the SSO, several papers have debated on the role of thalamic mechanisms in the origin and propagation of the SSO as well as in grouping fast rhythms (such as spindles). The presented data point out a thalamic role in modulating wake-like activities and electrical silence belonging to cortical SSOs.

The clinical interest of these findings rests on two main conclusions: 1) the study of SSO in presimptomatic FFI carriers could represent a useful tool for the early identification of pre-clinical thalamic dysfunctions; 2) the study of SSO will help establishing new diagnostic and therapeutic approaches that may ameliorate both symptoms and SSO activity in FFI patients. Possible approaches consist in techniques that have been shown to increase SSOs rate production, such as transcranial magnetic stimulation, and transcranial direct current stimulation.

Roles of wake-like activities and electrical silence of evoked SSOs (K-Complexes) in quenching consciousness and maintaining sleep

Using surface High-Density EEG, the cortical dynamics of evoked K-Complexes (eKCs) and how sensory stimuli are first processed and then quenched during sleep have been disclosed.

By means of three different sensory modalities of stimulation (acoustic, pallesthesic tactile and visual), the following questions have been addressed: (i) is topology of eKCs dependent or independent on sensory modality of stimulation? (ii) which eKC component starts sensory processing and (iii) which component quenches the following sensory processing? And more in general (iv) may eKCs study help us to understand sleep unconsciousness?

The main results of this study [35] are: (i) the earliest emerging component of eKCs, the so called P200 (which corresponds to the early positive bump of the aforementioned first study), origins in stimulation-related primary sensory areas, indicating a specific sensory-modality dependence; (ii) as any other cortical excitation, P200 travels on the cortical mantle for inducing a large scale sensory processing, but, (iii) brain is sleeping and reacts with a massive opening of K^+-channels which is the main basic mechanism for generating the giant negative component of eKCs, the so called N550 wave (which corresponds to the down-state of spontaneous SSOs). Owing to the higher proneness to bistability (in other words, the falling in down state) of fronto-central areas, the topology of N550 exactly involves a large amount of these cortical regions. This diffuse fronto-central

electrical silence quenches any temptation for creating large-scale functional connections between areas. The result is a quenching of sensory processing, hence maintenance of sleep and (iv) unconsciousness.

These findings are important for sleep physiology, since, from the discovery of the K-Complex (spontaneous or evoked), several papers [100, 135, 129, 37, 39, 118, 101, 50, 102, 113] debate on the dependence or independence from sensory modality, the topology of the different eKC components, and finally the KC as a mechanism for maintaining sleep or alternatively an arousal EEG index.

This study clarifies all points and settles this last controversy insofar as eKCs fully contain both properties with the traveling excitation P200 taking place almost exactly like in wakefulness (arousal) leaving the sleep-protection function to the classical bistable behavior (N550 and P900, the positive bump after the down state).

Moreover, these findings are also interesting for psychologists and clinicians since other conclusions open the door to explain phenomenologically known but still poorly understood sleep behaviors like: 1) sleep mentation, defined as presence of productive mental activity reported after awakening from Slow Wave Sleep [136], reflecting the P200 cortical travel; 2) the clear perception, till the level of full consciousness, of the kind of stimuli that provokes awakening, even in the case when stimuli were administered in deep sleep; 3) the fact that hyperarousal in insomniacs [137, 138, 139] makes these patients more prone to low-intensity stimuli awakenings.

Concluding remarks

In conclusion the results of the three studies allow drawing a peculiar scenario about sleep. Spontaneous or evoked SSOs need, for their ignition, a surplus of activity, i.e. the early positive bump for spontaneous SSOs and the P200 for the evoked ones (K-Complexes). These wake-like activities trigger the opening of activity-dependent K^+-channels, which in turn hyperpolarize the cortical neurons generating the electrical silence (down state). The down state has two effects: 1) it breaks down the functional and effective connectivity of distributed cortical neuronal pools, hence induces the formation of independent cortical modules, whose independence represents the substrate for sleep unconsciousness [32]; 2) it allows changes in the extracellular ionic concentration which triggers the neural discharge (network activity) characterizing the up state. We conjecture that this network activity takes place in each independent cortical module allowing the

communication between cortex and hippocampus, hence the consolidation of memory traces acquired during wake.

All these mechanisms are fine tuned by the thalamus through different mechanisms: a large component of wake-like activities of the early positive bump and of P200 (unpublished data) and of up states/P900 is composed by sigma activity, which represent the EEG band of the thalamic spindle rhythm. The role of this activity is different before and after the down state. Before the down state, sigma activity ensures the synchronization of wake-like activities allowing the emergence of an excitatory wave packet essential for the ignition of the down state. After the down state, sigma activity reflects only the activity of isolated thalamo-cortical modules involved in memory consolidation. These conjectures are supported by unpublished data of ours indicating that sigma activity of the early positive bump shows a higher large scale synchronization with respect to sigma crowned upon the up state.

Future works and research lines

There are several future works and research lines arising from this work that we are pursuing:

- Spectral characterization of evoked K-Complexes.
- Spectral characterization of the EEG baseline preceding the early positive bump/P200 of evoked K-Complexes, in order to identify a possible early thalamic engagement .
- Experiment aimed to identify the relationships between SSO phases and memory consolidation by using a paradigmatic task (rotation task [140]).
- Experiment aimed to identify the relationships between SSO phases/dynamics and *ad hoc* excitatory bumps evoked by transcranial magnetic stimulation.
- Experiments in pre-clinical and clinical conditions, such as stressful situations or primary insomnia.

Appendix A

The electrophysiological basis of sleeping brain

A.1 Sleep macro-architecture: stages and cycles

Sleep is a cyclical state which alternates with wakefulness, and in humans they have a circadian periodicity of about 24 hours. Since circadian rhythms are endogenous, they require the presence of an internal clock. In mammals, one major internal clock is the suprachiasmatic nucleus (SCN) of the anterior hypothalamus. Environmental light entrains this rhythm by means of the retinohypothalamic tract, a pathway that runs from the retina to the SCN, in fact the SCN is active during the day, both in diurnal and nocturnal animals. Even if the sleep patterns are under the influence of the SCN (and therefore the presence of environmental light), this neural centre is not responsible for the sleep itself. To understand which centre (or centres) of our brain regulates the sleep falling and its maintenance, it is necessary to focus and examine the sleep architecture in detail.
Behaviorally, the sleep is defined by four criteria:

(I) reduced or inhibited motor activity;

(II) decreased responsiveness both to internal and external stimuli;

(III) stereotypical postures;

(IV) relatively easy reversibility (which differentiates it from other states of altered consciousness).

These criteria are features of the whole sleep condition, but the sleep is not uniform and, in the course of night, it goes through an orderly progression of sleep stages

organized in cycles. Each sleep stage is strictly related to specific behavioral and neurophysiological activities which are promoted by different neural systems. Each neurophysiological activities can be recognized by electrical recordings: electroencephalogram (EEG), eye movements (EOG, electroculogram), and muscle tone (EMG, electromyogram). According to *American Academy of Sleep Medicine* (AASM) criteria [48], the humans sleep pattern is conventionally divided into four stages [48]:

N1 stage: is a transitional stage between the wakefulness and sleep and it is usually referred to as somnolence or drowsy sleep. The behavioral activities involve slow rolling eye movements, partial relaxation of voluntary muscles and decreased awareness of the external environment. The electrophysiological pattern is characterized by loss of alpha activity (prominent during during wakeful relaxation with closed eyes) and the appearance of a low-voltage activity with prominent theta one (4–8 Hz).

N2 stage: is recognizable on EEG by the appearance of bursts of *K-complexes* and *sleep spindles* and a background activity in theta band (similar to N1 stage). K-complexes are the largest graphoelement at the EEG level, and they are made up of a high-amplitude negative wave followed by a positive slow wave, and are often triggered by external stimuli. K-complexes are deal more in detail in the following sections. Sleep spindles are waxing and waning sinusoidal oscillations (12–15 Hz) that last about 1 second. Behaviorally, N2 stage is considering fully as sleep because people are completely disconnected from the external environment, meaning that they do not respond to the events around them and their arousal threshold is increased. The eye movements and muscle tone are much reduced with respect to N1 stage.

N3 stage: this sleep stage is also referred to as *slow wave sleep* (SWS) or delta sleep[1]. Since the threshold for arousal is higher than in N2 stage and it is characterized by the prevalence of delta activity (a minimum of 20% of frequencies in the range 1-4 Hz and amplitude higher then 75 μV) at the EEG level[2]. The eye movements is not present during stage N3 and EMG activity decreases further.

[1]In the previous sleep classification, the N3 stage was further considered divided into two stages (stage 3 and 4), which are characterized by different amount of delta band frequencies in EEG recordings.

[2]EEG standards define delta activity between 1 to 4 Hz, but in both the old sleep standards

REM Sleep: the EEG during REM sleep is similar to the EEG recorded in waking or N1, therefore this stage is also referred to as *paradoxical sleep*, but it is fully deep sleep, with an arousal threshold that is as high as in N3 stage. The name of this sleep stage was due to the peculiar *rapid eye movements* (REMs) recorded on EOG during this stage. On EEG, REM sleep is characterized by unstructured low-voltage fast-activity, with high power in the theta band. REM sleep is subdivided into tonic and phasic components. Tonic components of REM sleep comprehend the activated EEG and a generalized loss of muscle tone, excepting the extra-ocular muscles and the diaphragm. Phasic components of REM include irregular bursts of rapid eye movements and muscle twitches.

The stage N1, N2 and N3, ordered by their deepness, are usually referred to non-REM sleep (*NREM sleep*). Humans fall asleep by entering firstly into NREM sleep and then into REM sleep, typically the orderly progression is N1 $\rightarrow$ N2 $\rightarrow$ N3 $\rightarrow$ N2 $\rightarrow$ REM, this succession of NREM sleep stages followed by an episode of REM sleep is called a *sleep cycle*. In a normal night's sleep, a sleep cycle lasts approximately 70-120 minutes, and there are a total of 4-6 cycles. Slow wave sleep is prominent in the early sleep cycles of the night, and diminishes during the progression of the night. On the contrary, the periods of REM sleep become longer and show greater phasic activity with the night progression. The succession of the sleep stages, during the night of a subject, is well described by a diagram called hypnogram (for a example see Figure A.1). Typically, A human healthy young adult will spend about 5% of the sleep period in stage N1, about 50% in stage N2, 20–25% in stage N3, and 20–25% in REM sleep.

[141] and new guidelines [48] it has a range of 0.5–2 Hz. In this work we refer to delta activity as 1-4 Hz range.

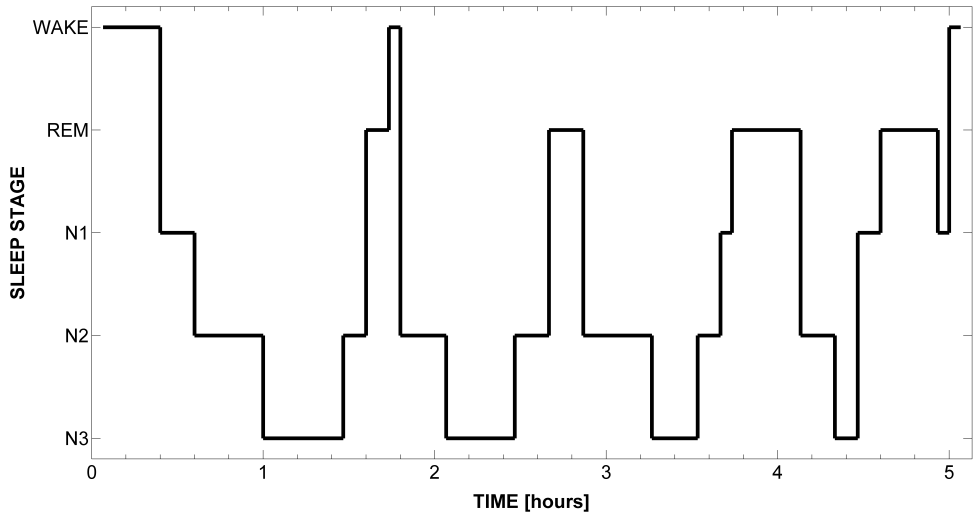

Figure A.1. Hypnogram of a representative healthy subject. REM, N1, N2 and N3 (Slow Wave Sleep) indicate sleep stages according to AASM scoring criteria.

A.2 Neurophysiology of Sleep and Wakefulness

A.2.1 Pioneering Steps

In the past, many scientists working on sleep explain the sleep falling as a result from reduced brain activity induced by the fatigue during awake state. They have argued that the wakefulness is sustained by the sensory stimulation, and the sleep arises when the sensory stimulation is reduced by the physical fatigue. This view about sleep was not completely fulfilling and many aspects remained unexplained.

The early successful studies about the explanation of the sleep role were conducted in the 1940s, when the neurophysiology of sleep have been widely investigated by Moruzzi and Magoun. In 1945, they found that transection of the ascending sensory pathways in the brain stem did not altered either sleep or wakefulness. On the contrary, they observed that lesions of the reticular formation of the brain stem induced behavioral stupor and an electroencephalographic pattern resembling sleep even though these lesions did not disturb the ascending sensory pathways. Based on these findings, Moruzzi and Magoun hypothesized the so-called *passive view* of sleep role: the tonic activity of the reticular formation (driven by sensory input) keeps the forebrain awake, and that a reduction in the activity of the reticular formation produces sleep. Then Moruzzi and Magoun developed the

concept of the *ascending activating reticular system*, and the reticular formation in the brainstem became the main candidate for "wakefulness brain centre".

The invention of the electroencephalograph[3] allowed scientists to study sleep in ways that were not previously possible. In the early 1950s, Kleitman[4] and his students used this electroencephalograph to discover that sleep has two distinct alternating phases: one characterized by rapid eye movements (*REM sleep*) and another one without eye movements (*NREM sleep*). Periodic REM sleep episodes (with low voltage and high frequencies EEG patterns) have been described since past times, they were termed *sonno profondo* (deep sleep) by Fontana around 1765, and in the late 1930s described as *Tiefen Schlaf* by Klaue [143]. The dichotomous aspect of the sleep (NREM/REM) influenced the following researches about sleep, that focused to investigate the specific brain centres e neurotransmitters responsible of each sleep state.

In the late 1950s, Moruzzi and his colleagues made a second great discovery: they transected the brain stem, including its reticular formation through the pons, and they observed that sleep was greatly reduced. They suppose that the reticular formation of the brain stem does not act uniformly in regulating sleep. Rather, the rostral portion of the reticular formation (the portion above the pons) contains neurons whose activity contributes to wakefulness. Normally, this activity is inhibited by neurons in the portion of the reticular formation below the pons. By founding a sleep-promoting specific brain centre, they rejected their initial hypothesis of passive role of the sleep.

While in their classic study Moruzzi and Magoun demonstrated that wakefulness and sleep are promoted by different neural systems, the works of Moruzzi and Kleitman proved that the sleep is an actively induced and highly organized brain state with different phases, and they displaced the idea that sleep is simply a state of reduced activity.

Some years later, Jouvet and his colleagues discovered that the oscillator for the REM sleep is located in the pontobulbar brainstem [144]. They also observed the

[3]Hans Berger recorded the first human EEG in 1924. Expanding on work previously conducted on animals by Richard Caton and others, Berger also invented the electroencephalogram, an invention described as "one of the most surprising, remarkable, and momentous developments in the history of clinical neurology".

[4]Nathaniel Kleitman was a leading proponent of the passive theory of sleep. He emphasized that there are not proofs that support the theory of active sleep and that what needs to be explained is not sleep, but wakefulness [142].

presence of muscular atonia and spiky pontine waves, thus establishing the signs that differentiate REM sleep from the other states of the sleep-waking cycle. After, Pompeiano and his colleagues described the mechanisms of muscular atonia, and they showed that both tonic and phasic inhibition of spinal reflexes occur during REM sleep in unrestrained cats [145].

A.2.2 Brain Mechanisms of Wakefulness and Sleep States

Wakefulness

Both wakefulness and sleep promotion can not be associated by only one neurotransmitter system or one brain structure. The human brain centres involved in the maintenance of wakefulness are the *reticular activating system* (RAS, situated in the upper pons and midbrain), the posterior hypothalamus and the basal forebrain. These neuronal groups are able to release over large brain regions the neurotransmitters and neuromodulators (acetylcholine, histamine, noradrenaline, glutamate and hypocretin) responsible of neural activation during wakefulness. All these neurotransmitters and neuromodulators induce cortical activation by closing the leakage potassium channels on the cell membrane of thalamic and cortical neurons, in this way these cells are kept depolarized and ready to fire.

The role of hypothalamus in the regulation of sleep and wakefulness is relate to the histaminergic neurons located in the *tuberomammillary nucleus* (a subnucleus of the posterior third of the hypothalamus). These neurons project over the cortex and are connected to cholinergic cells of the pons. The histaminergic cells fire at highest frequencies in waking and are inhibited during sleep (both NREM and REM).

In basal forebrain there are two structures named *pedunculopontine tegmental nucleus* (PPT) and *lateral dorsal tegmental nucleus* (LDT). The cholinergic neurons situated in these neuronal structures fire at high frequencies during both wakefulness and REM sleep and they reduce or stop firing during NREM sleep[5]. The cholinergic cells of PPT/LDT contribute to depolarize specific and intralaminar thalamic nuclei via their projections to the thalamus. The intralaminar thalamic nuclei project over large cortical areas and they fire at high rates during both

[5]Acetylcholine is released in high levels in waking, alertness and REM sleep. Its lowest levels have been found in NREM sleep (slow wave sleep) when there is no cortical arousal

wakefulness and REM sleep. These nuclei induce the cortical neurons to fire synchronized at EEG frequencies higher then 28 Hz. Activation inputs to cortex are also provided by cholinergic and glutamatergic neurons located in basal forebrain which receive projections from cholinergic cells of dorsal forebrain.
The glutamatergic neurons located in RAS and basal forebrain are also able to promote wakefulness, in fact glutamate can acts as a neuromodulator and it can influence the excitability of his target neurons.
In the *locus coeruleus* in the upper pons, there are present noradrenergic cells (LC-NA system) which fire tonically during wakefulness and start to fire with phasic burst in response to salient stimuli (behaviorally relevant and naturally evoke a behavioral reaction: intense stimuli, aversive stimuli or novel stimuli). Their firing decreases markedly during NREM sleep and disappears during REM sleep. The LC-NA system have dense excitatory projections to the majority of the cerebral cortex.
Serotonin is mostly produced in waking by the neurons of the *anterior raphe nucleus* in the reticular formation, which project widely to the hypothalamus and the cortex. Stimulation of the raphe nuclei produces cortical arousal and automatic motor behavior. The serotoninergic neurons fire at higher frequencies during wakefulness, lower during NREM sleep and stop firing in REM sleep.
Another important neurotransmitter for wakefulness promotion is dopamine, which originates in the cells of the *substantia nigra* and *ventral tegmental area*. These neurons connect with the frontal cortex, basal forebrain and limbic structures. The inhibition[6] of dopamine re-uptake increases dramatically wakefulness and alertness.
The hypocretin is released by cells in the posterior hypothalamus. These cells firing in waking state (in particular during motor activity and exploratory behavior) and they are inhibited during sleep (both NREM and REM sleep).

Sleep

The inhibition of wakefulness-promoting brain structures is essential for the initiation of the sleep. The brain structures responsible of this inhibition are located in the basal forebrain and anterior hypothalamus (in particular the *ventrolateral*

[6]The dopaminergic neurons not seem to change their firing with respect to behavioral state, but some dopamine agonists (as ritalin, cocaine and amphetamines) can enhance the release of dopamine.

preoptic area (VLPO, which came to be known as the "sleep centre") and the *median preoptic nucleus*). During NREM sleep the cells of these areas tend to fire and release GABA and galanin, in this way they inhibit the neuronal groups sited in wakefulness-promoting regions (including cholinergic, noradrenergic, histaminergic, hypocretinergic and serotoninergic neurons). The reduction of the waking-promoting neurotransmitters and neuromodulators provokes the opening of leak potassium channels in thalamus and cortex, and their neurons become hyperpolarized start to fire at very low frequencies.
The most important biochemical changes during REM sleep with respect to NREM sleep are the great amount of acetylcholine in the thalamus and the the presence of acetylcholine and glutamate in the basal forebrain. This biochemical condition induces an intense activity in the limbic system and in the cortex, similar to waking state. The brain generators of REM sleep are the pontine cholinergic cells (LDT and PPT, witch are members of wakefulness system), and cell groups in the medial pontine reticular formation and medulla. During REM sleep, the neurons in dorsal pons are activated and induce the tonic inhibition of muscle tone, and the cells of medial pontine reticular formation fire with a bursting patterns and provoke REMs and muscle twitches.

A.3 Environment and sleep: the conventional view

As above mentioned, one of the most relevant feature of the sleep state is the decreased responsiveness both to internal and external stimuli [146] and therefore a disconnection from environment. The environmental disconnection is gradually with respect to progression of sleep stages (from N1 to REM), and it can be monitored by the progressive (from N1 to N3) increase of the threshold for responding to external stimuli. But what means that during sleep the responsiveness to environment is reduced or inhibited and how much the degree of cognitive capabilities are weaken or vanish? Many experimental evidence show that the processing of external information is not completely disrupted during sleep, but the brain preserves some processing pathway (probably at low level) to elaborate external information. Certainly, the thalamocortical network is main brain director to acquire, analyze, store and retrieve sensory information both in waking and in sleep state. In fact, one of the main function of the thalamus is the selective control of the sensory information flow during different states of consciousness. In this contest, only the olfactory stimuli have a different processing pathway that is kept

out from the thalamic processing.
During wakefulness, the thalamocortical relay cells are tonic depolarized and they exhibit activity with tonic firing patterns, that is the groundwork for the desynchronized, low amplitude, high frequencies EEG waves typical of activated activities. From the peripheral sense organs, the sensory nerve impulses reach the thalamus and they produce excitatory postsynaptic potentials, which easily pass the low-level threshold of the thalamic cells. The thalamic neurons generate outgoing impulses, that are transmitted at the cortical areas related to the sensory modality of the stimuli (the cortical primary sensory areas).
Whereas, during NREM sleep the thalamocortical sensory pathway is considered partially closed (the so-called *thalamic gating*). Indeed, the sensory stimuli fail to reach at the cortex because they are stopped at thalamocortical level, due to the hyperpolarizations and subsequent neuronal bursting (spindles) of thalamocortical neurons. Besides, sleep spindles are able to blocking the incoming sensory stimuli, by decoupling the inputs from outputs via their intrinsic fast oscillations at thalamic levels. In spite of the thalamic gate during NREM sleep, it is possible to identify evoked responses on the cortex due to peripherally stimulations, and some neuroimaging studies have show that activations of primary sensory areas ensue the stimuli onset [ref]. The classical electrophysiological correlate of sensory stimulation during NREM sleep is the K-complex and it will treated more in detail in a next section. Some studies have suggested that during NREM sleep the lost of sensory information stream is due to the *breakdown* of cortical effective connectivity and not to the information gating at thalamic level. These studies show that the activation of sensory primary areas by TMS (transcranical magnetic stimulation) is not followed by the activation of higher-order cortical areas. Also during REM sleep the responsiveness to sensory stimulation is inhibited, and the brain seems to be focused on his internal activity. More in general, consciousness disappears during the deep stage of the sleep and it seems to reappear during dreams occurring in REM stage. Certainly, the consciousness during REM is altered, one of the most evident feature of the dream consciousness is the sensory-disconnection from the external world, in this case we can speak about *internal consciousness*.
Despite of the inhibition of high-level sensory information processing during sleep, it is well known that a sleeper can be awakened by both intense stimulus and not intense but meaningful ones. The threshold for awakening is lower for relevant stimuli than for stimuli of the same modality and intensity but non relevance for the subject. In [147] is shown that sleeping subjects are awakened faster when hearing their own names than other names. The latency from sleep to waking

state is shorter for stimuli having a special significance than neutral ones, as reported in [148]. Also the experiments using EEG evoked potentials during sleep support the discriminative proprieties of the sleeping brain with respect to sensory processing. The electrophysiological representation of auditory stimulation (using an oddball paradigm) seems to be the same both in wakefulness and in sleep [149], but it is found that during sleep the processing of auditory information is slower and delayed [150]. Bastuji and his colleagues [151] shown that the late components in auditory evoked responses were selectively enhanced after the presentation of the subject's own name with respect to presentation of other names. In an important combined EEG-fMRI human study [128] it was show how some areas of the prefrontal cortex are more activated by meaningful stimuli (subject's name) than not meaningful ones (acoustic tone), it was also reported that the auditory cortex is activated . All these studies conclude that the environmental information processing is maintained during NREM and REM sleep even thought it was reduced or altered with respect to wakefulness, but it is still controversial the degree to which the cortex receives external information during sleep. Indeed, the processing of external stimuli during sleep is very important for the survival and safety. Nevertheless more in general, the exact reduction of the degree of consciousness, in transition from waking to sleeping, remains difficult to establish. In sleep research, the averaged event-related potential (ERPs) are one of the most used electrophysiological methods for investigating the brain's responsiveness to external stimuli, since electrophysiological measures are independent of behavioral activity or state of consciousness. In most of the studies the used experimental protocol is the "oddball paradigm", in which infrequent target stimuli are presented within a series of rapidly standard stimuli. During wakefulness, the P300 component[7] of the ERP followed the target stimuli is associated to the active detection of the stimulus, since this component is not detectable when subject ignores or not recognizes the target stimulus. Interestingly, during NREM sleep the P300 was not detected [116], the N100 seems to be attenuated while the P200 is higher with respect to wakefulness. Besides, in NREM sleep are present some sleep-specific ERP components such as the N350, P450, N550 and P900. All these alterations in ERPs are associated with the decrease of cortical excitability and

[7]By convention, the ERP components are labeled considering both their electrical polarity - positive (P) or negative (N) - and average latency of maximum amplitude peak of the component. For example, P300 refers to the ERP component with positive electrical polarity and an average latency of its maximum amplitude at about 300 msec after the stimulus onset.

increase of inhibitory mechanism in the transition to sleep from waking state.

A.4 Electrophysiological correlates of NREM sleep

The changes of neural mechanisms between wakefulness, NREM sleep and REM sleep are reflected in different electrophysiological correlates, evaluable from EEG recordings.
During waking state, the cortical and thalamic neurons are ready to respond to each external or internal input, for this reason these cells are permanently depolarized close the firing threshold. This neuronal condition explains the presence of low-voltage fast-activity on EEG recordings (named as "activated") during wakefulness. On this background activity, it is possible to observe oscillatory EEG phenomena, which are distinctive frequency bands and cortical topographies[152]. The frequency ranges of these events are alpha (8-12 Hz), beta (13-30 Hz) and gamma (>30 Hz and unlimited in upper range). Alpha rhythm is the classical EEG correlate for a state of relaxed wakefulness with the eyes closed. It is attenuated or suppressed by alertness or stimuli (influx of light (eye opening), other afferent stimuli, and mental activities), and it is then supplanted by faster activity. The alpha activity is a manifestation of the posterior half of the head and is usually found over occipital, parietal and posterior temporal cortical regions. Beta activity is found in almost every healthy adult EEG, and it is associated with arousal of the cortex to higher state of alertness or tension, it also represents the retrieving of memories. Rhythmical beta activity is encountered chiefly over the frontal and central cortical regions, and its amplitude seldom exceeds 30 μV. Gamma activity seems to be involved in higher mental activity, including perception and consciousness, and it can be recorded from all lobes of the cerebrum. Historically, the term gamma was originally used for the designation of faster beta activity[8].
At a glance, the EEG recordings in REM sleep have similar patterns with respect to wakefulness or N1 stage: an activated, low-voltage high-frequency oscillation.

[8]The terms "alpha" and "beta" rhythms were introduced by Berger [153], the term "gamma" rhythm was subsequently used by Jasper and Andrews [154] in order to designate EEG activities above 30 or 35 Hz; these were essentially 35-45 Hz and superimposed on the occipital alpha rhythm [155]. This term was abandoned and "gamma" frequencies became a part of the beta range. During the 1990s, the term "gamma" rhythm was intensely recovered. It is ordinarily used in modern EEG researches, in light of the fact that, recently, there are found different properties and neuronal sources between gamma and beta rhythms [156, 157]

But this activity is combined with a more powerful theta band ground pattern, in particular with respect to the wakefulness. Besides during REM sleep, it is possible to identify the so-called *saw-tooth waves*, which are a special type of central theta activity that has a distinguishing morphology resembling the blade of a saw and usually occurs close to REMs.
On the other hand, the EEG recordings in NREM sleep (except for N1) is very different from ones during both waking and REM sleep. It is characterized by an ongoing oscillation in theta (during N2) and delta (prominently in N3) ranges.
Delta waves are generated between cortical layers 2 to 3 and 5. A delta oscillation can be induced by the interplay of two intrinsic currents of thalamocortical neurons (the hyperpolarization-activated cation current and the transient low-threshold Ca^{2+} current). The thalamocortical neurons, after the disconnection from the cortex, are hyperpolarized at about 10 mV and as a consequence they exhibit a spontaneous, self-sustained delta activity. However, this oscillation would be not be synchronized over large assembles of neurons (and thus not visible on EEG), but there are some factors that provide for the synchronization. The synchronization may be realized by both some local factors and the widespread connections from RTN and other thalamic nuclei. The simultaneous delta oscillations of thalamic cells are enhanced and synchronized by thalamocortical volleys, in fact the synchrony between different thalamic relay neurons during delta activity has not been found in decorticated animals [28]. It is demonstrated that delta activity during sleep may be essential for memory consolidation and memory formation [158, 6, 43].
On this background activity, there are abruptly superimposed some peculiar EEG signatures: ***sleep spindle wave***, ***Sleep Slow Oscillation*** (SSO) and ***K-complex*** (KC). This thesis is focused on the cerebral information processing during NREM sleep, so each electrophysiological correlate and the ongoing activity of the NREM sleep are described in detail in the next sections.

A.4.1 Sleep spindles

Sleep spindle oscillation appears in the thalamus and cortex during N2 stage or grouped with active phases of SSOs. It consists of waxing-and-waning field potentials at 12-15 Hz (for humans), which last 1-3 seconds and recur every 5-15 seconds. The spindle waves originate in the thalamus as a results of the interaction of neurons containing inhibitory γ-aminobutyric acid (GABA) of the *reticular thalamic nucelus* (RTN), the thalamocortical cells, and the cortical pyramidal cells [94, 159].

The TRN is positioned to uniquely influence the information flux between the cortex and the thalamic neurons: the reticular neurons receive excitatory inputs from axons collaterals both of thalamus that project to the cortex and of cortical cells that project to the thalamus. Thalamic reticular neurons project back to the rest of the thalamus, and innervate other cells of RTN. The neuronal oscillation at the spindle range are effectively generated into the RTN, as proved by the fact that the isolation of this neuronal structure from the rest of thalamus and the cortex abolished the spindle oscillations in dorsal thalamus and cortex, but the deafferented RTN can itself oscillate in frequency range of spindle. The reticular neurons generate bursts at spindle frequency range by low-threshold Ca^{2+} spikes, which are superimposed to slow depolarizing envelope. By means of GABA-containing axons of reticular cells, their spindle bursts inhibit a large population of thalamocortical neurons, which exhibit rhythmic inhibitory postsynaptic potentials (IPSPs) at spindle frequency These IPSPs can remove the inactivation of low-threshold Ca^{2+} current inducing a rebound of Ca^{2+}, that is associated with a burst of action potentials. These thalamocortical rhythmic bursts induce excitatory postsynaptic potentials (EPSPs) in cortical pyramidal neurons which are expressed by spindle waves on EEG. Concerning the functional role of spindle oscillations, it is shown that they are essential for memory formation [158] and for the short and middle term synaptic plasticity [160].

A.4.2 Sleep Slow Oscillations

As regards the oscillation processes at low frequencies during NREM sleep, the intracellular studies distinguish between delta oscillation and SSO. The former oscillates at 1-4 Hz and the second at less then 1 Hz, each of them are also characterized by distinct origins and cellular oscillating mechanisms. The SSO is one of the most examined phasic events in sleep EEG[9], it occurs during N2 and N3 sleep stages but not during N1 stage, REM sleep or wakefulness. As above mentioned, despite its low characterized frequency (<1Hz, mainly 0.3 to 1 Hz) it has different

[9]The first one who described the Sleep Slow Oscillation and its neuronal mechanisms was **Mircea Steriade** by using intracellular recordings in animals and field potential recordings during human sleep. He was also known for his pioneering studies about the identification of the neuronal properties in corticothalamic systems during wakefulness or different states of consciousness. Furthermore, he was the first to demonstrate the role of GABAergic thalamic reticular neurons in the generation of sleep spindles. All these important fundings have earned Steriade the reputation of the *Master of Rhythms* [sleep,2006].

origins with respect to delta waves. Intracellular studies showed that SSO arises from the layers 2 to 6 of several (sensory, motor and associational) cortical areas, and there are involved not only the neocortical pyramid cells but also inhibitory, local-circuit neurons. Probably, the slow depolarizations (expressed by SSOs) are induced by synaptic inputs, this mechanism is mediated by N-methyl-D-aspartate receptors (NMDAR) and it is also sustained by a persistent Na^+ current. Long-lasting hyperpolarizations follow these phases of depolarization, and they were synchronous with grouped EEG oscillations at similar frequencies (especially 0.2 to 0.5 Hz, but however less then 1 Hz). Electrophysiological studies in animal models have revealed that cortical neurons show a coordinated switching behavior of the membrane potential during the SSO: they synchronously oscillate between a state of hyperpolarization (*down state*) and a state of wake-like depolarization (*up state*), both lasting several hundreds of millisecondes. This behavior represents the fundamental cellular phenomenon underlying different slow and fast neural activities in SWS, such as K-complexes, delta waves and spindles. The SSO in the human EEG corresponds to a sharp negative peak (related to the down state) followed by a shallow positive half wave (related to the up state). The positive phase of each SSO has also the property of grouping spindles and faster activities. Indeed, it has been observed in animal models and in humans that periods of cortical hyperpolarization (down state) are followed by strong rebounds of spindle activity which represent the grouping influence of the SSO on thalamocortical cells. This property has been considered relevant for establishing reiterative processing of memories during NREM sleep. Furthermore, the SSO originates mainly in frontal regions and propagates across variable cortical territories at a typical speed of a few m/sec, preferentially in a fronto-posterior direction. From the point of view of scalp signal analysis, each SSO is concurrently detected on a variable set of EEG electrodes, with delays related to the propagation. Consequently, each set of quasi simultaneous SSO constitutes a propagating SSO event. From an anatomical standpoint, the SSO in cortex survives to extensive thalamic lesions or destruction of thalamocortical neurons, although it is detectable in thalamocortical neurons of various thalamic nuclei and in neurons belonging to the RTN. In addition, animal models indicate that intact thalamocortical circuits have substantial influence on the generation and synchronization of the cortical SSO. In this contest, it is still under debate if the human SSO is generated in the neocortex and then imposed on thalamic territories or it is generated by a mutual interplay between thalamus and cerebral cortex. In our recent study [30], we have studied the thalamic role in the cortical expression of the SSO in humans, by comparing SSO features in a case

of Fatal Familial Insomnia (FFI)[10] and a group of controls. The results of our study are reported and described in Chapter 2.

A.4.3 K-complexes

The late components of ERPs during NREM sleep (the N550 and P900) are a reflection of the so-called K-complex (KC). Historically, the term K-complex was referred to characterized large potential waves on EEG elicited by an acoustic stimulation during NREM sleep [36]. Because they are produced within the same network (the cortex), KCs had the same neurophysiological features of the previous described SSOs: frequency range less then 1 Hz, a hyperpolarized phase (down state) followed by a depolarized one (up state), a spindle grouping effect on up state and the traveling behavior on the cortex. As concerning of the scalp distribution of KC, in [135] was reported that the down state of the auditory-evoked K-complex was maximal over fronto-central areas of the scalp. The KCs is known to also occur both as a response to other sensory modality and not evoked by external stimuli. Traditionally, KCs are reputed as *non-specific*, *diffuse* and *delayed* electrophysiological responses [103]. In particular, the non-specificity of KC was related to the modality of eliciting sensory input [96]. Probably, this view of the KCs was mainly caused by the fact that, in the past, it was no possible to study accurately the dynamic and topology of this electrophysiological correlate because the EEG channel montage was very limited (due to the lack of high-density EEG methodology). More recently, in [105] it was studied the topology down state of KCs evoked by both acoustic and somatosensory (respiratory occlusion) stimuli thought a 29-channels EEG montage, they not found any differences about the resulting topographies between the two modalities of stimulation. The idea of evoked KC as a modality independent sleep response was after confirmed in [118], in this exhaustive review was also reported that the brain dynamic of evoked KCs not involves the sensory-relay thalamocortical pathways. In a recent combined EEG-fMRI work [108], it was observed that during sleep the auditory cortex is activated in response to acoustic stimulus only when there is a consequent elicitation of a KC, in addition, it was also found an activation of middle frontal

[10]Fatal familial insomnia is an autosomal dominant prion disease, caused by a mutation in codon 178 of the *PrP* gene. This disease interferes with sleep and leads to deterioration of mental and motor functions, and in general to alteration of the main autonomic functions. In FFI patients, death occurs within about 7 to 36 months after symptoms begin.

gyri and cingulate areas during an acoustic evoked KC. The functional role of KC remains a subject of debate. On the one hand, it is believed that the KC represents a electrophysiologic correlate of arousal process without awakening [96], on the other hand the KC is viewed as a sleep-protecting mechanism [118] by triggering anti-arousal reactions.

Bibliography

[1] M. Steriade, A. Nuñez, and F. Amzica. A novel slow (< 1 hz) oscillation of neocortical neurons in vivo: depolarizing and hyperpolarizing components. *J Neurosci*, 13(8):3252–3265, Aug 1993.

[2] A. Destexhe, D. Contreras, and M. Steriade. Spatiotemporal analysis of local field potentials and unit discharges in cat cerebral cortex during natural wake and sleep states. *J Neurosci*, 19(11):4595–4608, Jun 1999.

[3] A. Nuñez, F. Amzica, and M. Steriade. Electrophysiology of cat association cortical cells in vivo: intrinsic properties and synaptic responses. *J Neurophysiol*, 70(1):418–430, Jul 1993.

[4] I. Timofeev and S. Chauvette. Thalamocortical oscillations: local control of eeg slow waves. *Curr Top Med Chem*, 11(19):2457–2471, 2011.

[5] G. Buzsáki. Memory consolidation during sleep: a neurophysiological perspective. *J Sleep Res*, 7 Suppl 1:17–23, 1998.

[6] P. Maquet. The role of sleep in learning and memory. *Science*, 294(5544):1048–1052, 2001.

[7] P. Peigneux, S. Laureys, X. Delbeuck, and P. Maquet. Sleeping brain, learning brain. the role of sleep for memory systems. *Neuroreport*, 12(18):A111–A124, Dec 2001.

[8] M. Steriade and I. Timofeev. Neuronal plasticity in thalamocortical networks during sleep and waking oscillations. *Neuron*, 37(4):563–576, Feb 2003.

[9] Matthias Mölle, Lisa Marshall, Steffen Gais, and Jan Born. Learning increases human electroencephalographic coherence during subsequent slow sleep oscillations. *Proc Natl Acad Sci U S A*, 101(38):13963–13968, Sep 2004.

[10] P. Achermann and A. A. Borbély. Low-frequency (< 1 hz) oscillations in the human sleep electroencephalogram. *Neuroscience*, 81(1):213–222, Nov 1997.

[11] Marcello Massimini, Reto Huber, Fabio Ferrarelli, Sean Hill, and Giulio Tononi. The sleep slow oscillation as a traveling wave. *J Neurosci*, 24(31):6862–6870, Aug 2004.

[12] Matthias Mölle, Lisa Marshall, Steffen Gais, and Jan Born. Grouping of spindle activity during slow oscillations in human non-rapid eye movement sleep. *J Neurosci*, 22(24):10941–10947, Dec 2002.

[13] Danilo Menicucci, Andrea Piarulli, Ursula Debarnot, Paola d'Ascanio, Alberto Landi, and Angelo Gemignani. Functional structure of spontaneous sleep slow oscillation activity in humans. *PLoS One*, 4(10):e7601, 2009.

[14] Andrea Piarulli, Danilo Menicucci, Angelo Gemignani, Umberto Olcese, Paola d'Ascanio, Alessandro Pingitore, Remo Bedini, and Alberto Landi. Likeness-based detection of sleep slow oscillations in normal and altered sleep conditions: application on low-density eeg recordings. *IEEE Trans Biomed Eng*, 57(2):363–372, Feb 2010.

[15] A. Destexhe, D. Contreras, and M. Steriade. Cortically-induced coherence of a thalamic-generated oscillation. *Neuroscience*, 92:427–443, 1999.

[16] Maxim Bazhenov, Igor Timofeev, Mircea Steriade, and Terrence J. Sejnowski. Model of thalamocortical slow-wave sleep oscillations and transitions to activated states. *J Neurosci*, 22(19):8691–8704, Oct 2002.

[17] A. Compte, M.V. Sanchez-Vives, D.A. McCormick, and X. Wang. Cellular and network mechanisms of slow oscillatory activity (¡1 hz) and wave propagations in a cortical network model. *J Neurophysiol*, 89(5):2707–2725, May 2003.

[18] M. V. Sanchez-Vives and D. A. McCormick. Cellular and network mechanisms of rhythmic recurrent activity in neocortex. *Nat Neurosci*, 3(10):1027–1034, Oct 2000.

[19] D. Contreras and M. Steriade. Cellular basis of eeg slow rhythms: a study of dynamic corticothalamic relationships. *J Neurosci*, 15(1 Pt 2):604–622, Jan 1995.

[20] I. Timofeev, F. Grenier, M. Bazhenov, T. J. Sejnowski, and M. Steriade. Origin of slow cortical oscillations in deafferented cortical slabs. *Cereb Cortex*, 10(12):1185–1199, Dec 2000.

[21] R. Liguori, A. Vincent, L. Clover, P. Avoni, G. Plazzi, P. Cortelli, A. Baruzzi, T. Carey, P. Gambetti, E. Lugaresi, and P. Montagna. Morvan's syndrome: peripheral and central nervous system and cardiac involvement with antibodies to voltage-gated potassium channels. *Brain*, 124(Pt 12):2417–2426, Dec 2001.

[22] F. Provini, P. Cortelli, P. Montagna, P. Gambetti, and E. Lugaresi. Fatal insomnia and agrypnia excitata: sleep and the limbic system. *Rev Neurol (Paris)*, 164(8-9):692–700, 2008.

[23] Thien Thanh Dang-Vu, Manuel Schabus, Martin Desseilles, Geneviève Albouy, Mélanie Boly, Annabelle Darsaud, Steffen Gais, Géraldine Rauchs, Virginie Sterpenich, Gilles Vandewalle, Julie Carrier, Gustave Moonen, Evelyne Balteau, Christian Degueldre, André Luxen, Christophe Phillips, and Pierre Maquet. Spontaneous neural activity during human slow wave sleep. *Proc Natl Acad Sci U S A*, 105(39):15160–15165, Sep 2008.

[24] Victor I. Spoormaker, Michael Czisch, Pierre Maquet, and Lutz Jäncke. Large-scale functional brain networks in human non-rapid eye movement sleep: insights from combined electroencephalographic/functional magnetic resonance imaging studies. *Philos Trans A Math Phys Eng Sci*, 369(1952):3708–3729, Oct 2011.

[25] Danilo Menicucci, Andrea Piarulli, Paolo Allegrini, Marco Laurino, Francesca Mastorci, Laura Sebastiani, Remo Bedini, and Angelo Gemignani. Fragments of wake-like activity frame down-states of sleep slow oscillations in humans: New vistas for studying homeostatic processes during sleep. *Int J Psychophysiol*, Feb 2013.

[26] M. Steriade. Grouping of brain rhythms in corticothalamic systems. *Neuroscience*, 137(4):1087–1106, 2006.

[27] M. Steriade, D. Contreras, F. Amzica, and I. Timofeev. Synchronization of fast (30-40 hz) spontaneous oscillations in intrathalamic and thalamocortical networks. *J Neurosci*, 16(8):2788–2808, Apr 1996.

[28] I. Timofeev and M. Steriade. Low-frequency rhythms in the thalamus of intact-cortex and decorticated cats. *J Neurophysiol*, 76(6):4152–4168, Dec 1996.

[29] Vincenzo Crunelli and Stuart W. Hughes. The slow (<1 hz) rhythm of non-rem sleep: a dialogue between three cardinal oscillators. *Nat Neurosci*, 13(1):9–17, Jan 2010.

[30] A Gemignani, M Laurino, F Provini, A Piarulli, G Barletta, P d'Ascanio, R Bedini, R Lodi, D.N. Manners, P. Allegrini, D. Menicucci, and P. Cortelli. Thalamic contribution to sleep slow oscillation features in humans: a single case cross sectional eeg study in fatal familial insomnia. *Sleep Med*, 13(7):946–952, Aug 2012.

[31] Giulio Tononi. Consciousness as integrated information: a provisional manifesto. *Biol Bull*, 215(3):216–242, Dec 2008.

[32] P. Allegrini, P. Paradisi, D. Menicucci, M. Laurino, R. Bedini, A. Piarulli, and A. Gemignani. Sleep unconsciousness and breakdown of serial critical intermittency: New vistas on the global workspace. *Chaos, Solitons & Fractals*, 55(0):32–43, 2013.

[33] Giulio Tononi and Chiara Cirelli. Sleep and synaptic homeostasis: a hypothesis. *Brain Res Bull*, 62(2):143–150, Dec 2003.

[34] G. Tononi and C. Cirelli. Sleep function and synaptic homeostasis. *Sleep Med Rev*, 10(1):49–62, Feb 2006.

[35] Marco Laurino, Danilo Menicucci, Andrea Piarulli, Francesca Mastorci, Remo Bedini, Paolo Allegrini, and Angelo Gemignani. Disentangling different functional roles of evoked k-complex components: Mapping the sleeping brain while quenching sensory processing. *Neuroimage*, 86:433–445, Feb 2014.

[36] A.L. Loomis, E.N. Harvey, and G.A. Hobart. Distribution of disturbance-patterns in the human electroencephalogram with special reference to sleep. *J Neurophysiol*, 1938.

[37] F. Amzica and M. Steriade. The k-complex: its slow (<1-hz) rhythmicity and relation to delta waves. *Neurology*, 49(4):952–959, Oct 1997.

[38] F. Amzica and M. Steriade. Cellular substrates and laminar profile of sleep k-complex. *Neuroscience*, 82(3):671–686, Feb 1998.

[39] F. Amzica and M. Steriade. The functional significance of k-complexes. *Sleep Med Rev*, 6(2):139–149, Apr 2002.

[40] Alfredo Fontanini and James M. Bower. Slow-waves in the olfactory system: an olfactory perspective on cortical rhythms. *Trends Neurosci*, 29(8):429–437, Aug 2006.

[41] Trish Wolansky, Elizabeth A. Clement, Steven R. Peters, Michael A. Palczak, and Clayton T. Dickson. Hippocampal slow oscillation: a novel eeg state and its coordination with ongoing neocortical activity. *J Neurosci*, 26(23):6213–6229, Jun 2006.

[42] Reto Huber, M Felice Ghilardi, Marcello Massimini, Fabio Ferrarelli, Brady A. Riedner, Michael J. Peterson, and Giulio Tononi. Arm immobilization causes cortical plastic changes and locally decreases sleep slow wave activity. *Nat Neurosci*, 9(9):1169–1176, Sep 2006.

[43] Reto Huber, M Felice Ghilardi, Marcello Massimini, and Giulio Tononi. Local sleep and learning. *Nature*, 430(6995):78–81, Jul 2004.

[44] Lisa Marshall, Halla Helgadóttir, Matthias Mölle, and Jan Born. Boosting slow oscillations during sleep potentiates memory. *Nature*, 444(7119):610–613, Nov 2006.

[45] Jan Born. Slow-wave sleep and the consolidation of long-term memory. *World J Biol Psychiatry*, 11 Suppl 1:16–21, Jun 2010.

[46] Matthias Mölle, Oxana Eschenko, Steffen Gais, Susan J. Sara, and Jan Born. The influence of learning on sleep slow oscillations and associated spindles and ripples in humans and rats. *Eur J Neurosci*, 29(5):1071–1081, Mar 2009.

[47] M. Steriade. Corticothalamic resonance, states of vigilance and mentation. *Neuroscience*, 101(2):243–276, 2000.

[48] C. Iber, S. Ancoli-Israel, A. Chesson, and S.F. Quan. The aasm manual for the scoring of sleep and associated events: rules, terminology and technical specifications. *Westchester, IL: American Academy of Sleep Medicine*, pages 48–9, 2007.

[49] Michel Le Van Quyen, Richard Staba, Anatol Bragin, Clayton Dickson, Mario Valderrama, Itzhak Fried, and Jerome Engel. Large-scale microelectrode recordings of high-frequency gamma oscillations in human cortex during sleep. *J Neurosci*, 30(23):7770–7782, Jun 2010.

[50] Sydney S. Cash, Eric Halgren, Nima Dehghani, Andrea O. Rossetti, Thomas Thesen, Chunmao Wang, Orrin Devinsky, Ruben Kuzniecky, Werner Doyle, Joseph R. Madsen, Edward Bromfield, Loránd Eross, Péter Halász, George Karmos, Richárd Csercsa, Lucia Wittner, and István Ulbert. The human k-complex represents an isolated cortical down-state. *Science*, 324(5930):1084–1087, May 2009.

[51] Vincenzo Crunelli, David W. Cope, and Stuart W. Hughes. Thalamic t-type ca2+ channels and nrem sleep. *Cell Calcium*, 40(2):175–190, Aug 2006.

[52] Vladyslav V. Vyazovskiy, Umberto Olcese, Yaniv M. Lazimy, Ugo Faraguna, Steve K. Esser, Justin C. Williams, Chiara Cirelli, and Giulio Tononi. Cortical firing and sleep homeostasis. *Neuron*, 63(6):865–878, Sep 2009.

[53] D. Contreras, I. Timofeev, and M. Steriade. Mechanisms of long-lasting hyperpolarizations underlying slow sleep oscillations in cat corticothalamic networks. *J Physiol*, 494 (Pt 1):251–264, Jul 1996.

[54] Vincenzo Crunelli, Kate L. Blethyn, David W. Cope, Stuart W. Hughes, H Rheinallt Parri, Jonathan P. Turner, Tibor I. Tòth, and Stephen R. Williams. Novel neuronal and astrocytic mechanisms in thalamocortical loop dynamics. *Philos Trans R Soc Lond B Biol Sci*, 357(1428):1675–1693, Dec 2002.

[55] R. C. Dossi, A. Nuñez, and M. Steriade. Electrophysiology of a slow (0.5-4 hz) intrinsic oscillation of cat thalamocortical neurones in vivo. *J Physiol*, 447:215–234, Feb 1992.

[56] M. Steriade, R. C. Dossi, and A. Nuñez. Network modulation of a slow intrinsic oscillation of cat thalamocortical neurons implicated in sleep delta waves: cortically induced synchronization and brainstem cholinergic suppression. *J Neurosci*, 11(10):3200–3217, Oct 1991.

[57] F. Amzica, M. Massimini, and A. Manfridi. Spatial buffering during slow and paroxysmal sleep oscillations in cortical networks of glial cells in vivo. *J Neurosci*, 22(3):1042–1053, Feb 2002.

[58] S. Chauvette, M. Volgushev, and I. Timofeev. Origin of active states in local neocortical networks during slow sleep oscillation. *Cereb Cortex*, 20(11):2660–2674, Nov 2010.

[59] Tommaso Fellin, Michael M. Halassa, Miho Terunuma, Francesca Succol, Hajime Takano, Marcos Frank, Stephen J. Moss, and Philip G. Haydon. Endogenous nonneuronal modulators of synaptic transmission control cortical slow oscillations in vivo. *Proc Natl Acad Sci U S A*, 106(35):15037–15042, Sep 2009.

[60] Yousheng Shu, Andrea Hasenstaub, and David A. McCormick. Turning on and off recurrent balanced cortical activity. *Nature*, 423(6937):288–293, May 2003.

[61] Maxim Volgushev, Sylvain Chauvette, Mikhail Mukovski, and Igor Timofeev. Precise long-range synchronization of activity and silence in neocortical neurons during slow-wave oscillations [corrected]. *J Neurosci*, 26(21):5665–5672, May 2006.

[62] Maria V. Sanchez-Vives, Maurizio Mattia, Albert Compte, Maria Perez-Zabalza, Milena Winograd, Vanessa F. Descalzo, and Ramon Reig. Inhibitory modulation of cortical up states. *J Neurophysiol*, 104(3):1314–1324, Sep 2010.

[63] D. Contreras, A. Destexhe, T. J. Sejnowski, and M. Steriade. Control of spatiotemporal coherence of a thalamic oscillation by corticothalamic feedback. *Science*, 274(5288):771–774, Nov 1996.

[64] Brady A. Riedner, Vladyslav V. Vyazovskiy, Reto Huber, Marcello Massimini, Steve Esser, Michael Murphy, and Giulio Tononi. Sleep homeostasis and cortical synchronization: Iii. a high-density eeg study of sleep slow waves in humans. *Sleep*, 30(12):1643–1657, Dec 2007.

[65] Michael Murphy, Brady A. Riedner, Reto Huber, Marcello Massimini, Fabio Ferrarelli, and Giulio Tononi. Source modeling sleep slow waves. *Proc Natl Acad Sci U S A*, 106(5):1608–1613, Feb 2009.

[66] Reto Huber, Giulio Tononi, and Chiara Cirelli. Exploratory behavior, cortical bdnf expression, and sleep homeostasis. *Sleep*, 30(2):129–139, Feb 2007.

[67] David R. Euston, Masami Tatsuno, and Bruce L. McNaughton. Fast-forward playback of recent memory sequences in prefrontal cortex during sleep. *Science*, 318(5853):1147–1150, Nov 2007.

[68] Daoyun Ji and Matthew A. Wilson. Coordinated memory replay in the visual cortex and hippocampus during sleep. *Nat Neurosci*, 10(1):100–107, Jan 2007.

[69] Adrien Peyrache, Mehdi Khamassi, Karim Benchenane, Sidney I. Wiener, and Francesco P. Battaglia. Replay of rule-learning related neural patterns in the prefrontal cortex during sleep. *Nat Neurosci*, 12(7):919–926, Jul 2009.

[70] T. J. Sejnowski and A. Destexhe. Why do we sleep? *Brain Res*, 886(1-2):208–223, Dec 2000.

[71] Anton Sirota, Jozsef Csicsvari, Derek Buhl, and György Buzsáki. Communication between neocortex and hippocampus during sleep in rodents. *Proc Natl Acad Sci U S A*, 100(4):2065–2069, Feb 2003.

[72] M. Steriade, D. Contreras, R. Curró Dossi, and A. Nuñez. The slow (< 1 hz) oscillation in reticular thalamic and thalamocortical neurons: scenario of sleep rhythm generation in interacting thalamic and neocortical networks. *J Neurosci*, 13(8):3284–3299, Aug 1993.

[73] E. Lugaresi, R. Medori, P. Montagna, A. Baruzzi, P. Cortelli, A. Lugaresi, P. Tinuper, M. Zucconi, and P. Gambetti. Fatal familial insomnia and dysautonomia with selective degeneration of thalamic nuclei. *N Engl J Med*, 315(16):997–1003, Oct 1986.

[74] R. Medori, H. J. Tritschler, A. LeBlanc, F. Villare, V. Manetto, H. Y. Chen, R. Xue, S. Leal, P. Montagna, and P. Cortelli. Fatal familial insomnia, a prion disease with a mutation at codon 178 of the prion protein gene. *N Engl J Med*, 326(7):444–449, Feb 1992.

[75] L. G. Goldfarb, R. B. Petersen, M. Tabaton, P. Brown, A. C. LeBlanc, P. Montagna, P. Cortelli, J. Julien, C. Vital, and W. W. Pendelbury. Fatal familial insomnia and familial creutzfeldt-jakob disease: disease phenotype determined by a dna polymorphism. *Science*, 258(5083):806–808, Oct 1992.

[76] Pasquale Montagna. Fatal familial insomnia and the role of the thalamus in sleep regulation. *Handb Clin Neurol*, 99:981–996, 2011.

[77] E. Sforza, P. Montagna, P. Tinuper, P. Cortelli, P. Avoni, F. Ferrillo, R. Petersen, P. Gambetti, and E. Lugaresi. Sleep-wake cycle abnormalities in fatal familial insomnia. evidence of the role of the thalamus in sleep regulation. *Electroencephalogr Clin Neurophysiol*, 94(6):398–405, Jun 1995.

[78] P. Tinuper, P. Montagna, R. Medori, P. Cortelli, M. Zucconi, A. Baruzzi, and E. Lugaresi. The thalamus participates in the regulation of the sleep-waking cycle. a clinico-pathological study in fatal familial thalamic degeneration. *Electroencephalogr Clin Neurophysiol*, 73(2):117–123, Aug 1989.

[79] P. Cortelli, D. Perani, P. Parchi, F. Grassi, P. Montagna, M. De Martin, R. Castellani, P. Tinuper, P. Gambetti, E. Lugaresi, and F. Fazio. Cerebral metabolism in fatal familial insomnia: relation to duration, neuropathology, and distribution of protease-resistant prion protein. *Neurology*, 49(1):126–133, Jul 1997.

[80] Pietro Cortelli, Daniela Perani, Pasquale Montagna, Roberto Gallassi, Paolo Tinuper, Federica Provini, Provini Federica, Patrizia Avoni, Franco Ferrillo, Davide Anchisi, Rosa Maria Moresco, Ferruccio Fazio, Piero Parchi, Agostino Baruzzi, Elio Lugaresi, and Pierluigi Gambetti. Pre-symptomatic diagnosis in fatal familial insomnia: serial neurophysiological and 18fdg-pet studies. *Brain*, 129(Pt 3):668–675, Mar 2006.

[81] Bruce Fischl, André van der Kouwe, Christophe Destrieux, Eric Halgren, Florent Ségonne, David H. Salat, Evelina Busa, Larry J. Seidman, Jill Goldstein, David Kennedy, Verne Caviness, Nikos Makris, Bruce Rosen, and Anders M. Dale. Automatically parcellating the human cerebral cortex. *Cereb Cortex*, 14(1):11–22, Jan 2004.

[82] A. Delorme and S. Makeig. Eeglab: an open source toolbox for analysis of single-trial eeg dynamics including independent component analysis. *J Neurosci Methods*, 134(1):9–21, Mar 2004.

[83] F. Amzica and M. Steriade. Electrophysiological correlates of sleep delta waves. *Electroencephalogr Clin Neurophysiol*, 107(2):69–83, Aug 1998.

[84] V. Manetto, R. Medori, P. Cortelli, P. Montagna, P. Tinuper, A. Baruzzi, G. Rancurel, J. J. Hauw, J. J. Vanderhaeghen, and P. Mailleux. Fatal familial insomnia: clinical and pathologic study of five new cases. *Neurology*, 42(2):312–319, Feb 1992.

[85] P. Parchi, R. B. Petersen, S. G. Chen, L. Autilio-Gambetti, S. Capellari, L. Monari, P. Cortelli, P. Montagna, E. Lugaresi, and P. Gambetti. Molecular pathology of fatal familial insomnia. *Brain Pathol*, 8(3):539–548, Jul 1998.

[86] M. Steriade, A. Nuñez, and F. Amzica. Intracellular analysis of relations between the slow (¡ 1 hz) neocortical oscillation and other sleep rhythms of the electroencephalogram. *J Neurosci*, 13(8):3266–3283, Aug 1993.

[87] I. Timofeev, D. Contreras, and M. Steriade. Synaptic responsiveness of cortical and thalamic neurones during various phases of slow sleep oscillation in cat. *J Physiol*, 494 (Pt 1):265–278, Jul 1996.

[88] Morgane Le Bon-Jego and Rafael Yuste. Persistently active, pacemaker-like neurons in neocortex. *Front Neurosci*, 1(1):123–129, Nov 2007.

[89] F. Amzica and M. Steriade. Disconnection of intracortical synaptic linkages disrupts synchronization of a slow oscillation. *J Neurosci*, 15(6):4658–4677, Jun 1995.

[90] F. Amzica and M. Steriade. Short- and long-range neuronal synchronization of the slow (¡ 1 hz) cortical oscillation. *J Neurophysiol*, 73(1):20–38, Jan 1995.

[91] G. Marini, I. Gritti, and M. Mancia. Changes in eeg spindle activity induced by ibotenic acid lesions of medialis dorsalis thalamic nuclei in the cat. *Brain Res*, 500(1-2):395–399, Oct 1989.

[92] Pasquale Montagna, Pierluigi Gambetti, Pietro Cortelli, and Elio Lugaresi. Familial and sporadic fatal insomnia. *Lancet Neurol*, 2(3):167–176, Mar 2003.

[93] Pasquale Montagna. Fatal familial insomnia: a model disease in sleep physiopathology. *Sleep Med Rev*, 9(5):339–353, Oct 2005.

[94] M. Steriade and M. Deschenes. The thalamus as a neuronal oscillator. *Brain Research Reviews; Brain Research Reviews*, 1984.

[95] J. L. Velayos, M. Oliva, and F. Alfageme. Afferent projections to the mediodorsal and anterior thalamic nuclei in the cat. anatomical-clinical correlations. *Brain Pathol*, 8(3):549–552, Jul 1998.

[96] M. Roth, J. Shaw, and J. Green. The form voltage distribution and physiological significance of the k-complex. *Electroencephalogr Clin Neurophysiol*, 8(3):385–402, Aug 1956.

[97] R. D. Ogilvie, I. A. Simons, R. H. Kuderian, T. MacDonald, and J. Rustenburg. Behavioral, event-related potential, and eeg/fft changes at sleep onset. *Psychophysiology*, 28(1):54–64, Jan 1991.

[98] O. Winter, A. Kok, J. L. Kenemans, and M. Elton. Auditory event-related potentials to deviant stimuli during drowsiness and stage 2 sleep. *Electroencephalogr Clin Neurophysiol*, 96(5):398–412, Sep 1995.

[99] J. Gora, I. M. Colrain, and J. Trinder. Respiratory-related evoked potentials during the transition from alpha to theta eeg activity in stage 1 nrem sleep. *J Sleep Res*, 8(2):123–134, Jun 1999.

[100] C. Bastien and K. Campbell. The evoked k-complex: all-or-none phenomenon? *Sleep*, 15(3):236–245, Jun 1992.

[101] Péter Halász. K-complex, a reactive eeg graphoelement of nrem sleep: an old chap in a new garment. *Sleep Med Rev*, 9(5):391–412, Oct 2005.

[102] Florin Amzica. Comment on "the human k-complex represents an isolated cortical down-state". *Science*, 330(6000):35; author reply 35, Oct 2010.

[103] H. Davis, P.A. Davis, A.L. Loomis, EN Hervey, and G. Hobart. Electrical reactions of the human brain to auditory stimulation during sleep. *Journal of Neurophysiology; Journal of Neurophysiology*, 1939.

[104] M. O. Cunningham, D. D. Pervouchine, C. Racca, N. J. Kopell, C. H. Davies, R S G. Jones, R. D. Traub, and M. A. Whittington. Neuronal metabolism governs cortical network response state. *Proc Natl Acad Sci U S A*, 103(14):5597–5601, Apr 2006.

[105] IM Colrain, KE Webster, and G. Hirst. The effects of stimulus modality of the scalp topography of the evoked k-complex. *J. Sleep. Res*, 8:273–280, 1999.

[106] K. A. Cote, D. R. de Lugt, S. D. Langley, and K. B. Campbell. Scalp topography of the auditory evoked k-complex in stage 2 and slow wave sleep. *J Sleep Res*, 8(4):263–272, Dec 1999.

[107] C. Bastien, K. E. E. Crowley, and I.M. Colrain. Evoked potential components unique to non-rem sleep: relationship to evoked k-complexes and vertex sharp waves. *Int J Psychophysiol*, 46(3):257–274, Dec 2002.

[108] M. Czisch, R. Wehrle, A. Stiegler, H. Peters, K. Andrade, F. Holsboer, and P.G. Sämann. Acoustic oddball during nrem sleep: a combined eeg/fmri study. *PloS one*, 4(8):e6749, 2009.

[109] A.C. Evans, D.L. Collins, S.R. Mills, E.D. Brown, R.L. Kelly, and T.M. Peters. 3d statistical neuroanatomical models from 305 mri volumes. In *Nuclear Science Symposium and Medical Imaging Conference, 1993., 1993 IEEE Conference Record.*, 1993.

[110] Steve K. Esser, Sean L. Hill, and Giulio Tononi. Sleep homeostasis and cortical synchronization: I. modeling the effects of synaptic strength on sleep slow waves. *Sleep*, 30(12):1617–1630, Dec 2007.

[111] J. Carrier, I. Viens, G. Poirier, R. Robillard, M. Lafortune, G. Vandewalle, N. Martin, M. Barakat, J. Paquet, and D. Filipini. Sleep slow wave changes during the middle years of life. *Eur J Neurosci*, 33(4):758–766, Feb 2011.

[112] Vladyslav V. Vyazovskiy, Brady A. Riedner, Chiara Cirelli, and Giulio Tononi. Sleep homeostasis and cortical synchronization: Ii. a local field potential study of sleep slow waves in the rat. *Sleep*, 30(12):1631–1642, Dec 2007.

[113] M. Caporro, Z. Haneef, H.J. Yeh, A. Lenartowicz, C. Buttinelli, J. Parvizi, and J.M. Stern. Functional mri of sleep spindles and k-complexes. *Clin Neurophysiol*, 123(2):303–309, Feb 2012.

[114] John M. Stern, Matteo Caporro, Zulfi Haneef, Hsiang J. Yeh, Carla Buttinelli, Agatha Lenartowicz, Jeanette A. Mumford, Josef Parvizi, and Russell A. Poldrack. Functional imaging of sleep vertex sharp transients. *Clin Neurophysiol*, 122(7):1382–1386, Jul 2011.

[115] Brady A. Riedner, Bradley K. Hulse, Michael J. Murphy, Fabio Ferrarelli, and Giulio Tononi. Temporal dynamics of cortical sources underlying spontaneous and peripherally evoked slow waves. *Prog Brain Res*, 193:201–218, 2011.

[116] K.B. Campbell and I.M. Colrain. Event-related potential measures of the inhibition of information processing: Ii. the sleep onset period. *Int J Psychophysiol*, 46(3):197–214, 2002.

[117] Marcello Massimini, Mario Rosanova, and Maurizio Mariotti. Eeg slow (approximately 1 hz) waves are associated with nonstationarity of thalamocortical sensory processing in the sleeping human. *J Neurophysiol*, 89(3):1205–1213, Mar 2003.

[118] I.M. Colrain. The k-complex: a 7-decade history. *Sleep*, 28(2):255–273, Feb 2005.

[119] R. A. Velluti. Interactions between sleep and sensory physiology. *J Sleep Res*, 6(2):61–77, Jun 1997.

[120] E. G. Jones. The thalamic matrix and thalamocortical synchrony. *Trends Neurosci*, 24(10):595–601, Oct 2001.

[121] S. Kohsaka, T. Sakai, M. Kohsaka, N. Fukuda, and T. Ariga. Activation of the brainstem precedes and outlasts the k-complex in humans. *Neuroscience*, 202:243–251, Jan 2012.

[122] ER Kandel, JH Schwartz, TM Jessell, SA Siegelbaum, and AJ Hudspeth. *Principles of Neural Science, Fifth Edition*. McGraw-Hill Professional; 5th edition, 2012.

[123] Thien Thanh Dang-Vu, Maxime Bonjean, Manuel Schabus, Mélanie Boly, Annabelle Darsaud, Martin Desseilles, Christian Degueldre, Evelyne Balteau, Christophe Phillips, André Luxen, Terrence J. Sejnowski, and Pierre Maquet. Interplay between spontaneous and induced brain activity during human non-rapid eye movement sleep. *Proc Natl Acad Sci U S A*, 108(37):15438–15443, Sep 2011.

[124] Marcello Massimini, Fabio Ferrarelli, Steve K. Esser, Brady A. Riedner, Reto Huber, Michael Murphy, Michael J. Peterson, and Giulio Tononi. Triggering

sleep slow waves by transcranial magnetic stimulation. *Proc Natl Acad Sci U S A*, 104(20):8496–8501, May 2007.

[125] Pavlos Rigas and Manuel A. Castro-Alamancos. Thalamocortical up states: differential effects of intrinsic and extrinsic cortical inputs on persistent activity. *J Neurosci*, 27(16):4261–4272, Apr 2007.

[126] L. Domich, G. Oakson, and M. Steriade. Thalamic burst patterns in the naturally sleeping cat: a comparison between cortically projecting and reticularis neurones. *J Physiol*, 379:429–449, Oct 1986.

[127] J. Tsoukatos, Z. H. Kiss, K. D. Davis, R. R. Tasker, and J. O. Dostrovsky. Patterns of neuronal firing in the human lateral thalamus during sleep and wakefulness. *Exp Brain Res*, 113(2):273–282, Feb 1997.

[128] C.M. Portas, K. Krakow, P. Allen, O. Josephs, J.L. Armony, and C.D. Frith. Auditory processing across the sleep-wake cycle: simultaneous eeg and fmri monitoring in humans. *Neuron*, 28(3):991–999, 2000.

[129] I.M. Colrain, K.E. Webster, and G. Hirst. The n550 component of the evoked k-complex: a modality non-specific response? *J Sleep Res*, 8(4):273–280, Dec 1999.

[130] Lifshitz EM Landau LD. *Course of theoretical physics*. Pergamon Press, 1965.

[131] Marcello Massimini, Fabio Ferrarelli, Reto Huber, Steve K. Esser, Harpreet Singh, and Giulio Tononi. Breakdown of cortical effective connectivity during sleep. *Science*, 309(5744):2228–2232, Sep 2005.

[132] M. Steriade, V. Apostol, and G. Oakson. Control of unitary activities in cerebellothalamic pathway during wakefulness and synchronized sleep. *J Neurophysiol*, 34(3):389–413, May 1971.

[133] D. A. McCormick and T. Bal. Sleep and arousal: thalamocortical mechanisms. *Annu Rev Neurosci*, 20:185–215, 1997.

[134] Kolja Jahnke, Frederic von Wegner, Astrid Morzelewski, Sergey Borisov, Marcella Maischein, Helmuth Steinmetz, and Helmut Laufs. To wake or not to wake? the two-sided nature of the human k-complex. *Neuroimage*, 59(2):1631–1638, Jan 2012.

[135] Y. Niiyama, M. Fushimi, A. Sekine, and Y. Hishikawa. K-complex evoked in nrem sleep is accompanied by a slow negative potential related to cognitive process. *Electroencephalogr Clin Neurophysiol*, 95(1):27–33, Jul 1995.

[136] J Allan Hobson and Edward F. Pace-Schott. The cognitive neuroscience of sleep: neuronal systems, consciousness and learning. *Nat Rev Neurosci*, 3(9):679–693, Sep 2002.

[137] Chiara Baglioni, Kai Spiegelhalder, Caterina Lombardo, and Dieter Riemann. Sleep and emotions: a focus on insomnia. *Sleep Med Rev*, 14(4):227–238, Aug 2010.

[138] Dieter Riemann. "hyperarousal and insomnia: state of the science". *Sleep Med Rev*, 14(1):17, Feb 2010.

[139] Dieter Riemann, Kai Spiegelhalder, Bernd Feige, Ulrich Voderholzer, Mathias Berger, Michael Perlis, and Christoph Nissen. The hyperarousal model of insomnia: a review of the concept and its evidence. *Sleep Med Rev*, 14(1):19–31, Feb 2010.

[140] M. Ghilardi, C. Ghez, V. Dhawan, J. Moeller, M. Mentis, T. Nakamura, A. Antonini, and D. Eidelberg. Patterns of regional brain activation associated with different forms of motor learning. *Brain Res*, 871(1):127–145, Jul 2000.

[141] A. Rechtschaffen and A. Kales. A manual of standardized terminology, techniques, and scoring systems for sleep stages of human subjects. *Brain Research Institute*, 1968.

[142] N. Kleitman. *Sleep and wakefulness*. University of Chicago Press, 1963.

[143] G. Moruzzi. Active processes in the brain stem during sleep. *Harvey Lect*, 58:233, 1963.

[144] M. Jouvet. Recherches sur les structures nerveuses et les mécanismes responsables des différentes phases du sommeil physiologique. *Arch Ital Biol*, 100(March 21):125–206, 1962.

[145] O. Pompeiano. Mechanisms of sensorimotor integration during sleep. *Progr. Physiol. Psychol*, 3:1–179, 1970.

[146] AML Coenen and W. Drinkenburg. Animal models for information processing during sleep. *Int J Psychophysiol*, 46(3):163–175, 2002.

[147] I. Oswald, A.M. Taylor, and M. Treisman. Discriminative responses to stimulation during human sleep. *Brain: a journal of neurology*, 1960.

[148] GW Langford, R. Meddis, and AJD Pearson. Awakening latency from sleep for meaningful and non-meaningful stimuli. *Psychophysiology*, 11(1):1–5, 2007.

[149] H. Nordby, K. Hugdahl, R. Stickgold, K.S. Bronnick, et al. Event-related potentials (erps) to deviant auditory stimuli during sleep and waking. *Neuroreport: An International Journal for the Rapid Communication of Research in Neuroscience*, 1996.

[150] Sirel Karakaay, Emine D. Atakmak, Belma Bekasi, and Hamdullah Aydan. Oscillatory responses representing differential auditory processing in sleep. *Int J Psychophysiol*, 65(1):40 – 50, 2007.

[151] F. Perrin, L. Garcia-Larrea, F. Mauguiare, and H. Bastuji. A differential brain response to the subject's own name persists during sleep. *Clin Neurophysiol*, 110(12):2153–2164, 1999.

[152] E. Niedermeyer. Sleep and eeg. *Electroencephalography: Basic Principles, Clinical Applications, and Related Fields, 3rd edn Williams & Wilkins: Baltimore, MD*, pages 153–166, 1993.

[153] H. Berger. Über das elektrenkephalogramm des menschen. *Eur Arch Psychiatry Clin Neurosci*, 87(1):527–570, 1929.

[154] H.H. Jasper and H.L. Andrews. Electroencephalography. iii. normal differentiation of occipital and precentral regions in man. *Archives of Neurology & Psychiatry (Chicago); Archives of Neurology & Psychiatry (Chicago)*, 1938.

[155] F. Dutertre. *"Catalog of the main EEG-patterns." Handbook of Electroencephalography and Clinical Neurophysiology*, volume 2. Elsevier Scientific Publishing Company, Amsterdam, 1977.

[156] N. Kopell, GB Ermentrout, MA Whittington, and RD Traub. Gamma rhythms and beta rhythms have different synchronization properties. *Proceedings of the National Academy of Sciences*, 97(4):1867–1872, 2000.

[157] E. Başar and T.H. Bullock. *Induced rhythms in the brain*. Birkhauser, 1992.

[158] S. Gais and J. Born. Declarative memory consolidation: mechanisms acting during human sleep. *Learning & Memory*, 11(6):679–685, 2004.

[159] M. Von Krosigk, T. Bal, D.A. McCormick, et al. Cellular mechanisms of a synchronized oscillation in the thalamus. *Science*, 261:361–361, 1993.

[160] M. Steriade, I. Timofeev, et al. Neuronal plasticity in thalamocortical networks during sleep and waking oscillations. *Neuron*, 37(4):563–576, 2003.